

الجمهورية الجزائرية الديمقراطية الشعبية
République Algérienne démocratique et populaire

وزارة التعليم العالي و البحث العلمي
Ministère de l'enseignement supérieur et de la recherche scientifique

جامعة سعد دحلب البليدة
Université SAAD DAHLAB de BLIDA

كلية التكنولوجيا
Faculté de Technologie

قسم الإلكترونيك
Département d'Électronique



Eye and Optical System Design and Simulation using Blender and Matlab for Retina Laser PhotoCoagulation

A dissertation submitted in partial fulfillment of the requirements for a

Master's degree

In Génie Electrique

Specialty: Embedded Systems Electronics

Supervised by : **MS. BOUGHERIRA HAMIDA**

Accomplished by :

- **HAFSAOUI ALA EDDINE**
- **YOUSFI MOHAMED RYAD**

Academic Year 2023/2024

ACKNOWLEDGMENT

We would like to express our sincere gratitude to all those who have contributed to the successful completion of this project.

First and foremost, we extend our deepest appreciation to Ms Bougherira Hamida for her invaluable guidance, expertise, and unwavering support throughout this endeavor. Her insightful feedback and encouragement were instrumental in shaping our work.

We are grateful to the esteemed members of the jury for accepting to evaluate our work. Your expertise and willingness to assess our project are highly valued, and we appreciate your commitment. Your insights will undoubtedly contribute to the refinement of our project.

We would also like to acknowledge the technical staff and administrative personnel who provided assistance and resources crucial to our research.

To our families, we express our profound gratitude for their unwavering support, patience, and encouragement throughout our academic journey. Your love and belief in us have been a constant source of strength and motivation.

Finally, we extend our appreciation to all others who have contributed in any way to this project. Your support, however big or small, has not gone unnoticed and has played a part in our success.

Dedication

To our loving families, our beloved mothers, our supporting fathers and our siblings, for their advice, love and faith.

Abstract: Eye and Optical System Modeling for Retina Laser Photo-Coagulation

This study integrates Blender and MATLAB to model and optimize the eye and optical system used in retina laser photo-coagulation. Blender provides detailed 3D visualizations of the eye and optical components, aiding in understanding the laser's path and impact on the retina. MATLAB calculates the beam expander parameters to achieve the desired laser spot size and intensity. This combined approach enhances precision in retina laser treatments and offers a valuable framework for future ophthalmic laser applications.

ملخص: نمذجة العين والنظام البصري لعلاج تخثر الشبكية بالليزر

لنمذجة وتحسين النظام البصري والعين MATLAB و Blender تدمج هذه الدراسة بين برنامج تصورات ثلاثية الأبعاد مفصلة للعين والمكونات Blender المستخدم في علاج تخثر الشبكية بالليزر. يوفر بحساب معلمات ممدد MATLAB البصرية، مما يساعد في فهم مسار الليزر وتأثيره على الشبكية. يقوم الشعاع لتحقيق حجم البقعة وشدة الليزر المطلوبة. يعزز هذا النهج المدمج الدقة في علاجات الليزر للشبكية. ويوفر إطار عمل قيم لتطبيقات الليزر المستقبلية في طب العيون.

Résumé : Modélisation de l'œil et du système optique pour la photocoagulation rétinienne au laser

Cette étude intègre Blender et MATLAB pour modéliser et optimiser l'œil et le système optique utilisés dans la photocoagulation rétinienne au laser. Blender offre des visualisations 3D détaillées de l'œil et des composants optiques, aidant à comprendre le trajet du laser et son impact sur la rétine. MATLAB calcule les paramètres de l'expandeur de faisceau pour obtenir la taille et l'intensité souhaitées du point laser. Cette approche combinée améliore la précision des traitements au laser rétinien et offre un cadre précieux pour les futures applications laser en ophtalmologie.

Table of Contents

LISTE of FIGURES AND TABLES	8
LISTE OF SYMBOLES AND ABBREVIATIONS.....	12
GENERAL INTRODUCTION.....	13
I.....Chapter 1 : Background on Retina Diseases and Laser PhotoCoagulation Devices	
I.1.INTRODUCTION :	16
I.2.Retinopathies :	16
I.2.1.Anatomy of the EYE :	16
I.2.2.Retina pathologies.....	18
I.2.3.Laser treatment of retinal diseases	19
I.3.DIAGNOSTIC :	20
I.3.1.Diagnostic Tools and Techniques	20
I.3.1.1.Digital Fundus Photography:.....	20
I.3.1.2.Wide Angle Fluorescein Angiography.....	21
I.3.1.3.Optical Coherence Tomography (OCT)	22
I.3.2.Pre-Treatment Assessment:	24
I.4.Treatment :	24
I.4.1.LASER :	24
I.4.2.Laser Tissue Interactions :	25
I.4.3.Laser Tissue interactions with DMD :	26
I.4.4.Laser Types in Retina :	27
I.4.5.Laser-Tissue Absorption in the Retina :	28
I.5.Retinal Photocoagulation Hardware and Devices :.....	29
I.5.1.Laser Console :	30
I.5.2.Delivery Systems :.....	31
I.5.2.1.Slit Lamp :	31
I.5.2.2.Operating Microscope :	32
I.5.2.3.Indirect Ophthalmoscope :	34
I.5.2.4.Endoprobe :	34
I.5.3.Gonio Lens :	35
I.5.4.Safety Filters :	35
I.6.Guidance and Focusing System :.....	36
I.6.1.SingleSpot :	36
I.6.1.1.System 1 (only Galvo):.....	36
I.6.2.MultiSpot :	37
I.6.2.1.System 2 (LCD with Galvo) :	37
I.6.2.2.System 3 (DMD):.....	37
I.7.Conclusion :.....	38

II.Chapter 2 : Design of optical system for Retina

PhotoCoagulation

II.1.INTRODUCTION :	40
II.2.LASER Parameters :	41
II.3.Beam Combiner (Dichroic filter) :	42
II.4.Beam Expander :	43
II.4.1.Types of Beam Expanders.....	43
II.4.2.Components and Principle of Galilean Beam Expander	43
II.4.3.Magnification of Galilean Beam Expander	44
II.4.4.Beam Diameter Expansion	44
II.4.5.Lens Separation	44
II.5.Lenses	45
II.5.1.Type Of Lenses.....	45
II.5.2.Lensmaker's Equation.....	46
II.5.3.Plano Concave & Plano Convex	47
II.6.Gonio Lens	48
II.6.1.Direct Lenses	48
II.6.2.Indirect Lenses.....	49
II.6.3.Ocular 3 Mirror Universal Goldmann	50
II.7.Physics of the EYE :	51
II.7.1.RELAXED and ACOMODATION :	51
II.8.Index of Refraction (IOR) :	52
II.8.1.Snell's law	52
II.8.2.IOR of the Eye	53
II.9.DMD VIALUX V-7000 Module	54
II.9.1.Overview	54
II.9.2.Technical Data	55
II.9.3.ALP 4.2 Controller Suite.....	56
II.10. Conclusion	57

III.Chapter 3 : Modeling & Simulation Eye and Optical System

- III.1.INTRODUCTION :59**
- III.2.Dimensions and Measurements of the Eye :60**
 - III.2.1.Axial length (AL):..... 60
 - III.2.2.Transverse diameter :..... 60
 - III.2.3.Cornea: 61
 - III.2.4.Sclera : 62
 - III.2.5.Anterior chamber: 63
 - III.2.6.Aqueous humor: 63
 - III.2.7.Pupil:..... 63
 - III.2.8. Iris: 63
 - III.2.9.Lens: 64
 - III.2.10.Ciliary Body : 65
 - III.2.11.Vitreous: 66
 - III.2.12.Retina :..... 66
 - III.2.13.Macula:..... 67
 - III.2.14.Fovea : 67
 - III.2.15.Optic nerve : 68
- III.3.Modeling :.....69**
 - III.3.1.Blender : 69
 - III.3.2. Modeling EYE : 70
 - III.3.2.1.Modeling Sclera : 70
 - III.3.2.2.Modeling Cornea : 71
 - III.3.2.3.Modeling Ciliary Muscle : 72
 - III.3.2.4.Modeling Choroid & Retina : 72
 - III.3.2.5.Modeling Iris : 73
 - III.3.2.6.Modeling Vitreous : 73
 - III.3.2.7.Modeling Crystalline Lens : 74
 - III.3.2.8.EYE (All in One) : 76
 - III.3.3.Modeling & Calculation of Beam Expander :..... 77
 - III.3.4.Modeling DMD : 80
 - III.3.5.OptoMechanics Component :..... 82
 - III.3.6.Modeling OptoMechanics : 82
- III.4.Simulation :.....84**
 - III.4.1.LuxCoreRender : 84
 - III.4.2.DMD PATTERN Simulation :..... 85
 - III.4.3.Result : 86
- III.5.Conclusion.....88**
- General Conclusion 89**
- Annex..... 90**
- Bibliography 94**

LISTE of FIGURES AND TABLES

Chapter 1

Figure I.1 : Anatomy of the eye	16
Figure I.2 : Retina Elements of Visual Perception.....	18
Figure I.3 : Types of diabetic retinopathy	19
Figure I.4 : Schematic drawing of various vascular coagulations	19
Figure I.5 : hand-held fundus camera	20
Figure I.6 : wide field fundus fluorescein angiography.....	21
Figure I.7 : Schema of a basic OCT acquisition system	22
Figure I.8 : OCT 3D color coded cross-section images of the eye.....	23
Figure I.9 : Illustration of the OCT scanning protocol and image analyses	23
Figure I.10 : various laser tissues interactions and the type of laser involved	25
Figure I.11 : Laser-Tissue Absorption.....	28
Figure I.12 : Components of a Laser System for retinal photocoagulation	29
Figure I.13 : bloc diagram of a laser system for retinal photocoagulation	29
Figure I.14 : Laser Console.....	30
Figure I.15 : Schema Optic of Diode Laser with Slit Lamp	31
Figure I.16 : Assistant Operating Microscope.....	32
Figure I.17 : Diagram of biomicroscopic delivery system	33
Figure I.18 : Binocular indirect ophthalmoscopy and Laser Integration....	34
Figure I.19 : Endoprobe	34
Figure I.20 : Table 1 Contact Lenses used for PRP	35
Figure I.21 : Table 2 Contact Lenses used for Focal/Grid Lasers	35
Figure I.22 : Safety filters.....	35
Figure I.23 : Guidance and Focusing System	36
Figure I.24 : Galvo Laser	36
Figure I.25 : Transmissive LCD Display Working	37
Figure I.26 : DMD chip and micromirrors	37
Figure I.27 : DMD Control each Mirror independently.....	38

Chapter 2

Figure II.1 : Design of Optical System for Retina PhotoCoagulation.....	40
Figure II.2 : Power Density (J/cm ²).....	41
Figure II.3 : Beam Combiner	42
Figure II.4 : Dichroic Combine / Separate	42
Figure II.5 : Magnification of Galilean & Keplerian Beam Expander.....	43
Figure II.6 : Galilean Beam Expander.....	44
Figure II.7 : Type of Lenses	45
Figure II.8 : Negative and Positive Lens	45
Figure II.9 : The Lens Maker Variables.....	46
Figure II.10 : Plano-Concave Lens	47
Figure II.11 : Plano-Convex Lens	47
Figure II.12 : Volk Gonio Lens	48
Figure II.13 : Koeppel lens	48
Figure II.14 : Direct vs Indirect gonio lens	49
Figure II.15 : Goldmann Three Mirror.....	49
Figure II.16 : Goldmann three mirrors angles.....	50
Figure II.17 : Goldmann Ocular Three Mirror Universal Lenses	50
Figure II.18 : Relaxed and accommodated vision	51
Figure II.19 : IOR & Snell's Law	52
Figure II.20 : Refractive indices of the Eye.....	53
Figure II.21 : Refractive index in Crystalline Lens	53
Figure II.22 : VIALUX V-7000 Module	54
Figure II.23 : Control and Data Flow	56

Chapter 3

Figure III.1 : Ocular biometric measurements	60
Figure III.2 : Cornea Horizontal Vertical Diameter	61
Figure III.3 : Cornea semi-Sclera Sclera Diameter.....	61
Figure III.4 : Cornea Thickness	61
Figure III.5 : Cornea Layers	61
Figure III.6 : AST for all 8 meridians	62
Figure III.7 : Eye Axes	62
Figure III.8 : Sclera Thickness.....	62
Figure III.9 : OCT image of the temporal sclera (A). Ciliary muscle (B); Scleral spur (SS).....	62
Figure III.10 : Anterior segment parameters	63
Figure III.11 : Pupil Light Reflex	63
Figure III.12 : Crystalline Lens Dimension.....	64
Figure III.13 : Crystalline Lens Parameters	64
Figure III.14 : Crystalline Lens Diagram	64
Figure III.15 : Crystalline Lens Dimension/age.....	64
Figure III.16 : Ciliary Body Thickness/SS/Age.....	65
Figure III.17 : Ciliary Body Parameters.....	65
Figure III.18 : Ciliary Body thickness during Accommodationpars.....	65
Figure III.19 : plana/Ora serrata	65
Figure III.20 : Scattergram length of the ciliary body/sagittal	65
Figure III.21 : The vertical extent of the retina across the horizontal meridian	66
Figure III.22 : Foveola-Fovea-centralis-Parafovea-Perifovea	67
Figure III.23 : Blender Workspace Environment	69
Figure III.24 : 3D Sclera Topology	70
Figure III.25 : 3D Sclera side view	70
Figure III.26 : 3D Sclera Wireframe.....	70
Figure III.27 : 3D Sclera Thickness.....	70
Figure III.28 : 3D Sclera Solid View	70
Figure III.29 : 3D Cornea side view	71
Figure III.30 : 3D Cornea Solid view	71
Figure III.31 : 3D Cornea Wireframe Front view	71

Figure III.32 : 3D Cornea Wireframe Back view	71
Figure III.33 : 3D Ciliary Muscle side view.....	72
Figure III.34 : 3D Ciliary Muscle Wireframe	72
Figure III.35 : 3D Ciliary Muscle Measurment.....	72
Figure III.36 : 3D Ciliary Muscle Solid view	72
Figure III.37 : 3D Retina and Choroid side & front view	72
Figure III.38 : 3D Iris side & front view	73
Figure III.39 : 3D Vitreous (side & front view)	73
Figure III.40 : 3D Crystalline Lens Measurment (side & front view)	74
Figure III.41 : 3D Crystalline Lens Parameters (focal Length-R1-R2)	75
Figure III.42 : EYE (All in One)	76
Figure III.43 : Matlab Code for GUI.....	77
Figure III.44 : Matlab GUI Beam Expander Calculator	78
Figure III.45 : Plano Concave and Plano Convex Parameters	79
Figure III.46 : Beam Expander Dimension.....	79
Figure III.47 : DMD Dimensions	80
Figure III.48 : DMD ACTIVE ARRAY and WINDOW SHIELD APERTURE	80
Figure III.49 : 3D Model and Render of DMD	81
Figure III.50 : BreadBoard & OptoMechanics	82
Figure III.51 : Assembly all Components in BreadBoard.....	82
Figure III.52 : Full Optical System (Front view)	83
Figure III.53 : Full Optical System (Top view).....	83
Figure III.54 : DMD Pattern 1024x768 (example)	85
Figure III.55 : DMD Pattern Parameters in Editor.....	85
Figure III.56 : Render of DMD Pattern Reflect Laser.....	85
Figure III.57 : Render the Optical System (front view)	86
Figure III.58 : Render the Optical System (side view)	86
Figure III.59 : Render and Test Full Optical System	87
Figure III.60 : Simulate Full Optical System	87
Figure III.61 : Simulation Laser on Retina (view inside eye)	88

LISTE OF SYMBOLES AND ABREVIATIONS

DMD	Digital Micromirror Device
DLP	Digital light processing
LCD	Liquid Crystal Display
PASCAL	Pattern Scan Laser
GUI	Graphical User Interface
DLL	Dynamic Link Library
LASER	Light Amplification by Stimulated Emission of Radiation
ND:YAG	Neodymium-Doped Yttrium Aluminum Garnet
OCT	Optical Coherence Tomography
OD	Optical Density
FA	Fluorescein Angiography
PDT	Photodynamic therapy
RPE	Retinal Pigment Epithelium
BIO	Binocular indirect ophthalmoscope
LED	Light Emitting Diode
CMOS	Complementary metal–oxide–semiconductor
EVM	Evaluation Module
MEMS	Micro Electro Mechanical System
IOR	Index Of Refraction

GENERAL INTRODUCTION

Laser technology is used in medicine, particularly in retinal photocoagulation to treat conditions like diabetic retinopathy.

The laser produces a high-intensity, monochromatic, and coherent light beam, which is used to precisely destroy abnormal tissue on the retina.

Laser photocoagulation, while effective for treating various retinal conditions, presents notable risks and limitations. These include potential vision impairment from scarring or inadvertent macular damage, long-term retinal complications, recurrent neovascularization, and intraocular hemorrhage. Patients may experience diminished color perception and night vision.[1]

Current devices often lack precision, generate excessive heat, and deliver inconsistent energy, leading to patient discomfort and anxiety. Treatment outcomes can be unpredictable, with the possibility of induced vision loss rivaling that of the original condition.

These challenges highlight the need for more advanced, safer technologies and emphasize the importance of careful patient selection and comprehensive informed consent processes. Ongoing research aims to enhance treatment precision and minimize adverse effects, ultimately improving both clinical outcomes and patient comfort.

The aim of our project is to implement and simulate a system to demonstrate the possibility to use the DMD to shape a Laser beam to photocoagulation simultaneous wounded retina vessels.

Previous projects at the Lats, Lab in EE have used the DMD programmed and controlled Mirrors(the DLP7000) Directly showing its capability to modulate a laser beam, and reach multiple moving target in realtime.

however these Project did not take into account the anatomy of the eye of which complex optical properties must be considered for the laser to hit precisely specific points. Refractions of a same laser ray at different levels of the eye (aqueous humor, cornea, iris, vitreous humor) and the curved shape of the retina, make it impossible for the laser ray to hit its target directly.

Thus our, project objective is to design an optical system, and a realistic optically parameterized eye, and implement and simulate an experiment that shows the feasibility of the multispot photocoagulation of the retina using a DMD.

The Digital Micromirror Device (DMD) is an electromechanical system containing microscopic mirrors that accurately control the light beam, improving the precision and speed of laser treatment by shaping and modulating the beam directed at the retina.

The integration of laser technology and DMD allows for increased precision by accurately targeting abnormal tissue, reducing treatment time thanks to high speed and efficiency, and minimizing side effects by reducing damage to surrounding healthy tissue.

This integration enhances precision and efficiency, and leads to better patient outcomes.

To describe our work, we have organized our dissertation as follows:

Chapter 1 gives an overview of the retina and the eye, and the retina diseases requiring laser photocoagulation treatments. It shows methods and equipment used for diagnostics and treatment of the retina by laser photocoagulation.

In chapter 2 we study the anatomy of the eye, determine its optical parameters and design a corresponding optical system. We use matlab for beam propagation equations in different materials, the optical lenses parameters, to design beam expansion, collimation and combination, needed for our experiment. we design a DMD integrale in our experiment.

In chapter 3 we implement each part designed in chapter 2 in a Blender environnement, show the results for each element, and integrate them into our experiment. last we show the results of the multispot laser photocoagulation using the DMD, an optical system and a realistic eye.

CHAPTER I

Background on Retina Diseases and Laser PhotoCoagulation Devices

I. Chapter 1 : Background on Retina Diseases and Laser PhotoCoagulation Devices

I.1. INTRODUCTION :

Retinal laser applications, such as retinal photocoagulation, utilize precise laser systems to treat various retinal disorders, including diabetic retinopathy, retinal vein occlusions, and retinal tears. Designing the guidance and focusing system requires a precise understanding of the targeted surgical procedure and the tissues to be corrected, in addition to using appropriate and advanced technology to ensure the accuracy and effectiveness of the guidance and focusing process. The hardware for these applications is designed to deliver controlled laser energy to specific areas of the retina with high precision and safety. In this chapter we shall examine some of these systems, showing their relevance and efficiency, with an emphasis on the DMD since our design is based on it, in addition to some basic information about the eye and retina diseases like diabetic retinopathy.

I.2. Retinopathies :

I.2.1. Anatomy of the EYE :[2]

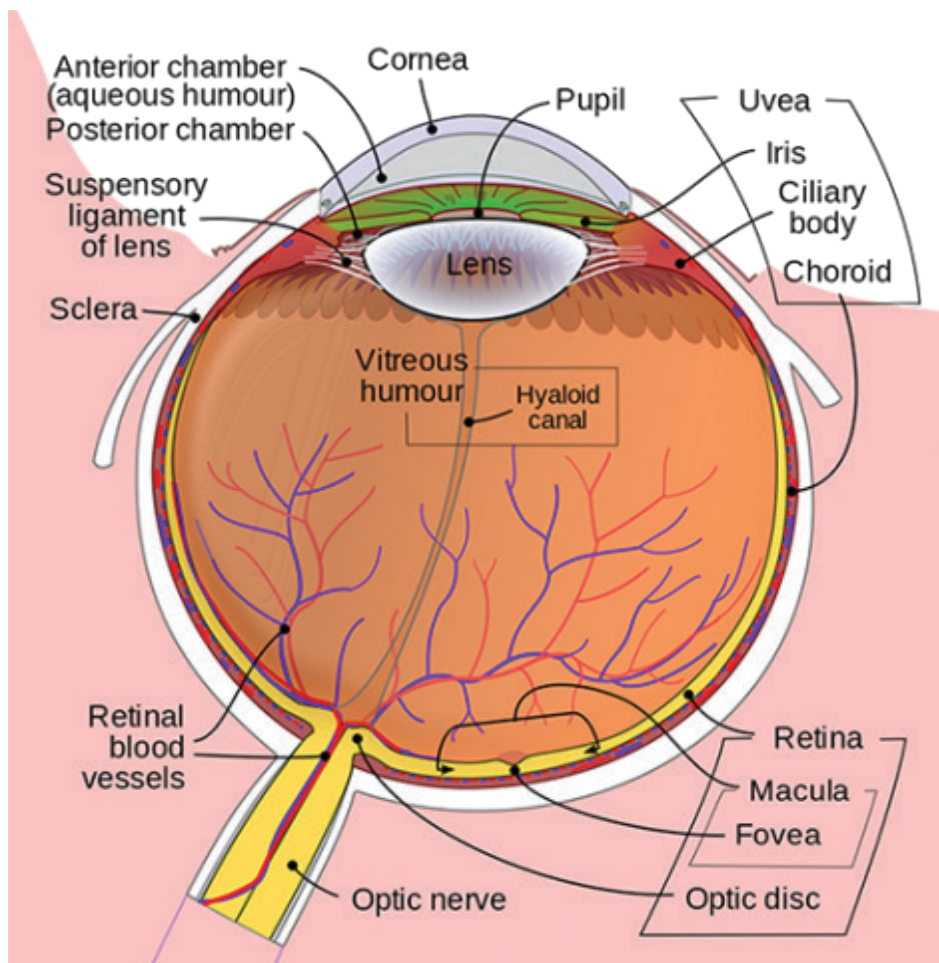


Figure I.1 : Anatomy of the eye

- **Choroid** : Layer containing blood vessels that lines the back of the eye and is located between the retina (the inner light-sensitive layer) and the sclera (the outer white eye wall).
- **Ciliary Body** : Structure containing muscle and is located behind the iris, which focuses the lens.
- **Cornea** : The clear front window of the eye which transmits and focuses (i.e., sharpness or clarity) light into the eye. Corrective laser surgery reshapes the cornea, changing the focus.
- **Fovea** : The center of the macula which provides the sharp vision.
- **Iris** : The colored part of the eye which helps regulate the amount of light entering the eye. When there is bright light, the iris closes the pupil to let in less light. And when there is low light, the iris opens up the pupil to let in more light.
- **Lens** : Focuses light rays onto the retina. The lens is transparent, and can be replaced if necessary. Our lens deteriorates as we age, resulting in the need for reading glasses. Intraocular lenses are used to replace lenses clouded by cataracts.
- **Macula** : The area in the retina that contains special light-sensitive cells. In the macula these light-sensitive cells allow us to see fine details clearly in the center of our visual field. The deterioration of the macula is a common condition as we get older (age related macular degeneration or ARMD).
- **Optic Nerve** : A bundle of more than a million nerve fibers carrying visual messages from the retina to the brain. (In order to see, we must have light and our eyes must be connected to the brain.) Your brain actually controls what you see, since it combines images. The retina sees images upside down but the brain turns images right side up. This reversal of the images that we see is much like a mirror in a camera. Glaucoma is one of the most common eye conditions related to optic nerve damage.
- **Pupil** : The dark center opening in the middle of the iris. The pupil changes size to adjust for the amount of light available (smaller for bright light and larger for low light). This opening and closing of light into the eye is much like the aperture in most 35 mm cameras which lets in more or less light depending upon the conditions.
- **Retina** : The nerve layer lining the back of the eye. The retina senses light and creates electrical impulses that are sent through the optic nerve to the brain.
- **Sclera** : The white outer coat of the eye, surrounding the iris.
- **Vitreous Humor** : The, clear, gelatinous substance filling the central cavity of the eye.

I.2.2. Retina pathologies

The retina is a multilayered, light sensitive neural tissue lining the inner eye ball. Light is focused onto the retina and then transmitted to the brain through the optic nerve.

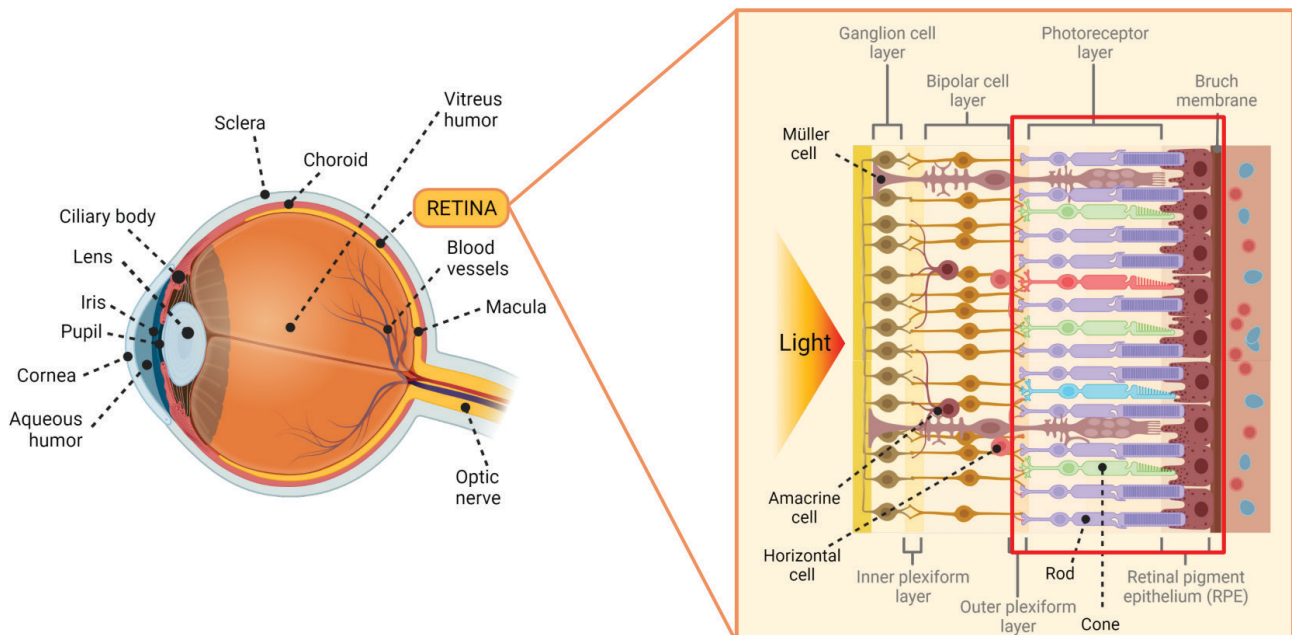


Figure I.2 : Retina Elements of Visual Perception

There are different varieties of retinal problems, conditions and diseases. This is a short list of common retinal problems.

- Retinal detachment.
- Age-related macular degeneration (AMD).
- Epiretinal membranes and macular holes.
- retinopathies, including diabetic retinopathy.

Our greatest concern in this work goes to diabetic retinopathy. Eye damage linked to unbalanced diabetes remains among the leading causes of blindness in industrialized countries. Diabetic retinopathy is a consequence of chronic hyperglycemia. In the event of excess sugar in the blood, such as during diabetes, the wall of the capillaries is weakened and loses its tightness. This then results in a bursting of the retinal vessels. This is called a “micro-aneurysm”.

There are two main types of retinopathy: non-proliferative retinopathy characterized by some micro-hemorrhages and proliferative retinopathy with the appearance of new vessels. Proliferative retinopathy is characterized by more significant hemorrhages.

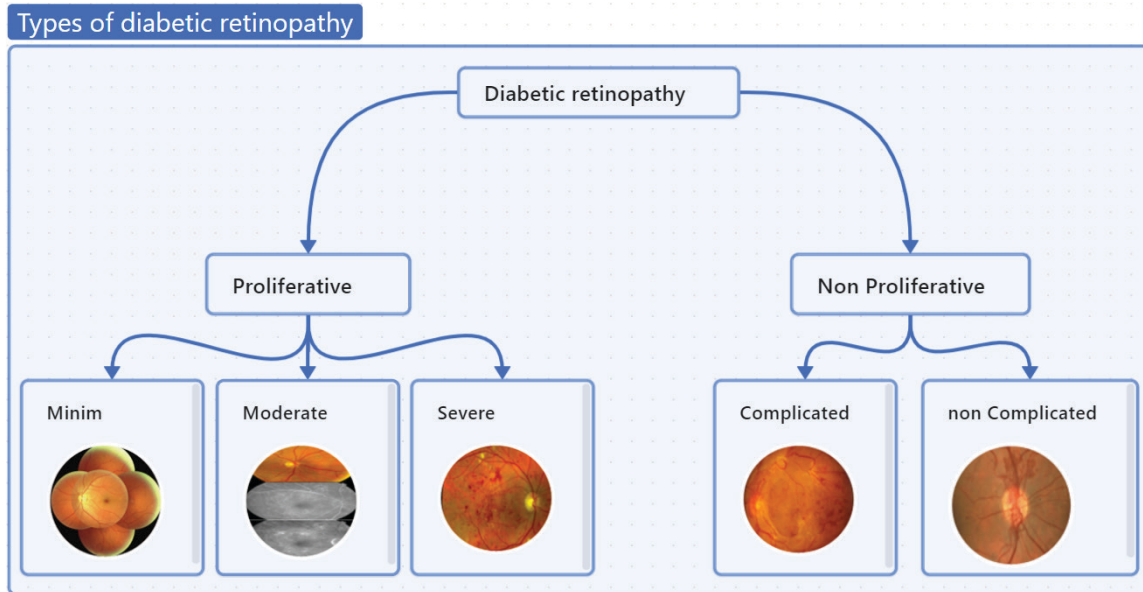


Figure I.3 : Types of diabetic retinopathy

I.2.3. Laser treatment of retinal diseases

Laser photocoagulation of the retina is indicated in all cases of proliferative diabetic retinopathy, and, in a preventive manner, in other types of diabetic retinopathy.

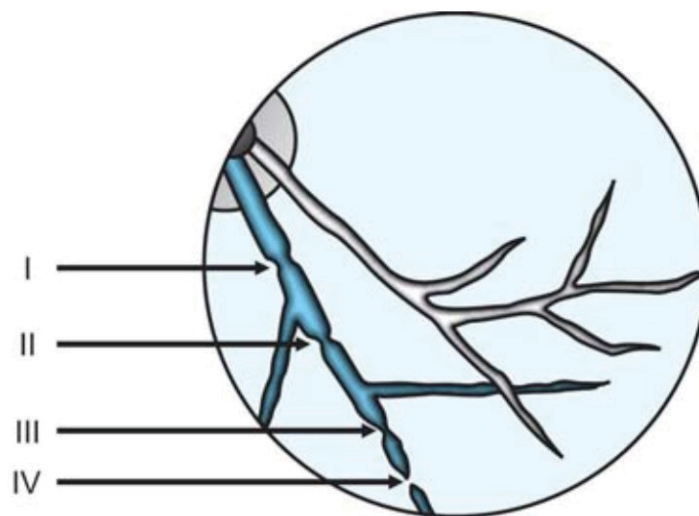


Figure I.4 : Schematic drawing of various vascular coagulations

I = Minimal visible constriction of the vessel

II = Total constriction and spasm of the vessel

III = Total constriction of the vessel along with coagulations of the surrounding tissue and

IV = Total constriction, charring of the vessel, coagulations of the surrounding tissue

I.3. DIAGNOSTIC :

Diagnostic tools play a crucial role in the effective use of retinal laser hardware. These tools aid in the assessment, planning, and monitoring of retinal treatments, ensuring precision and safety. Here are the primary diagnostic tools and techniques used in conjunction with retinal laser hardware:

I.3.1. Diagnostic Tools and Techniques

I.3.1.1. Digital Fundus Photography:

This test uses specialized equipment to take a panoramic view of the inside of your eye in order to capture a detailed image of the retina, optic nerve, retinal blood vessels, and outer edges of the retina.[3]

Integration: Often used before and after laser treatments to assess the effectiveness of the intervention.

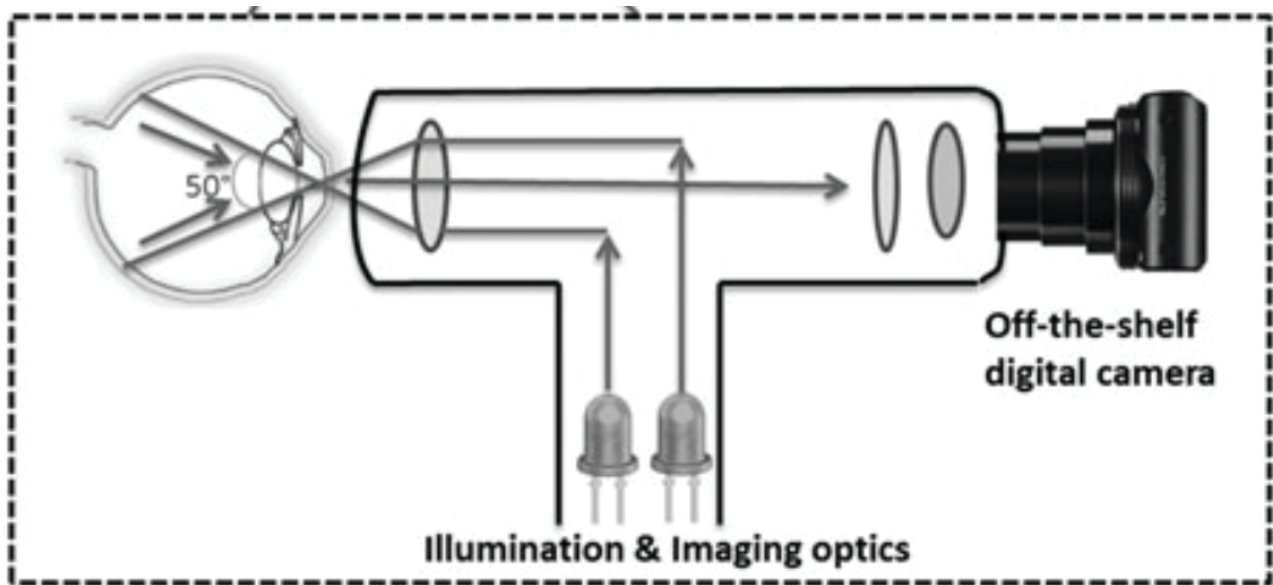


Figure I.5 : hand-held fundus camera

I.3.1.2. Wide Angle Fluorescein Angiography

Whereas a fundus photograph is a snapshot of retinal vessels taken at one point in time, angiography is a moving image technique that visualizes blood flow through the retinal vessels over a short period of time.[4]

As the only test that allows us to monitor retinal blood flow in real-time, Fluorescein Angiography (FA) provides valuable diagnostic information needed to treat certain retinal conditions, like diabetic retinopathy and wet macular degeneration, among others.

The wide-angle capacity allows us to visualize 200 degrees of the retinal surface so that we can get a good look at the entire retina.

FA involves administering sodium fluorescein dye into your bloodstream through a vein on your arm or hand. This dye is not iodine-based and is very well tolerated by most patients.

When the dye makes its way to the blood vessels of the retina, it gives off a fluorescent color when specially filtered light is focused on the retina. A real-time video of the blood flowing through the eye is then taken.

Integration: Used to map out areas needing laser treatment, particularly in conditions like diabetic retinopathy and retinal vein occlusions.

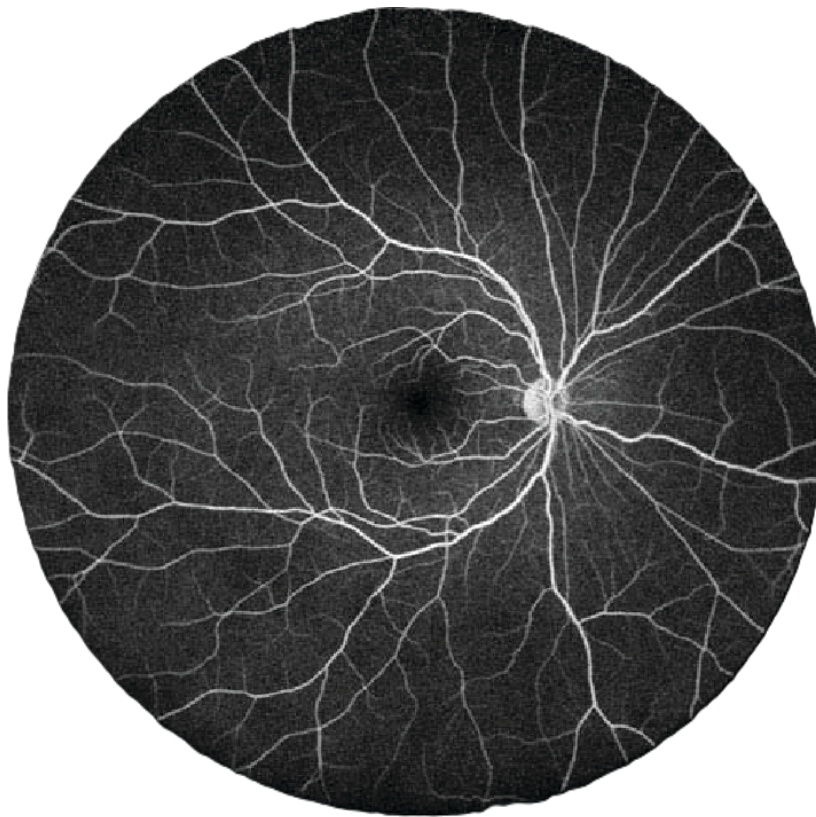


Figure I.6 : wide field fundus fluorescein angiography

I.3.1.3. Optical Coherence Tomography (OCT)

Optical coherence tomography (OCT) is one of the most common tests performed by a retinal specialist. OCT works essentially like an ultrasound, but instead of using sound waves, OCT uses light waves to obtain images of the retinal layers with higher resolution and magnification.[5]

also OCT functions by using light waves to produce 3D color coded cross-section images of the eye. It's safe, non-invasive and allows our doctors to see the eye's many components without harming tissue.[6]

OCT scans the central retina (known as the macula) and provides a magnified cross-section view of the full thickness of the macula, much like looking at the slice of cake and all its layers from the side.

Integration: Critical for planning laser treatments by identifying precise target areas and monitoring changes post-treatment.

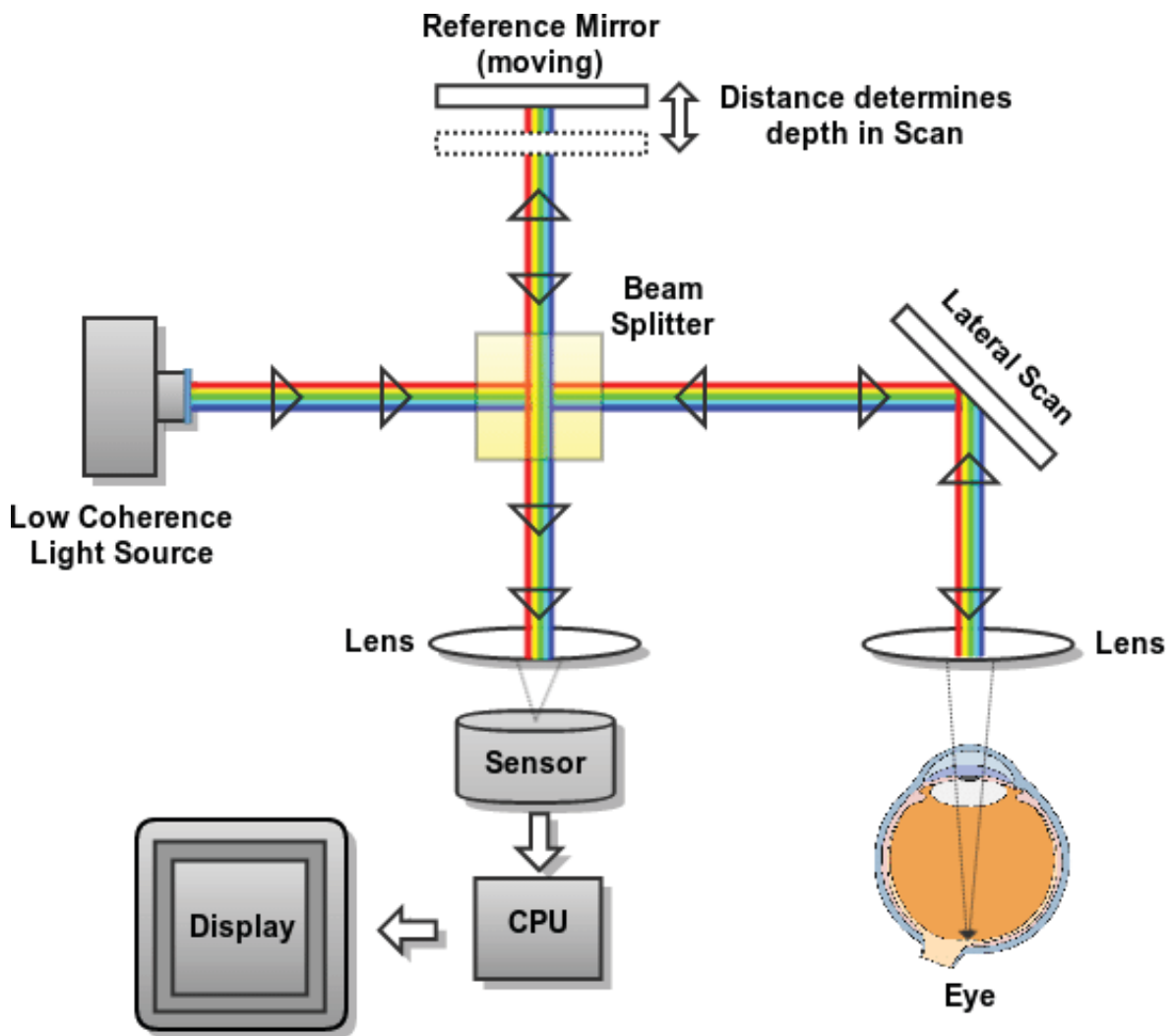


Figure I.7 : Schema of a basic OCT acquisition system

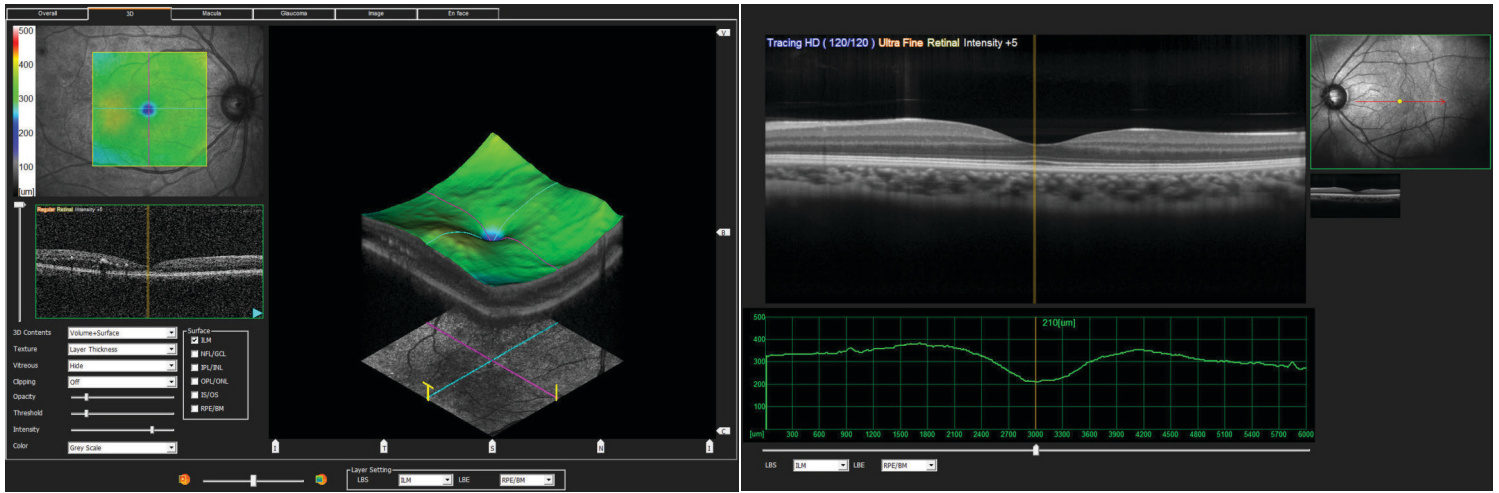


Figure I.8 : OCT 3D color coded cross-section images of the eye

Image Acquisition

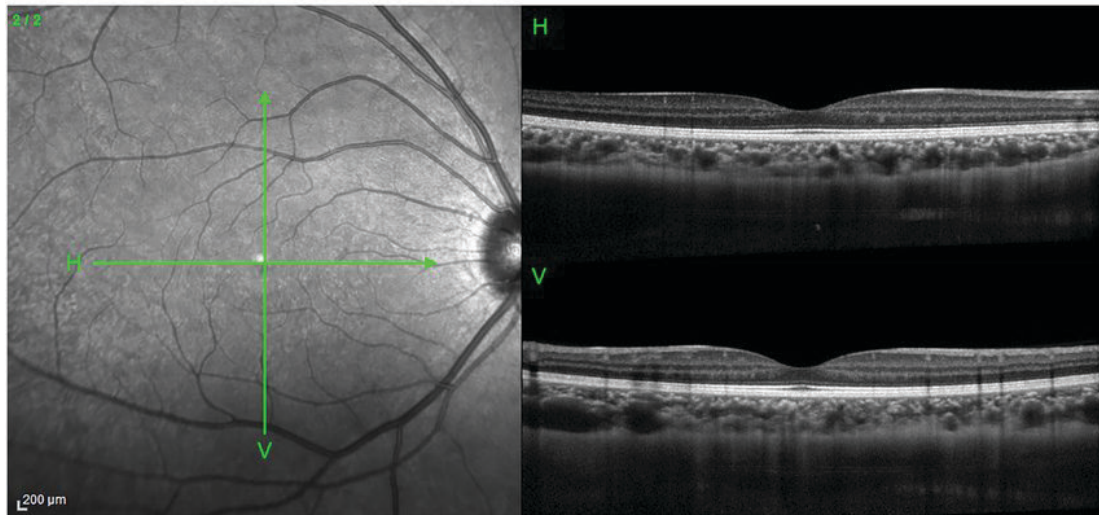


Image Analysis

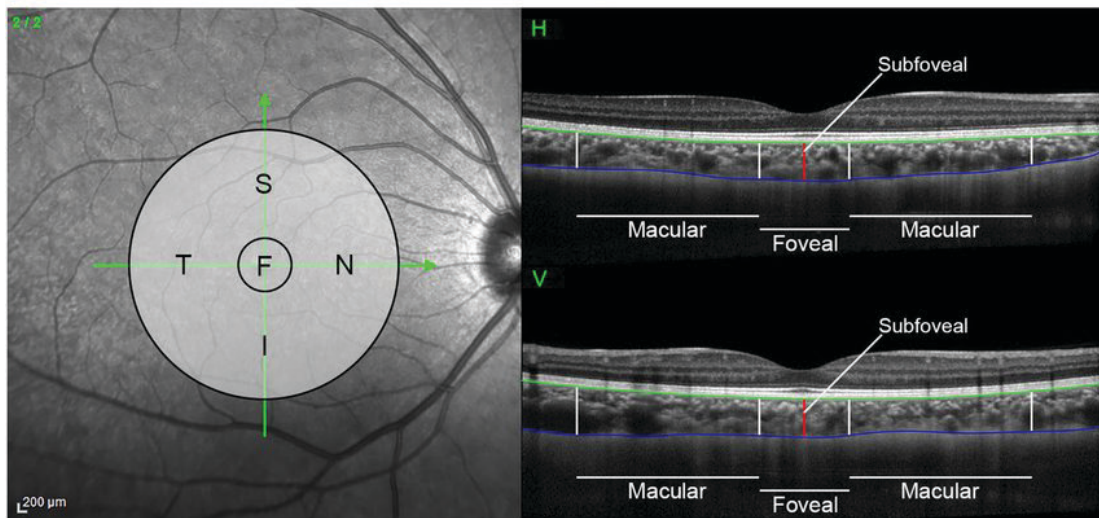


Figure I.9 : Illustration of the OCT scanning protocol and image analyses

I.3.2. Pre-Treatment Assessment:

- **Personalization:** Diagnostics enable personalized treatment plans based on the specific retinal pathology and its location, improving treatment outcomes.
- **Planning:** Diagnostic images are used to plan the laser treatment, determining the exact locations, patterns, and parameters for the laser application, reducing the risk of damage to healthy retinal tissue.

I.4. Treatment :

I.4.1. LASER :

Definition : LASER (an abbreviation for Light Amplification by Stimulated Emission of Radiation) is the equipment capable of emitting a powerful, highly monochromatic and coherent beam of electromagnetic radiation. Monochromatic electromagnetic radiation is meant for single frequency or single wavelength and eliminates chromatic aberration. Coherent beam means all photons produced are in phase with each other with limited divergence.[7]

Properties : Monochromatic, Coherent, Collimated

- Lasers have properties to produce highly monochromatic coherent beam that is **Collimated** and has limited divergence.
- **Monochromatic** electromagnetic wave means that it has single wavelength eliminating chromatic aberration.
- **Coherence** of lasers is classified as either **spatial or temporal**. **Spatial coherence** allows precise focusing of the laser beam to widths as small as a few microns, while **Temporal coherence** allows selection of specific monochromatic wavelengths within a single laser or a group of lasers.

Practically, **spatial coherence**, allow extremely small burns to pathologic tissue, with minimal disturbance to surrounding normal tissue; on the other hand, **temporal coherence** allows treatment of specific tissue sites by selecting laser wavelengths that are preferentially absorbed by these tissue sites.[8]

I.4.2. Laser Tissue Interactions :

Laser interaction with various tissues of the eye may be classified into following categories :[9]

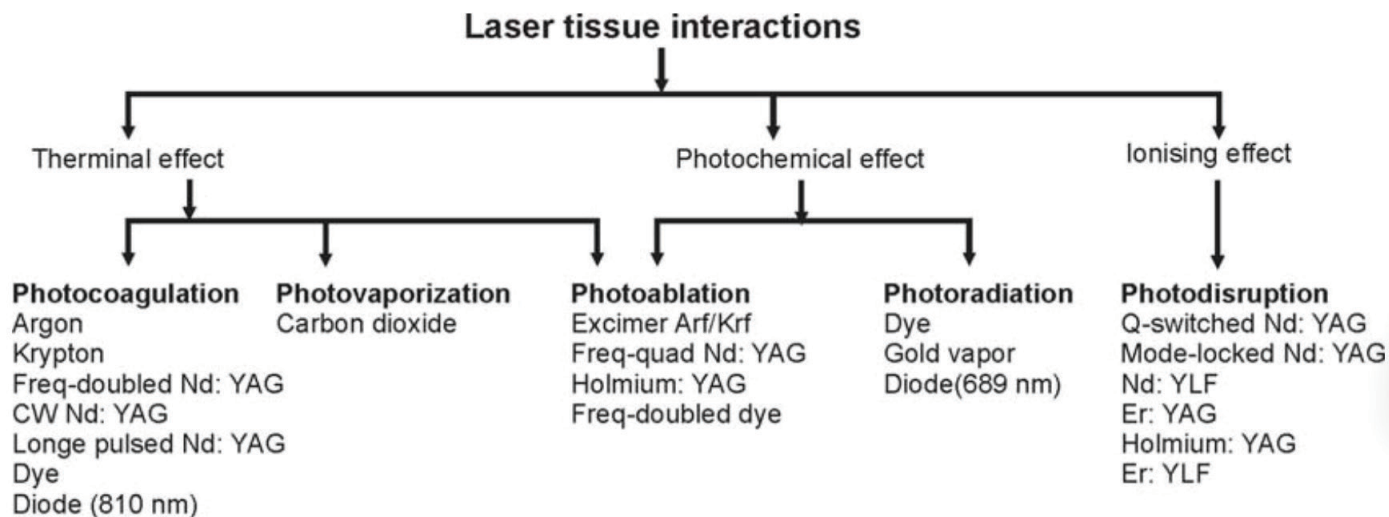


Figure I.10 : various laser tissues interactions and the type of laser involved

Photothermal (photocoagulation and photovaporization) :

- **Photocoagulation**, absorption of light by the target tissue results in a temperature rise, which causes denaturation of proteins. Typically, argon, krypton, diode (810nm) and Frequency doubled ND:YAG lasers cause this type of effect.
- **Photovaporization** occurs when higher energy laser light is absorbed by the target tissue, resulting in vaporization of both intracellular and extracellular water. The advantage of this type of tissue response is that adjacent blood vessels are also treated, resulting in a bloodless surgical field. The carbon dioxide laser, with its wavelength in the far infrared (10,600 nm), uses this method of action.

Photochemical (photoablation and photoradiation)

- **Photoradiation**, intravenous administration of photosensitizing agent, which is taken up by the target tissue, causes sensitization of the target tissue. Exposure of this sensitized tissue to red laser light (690 nm) induces the formation of cytotoxic free radicals.
- **Photoablation** occurs when high-energy laser wavelengths in the far ultraviolet (< 350 nm) region of the spectrum and are used to break long-chain tissue polymers into smaller volatile fragments. The exposure times in the photoablation process is usually much shorter (nanoseconds) compared to photoradiation. Photodynamic therapy (PDT) is an example of photoradiation therapy while Excimer laser is a photoablative process.

Photoionizing (photodisruption)

- **Photoionization** high-energy light (1064 nm) is deposited over a short interval to target tissue, stripping electrons from the molecules of that tissue which then rapidly expands, causing an acoustic shock wave that disrupts the treated tissue. The ND:YAG laser works via a photodisruptive mechanism.

I.4.3. Laser Tissue interactions with DMD :

The suitability of laser tissue interactions with Digital Micromirror Devices (DMDs) varies significantly :

- **Photocoagulation** is highly compatible with DMDs, as these devices excel at creating precise patterns for controlled thermal effects using visible and near-infrared wavelengths.
- **Photoradiation** is moderately suitable, particularly for some photodynamic therapies, though limited by the power handling capabilities of DMDs.

Several laser tissue interactions face challenges with DMD implementation.

- **Photovaporization** is limited due to the high power requirements and potential thermal management issues in DMDs.
- **Photoablation's** applicability is restricted because DMDs struggle with the UV wavelengths often used and have power limitations that may affect treatment efficacy.
- **Photodisruption** is the least suitable, as the ultrashort pulses and extremely high peak powers required exceed DMD capabilities, and the temporal resolution of DMDs is insufficient for this interaction.

These limitations stem from the fundamental design and operating principles of DMDs[X], which are optimized for specific wavelength ranges, power levels, and switching speeds that don't align with the demands of these more intense or specialized laser-tissue interactions.

I.4.4. Laser Types in Retina :[10]

Argon blue-green Laser (70% blue (488 nm) and 30% green(514nm)) :

- Absorbed selectively at retinal pigment epithelial layer (RPE), hemoglobin pigments, choriocapillaries, inner and outer nuclear layer of the retina.
- It coagulates tissues between the choriocapillaris and inner nuclear layer.
- The main adverse effects of these lasers are high intraocular scattering, macular damage in photocoagulation near the fovea, and choroidal neovascularization (if Bruch's membrane is ruptured).

Frequency-doubled Nd-YAG Laser (532 nm) :

- Highly absorbed by hemoglobin, melanin in retinal pigment epithelium and trabecular meshwork. It can be used either continuously or in pulsed mode.
- PASCAL (Pattern Scan Laser) is one such type of laser that incorporates semi-Automated multiple pattern, short pulse, multiple shots with precise burn in very short duration using frequency-doubled Nd-YAG Laser (532 nm). It is commonly used nowadays in treatment of many retinal conditions (proliferative diabetic retinopathy, diabetic macular edema, vein occlusions etc.). It has many advantages when compared with conventional single spot laser, as it is produced at a very short duration (10-20 msec) compared to (100-200 msec) of conventional single spot one which leads to less collateral retinal damage. Other advantages include relatively stable scar size, less destructive same efficiency.
- It also permits the application of different patterns that gives more regular spots on retina with less duration.

Krypton Red (647 nm) :

- Well absorbed by melanin and can pass through hemoglobin which makes it suitable for treatment of subretinal neovascular membrane.
- It also has low intraocular scattering with good penetration through media opacity or edematous retina and has ability to coagulate the choriocapillaries and the choroid.

Diode Laser (805-810 nm) :

- It is well absorbed by melanin.
- The near to infrared spectrum (near invisible) makes it more comfortable to use due to absence of flashes of light.
- It has very deep penetration through the retina and choroid making it the laser of choice in treatment of Retinopathy of Prematurity (ROP) and some types of retina lesions.

- It is also used via trans-scleral route to treat the ciliary body in some cases of refractory glaucoma.

I.4.5. Laser-Tissue Absorption in the Retina :[11]

Melanin :

- Found mainly in the RPE (Retinal pigment epithelium) and choroid, and absorbs mainly wavelength between 400-700 nm.
- The longer the wavelength of light, the more the melanin is penetrated. For example, Diode laser with wavelength of 810 nm can penetrate deeply into the choroid.

Macular xanthophyll :

- Located in the inner and outer plexiform retinal layers.
- It protects the photoreceptors from short-wavelength light damage, but can be damaged by blue light which is why Argon green is preferred in macular photocoagulation over Argon blue.

Hemoglobin :

- Absorption varies according to oxygen saturation.
- It absorbs yellow, green, and blue wavelengths, but red light is absorbed poorly. Thus, macular lasers may, uncommonly, damage retinal vessels.

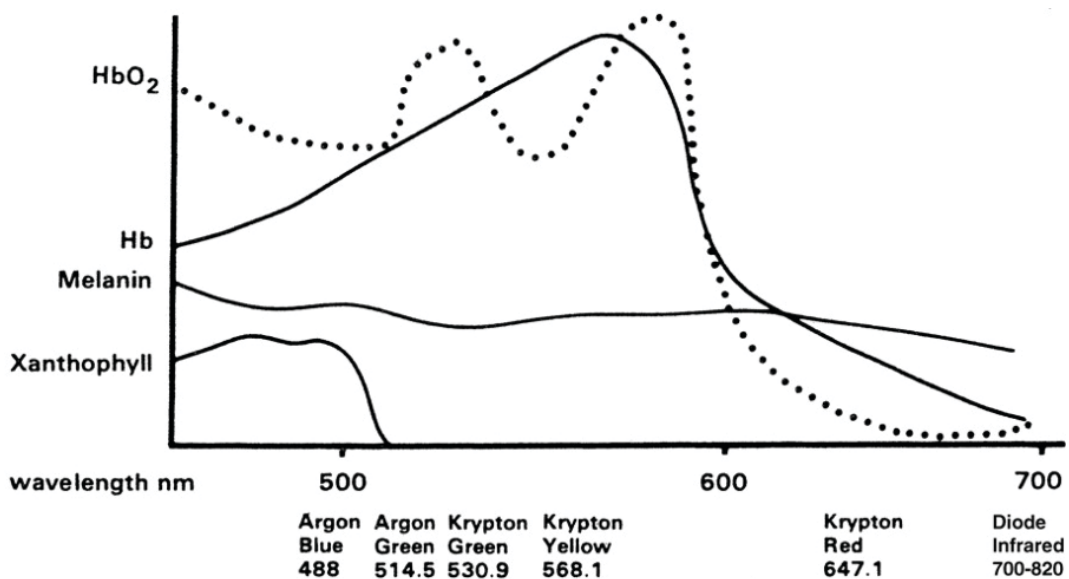
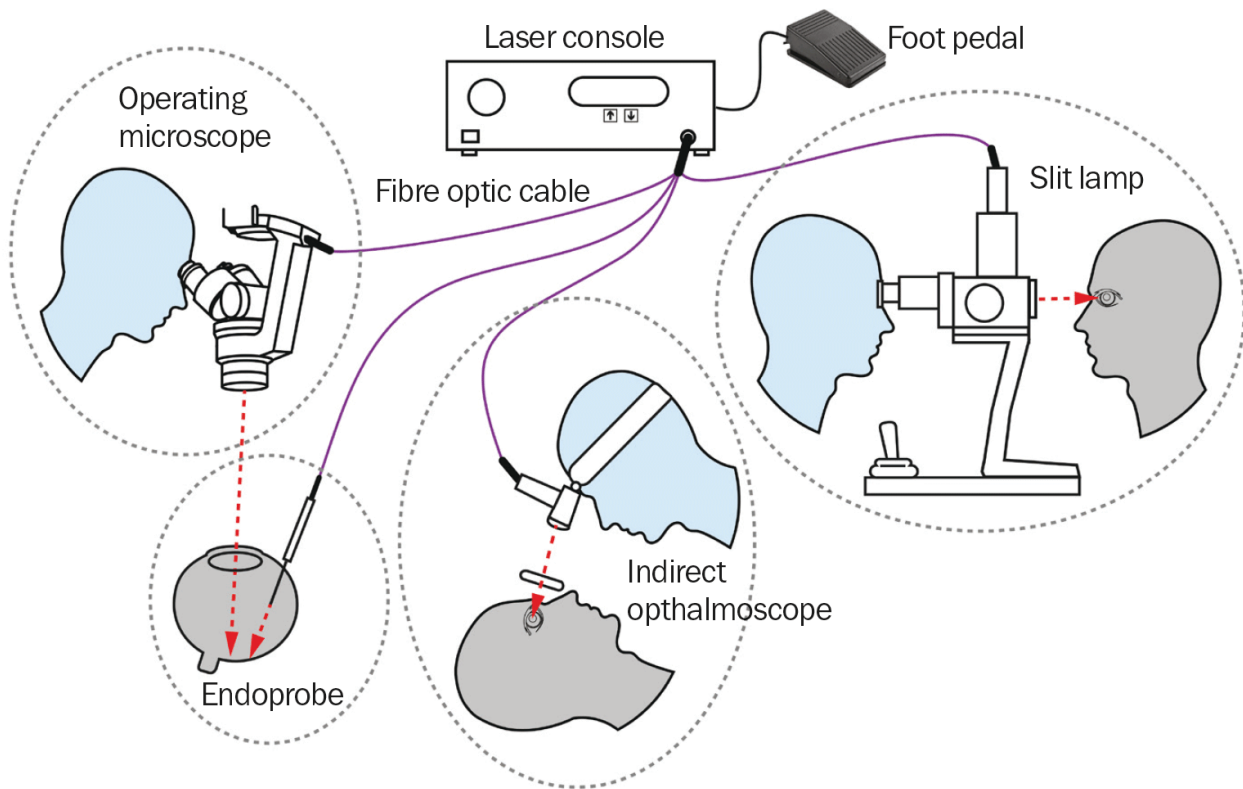


Figure I.11 : Laser-Tissue Absorption

I.5. Retinal Photocoagulation Hardware and Devices :



Ismael Cordero

Figure I.12 : Components of a Laser System for retinal photocoagulation

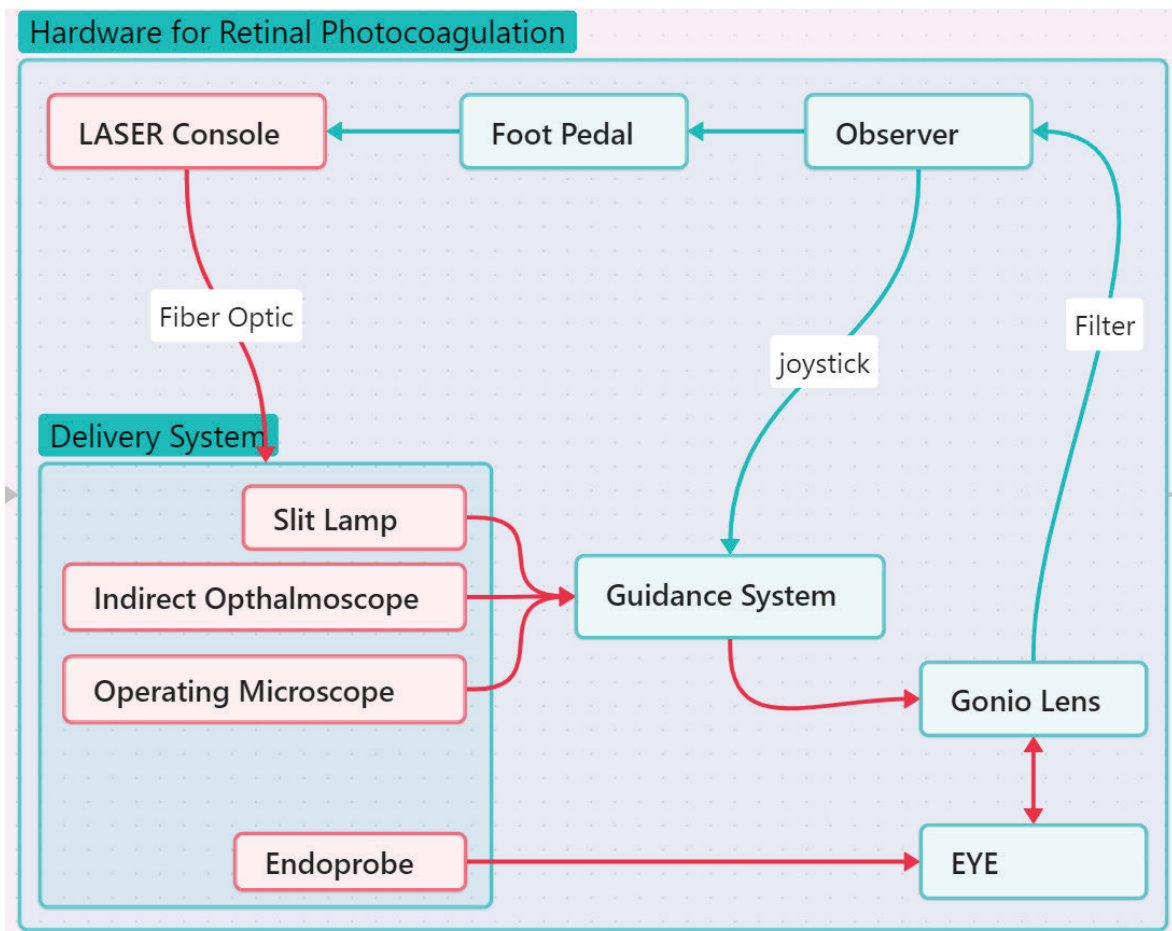


Figure I.13 : bloc diagram of a laser system for retinal photocoagulation

The main components of a laser system are the laser console, the foot pedal, and the laser delivery system.

- Different delivery systems, connected to the console by a fibre optic cable, can be used to transmit the laser energy to the patient's eye (**Figure**): an endoprobe (a small fibre optic probe that is inserted into the eye), a slit lamp, an operating microscope, or an indirect ophthalmoscope[12]
- These systems are designed to provide high precision, better control, and flexibility in use for various applications in ophthalmology. They were designed with consideration for factors such as ease of use, safety, and accuracy in guidance and focusing.[13]

I.5.1. Laser Console :

Five parameters should be considered each time a laser or light-based device is used: wavelength, power, spot size, pulse width, and cooling.[14]

If a laser device allowed control of each of these parameters independent of the other, you would be able to adjust the treatment more precisely to match your patient. Devices that allow the practitioner the freedom to individualize these 5 settings create the ideal environment for maximum efficiency at minimal risk.

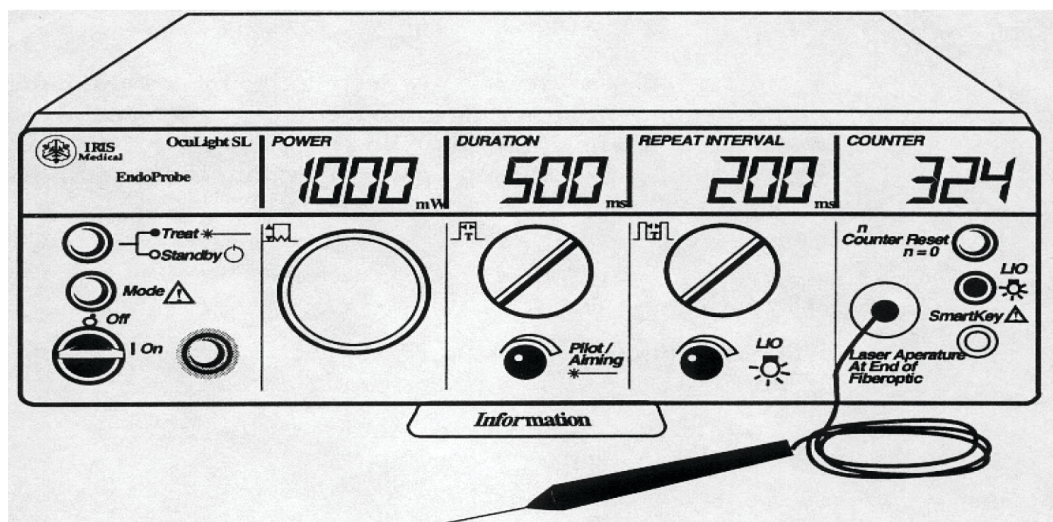


Figure I.14 : Laser Console

I.5.2. Delivery Systems :

I.5.2.1. Slit Lamp :

A slit lamp is a special microscope with a bright light attached to it that your eye care specialist will use to look at the different parts of your eyes. They'll adjust the light to see into and through the layers of your eyes. They'll check the overall health of your eyes and diagnose any issues or symptoms you're having.[15]

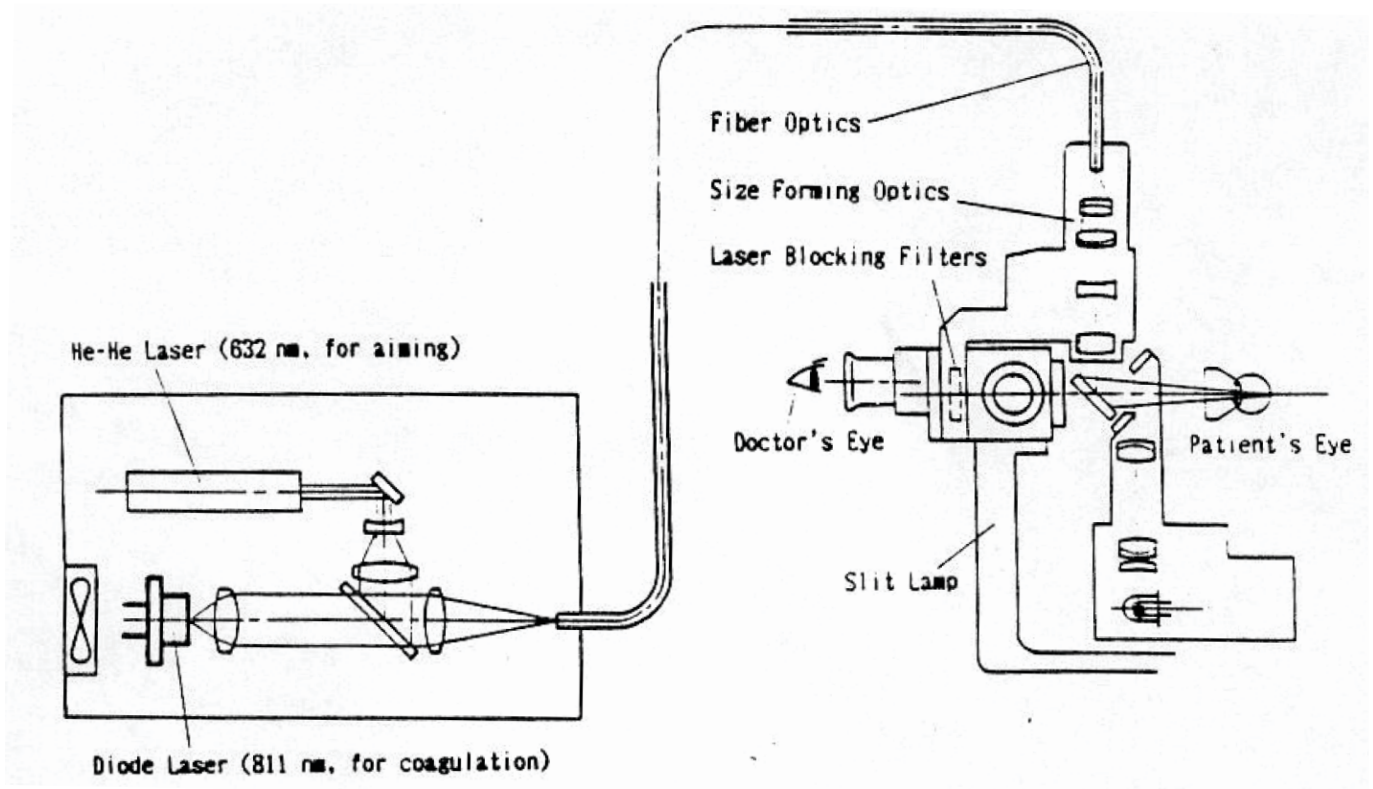


Figure I.15 : Schema Optic of Diode Laser with Slit Lamp

I.5.2.2. Operating Microscope :

An operating or surgical microscope is an optical instrument that provides the surgeon with a stereoscopic, high quality magnified and illuminated image of the small structures in the surgical area.[16]

Design features of an operating microscope are: magnification typically in the range from 4x-40x, There is often a prism that allows splitting of the light beam in order that assistants may also visualize the procedure.[17]

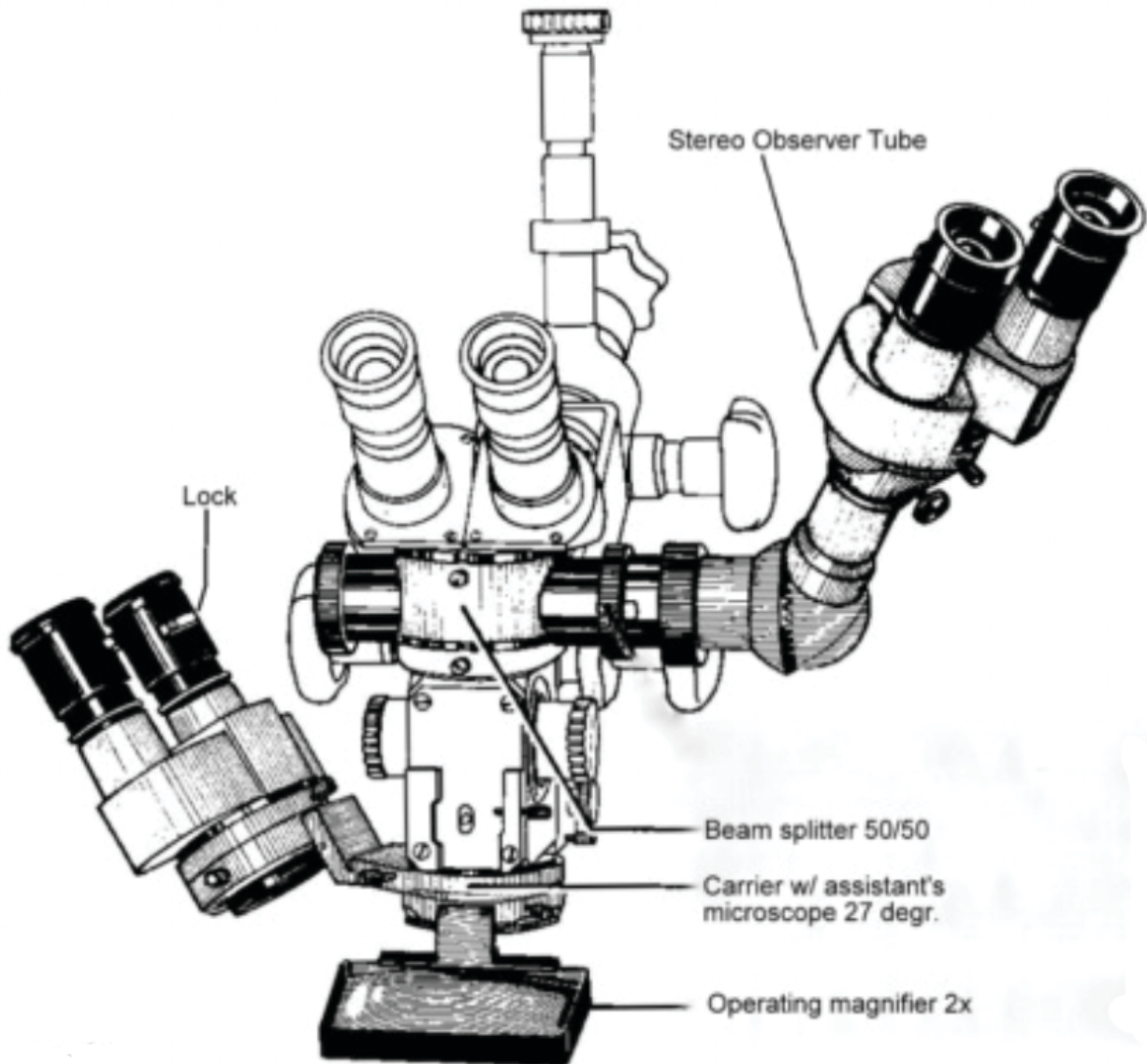


Figure I.16 : Assistant Operating Microscope

Diagram of biomicroscopic delivery system for anterior segment (and selected paramacular) photocoagulation with argon laser radiation. The beam passes through a triggered shutter and relay system to the beam

splitter cube. The dichroic diagonal face of the cube reflects the argon beam through the magnification selector to the

patient's eye. Simultaneous examination and photography are performed through protective anti-argon filters. [18]

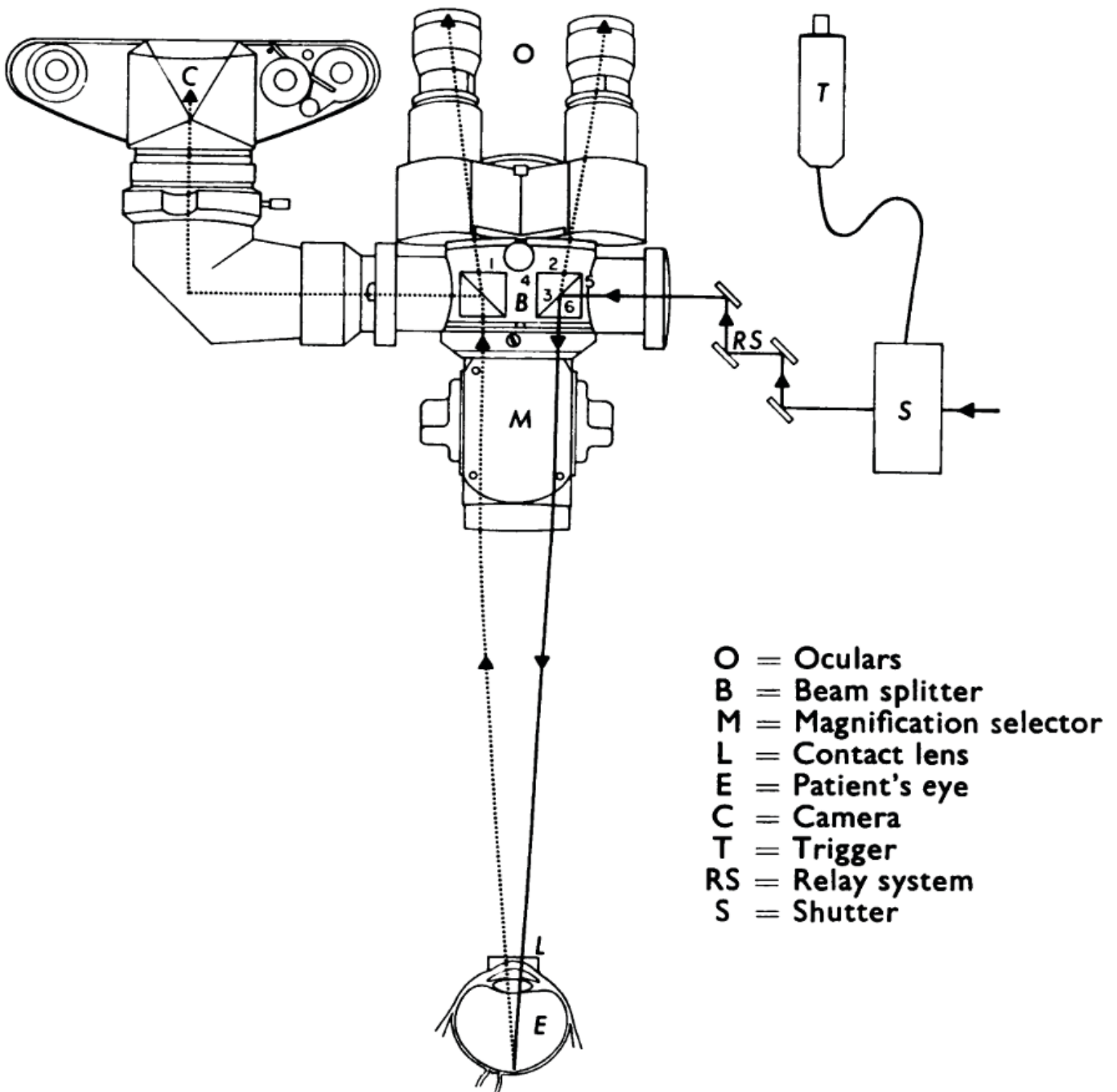


Figure I.17 : Diagram of biomicroscopic delivery system

I.5.2.3. Indirect Ophthalmoscope :

Binocular indirect ophthalmoscope (BIO) provides a wider view of fundus with stereopsis contrary to the direct one. The illumination unit of BIO utilized high flux LED as a light source, LED condensing lens cap for beam focusing, color filters and small lithium ion battery. In optics unit of BIO, beam splitter used to distribute an examinee's fundus image both to examiner's eye and to CMOS camera module attached to device.[19]

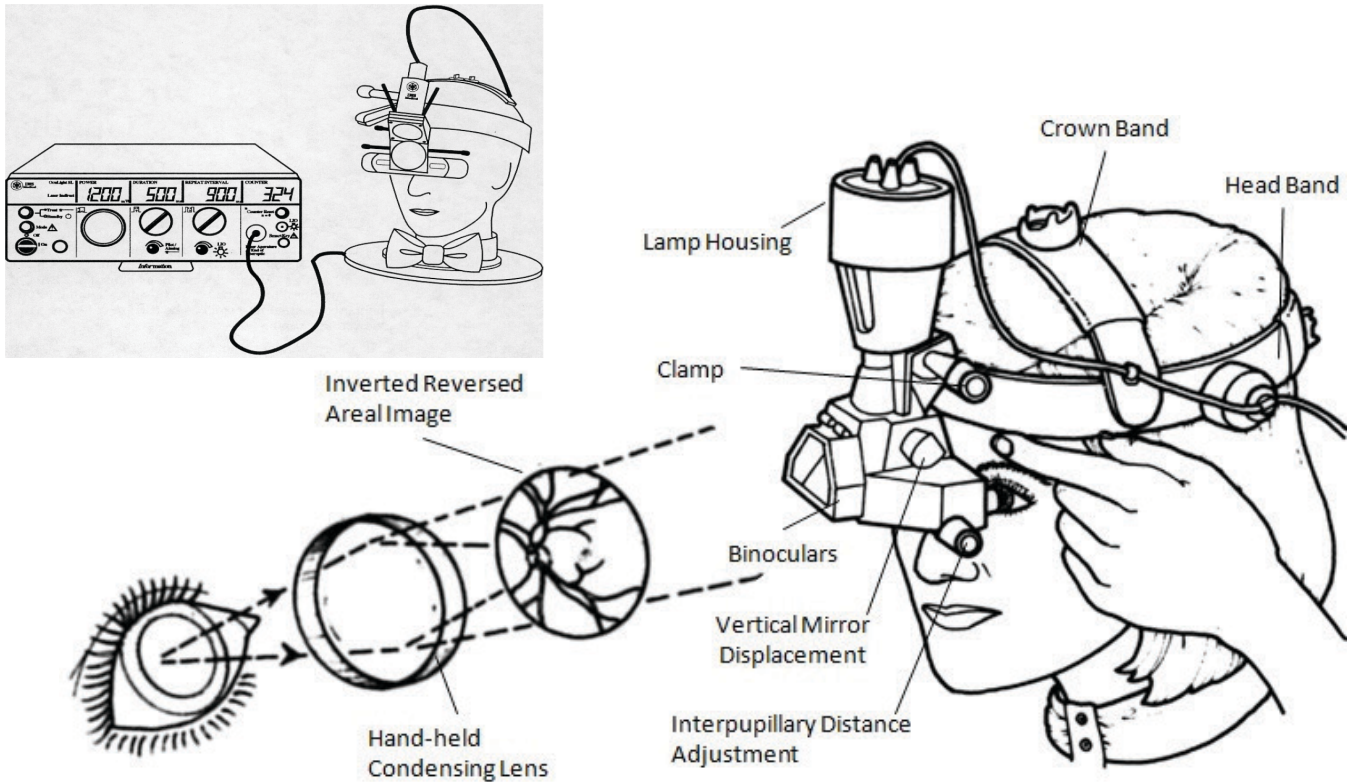


Figure I.18 : Binocular indirect ophthalmoscopy and Laser Integration

I.5.2.4. Endoprobe :

Endoprobe instrumentation targets the retina to deliver precise energy exactly where you need it. With a wide array of models, there is an Endoprobe for every vitreoretinal laser case.[20]

- Dual function - white-light illumination with laser delivery in one convenient design.
- Offers bimanual operation - one hand manages illumination and laser delivery, freeing the other hand to operate additional instruments.

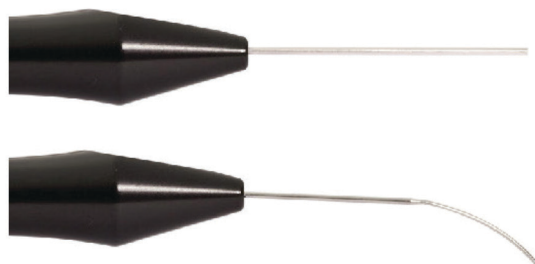


Figure I.19 : Endoprobe

I.5.3. Gonio Lens :

Selection of lens depend on many factors include, desired field of view, amount of magnification, area to be treated, and ophthalmologist preference. The commonly used contact lenses for panretinal and focal/grid retinal photocoagulation are listed in table 1 and 2.

It is important to remember that most of the commonly used lenses magnify the image size thus, the laser spot size on the machine must be set accordingly.[21]

Lens	Image Magnification	Laser Spot Magnification	Field of View
Goldmann 3-mirror	0.93x	1.08x	140°
Mainster Widefield	0.68x	1.5x	118-127°
Mainster PRP 165	0.51x	1.96x	165-180°
Volk Quadraspheric	0.51x	1.97x	120-144°
Volk Super Quad 160	0.50x	2.00x	160-165°

Figure I.20 : Table 1 Contact Lenses used for PRP

Lens	Image Magnification	Laser Spot Magnification	Field of View
Goldmann 3-mirror	0.93x	1.08x	140°
Mainster standard	0.96x	1.05x	90-121°
Mainster high magnification	1.25x	0.8x	75-88°
Ocular PDT 1.6X	0.63x	1.6x	120-133°
Volk area centralis	1.06x	0.94x	70-84°

Figure I.21 : Table 2 Contact Lenses used for Focal/Grid Lasers

I.5.4. Safety Filters :

- Safety filters (**Figure**) protect the physician from back-scattered laser light. Integral eye safety filters should be permanently installed in every slit lamp and laser indirect ophthalmoscope.[22]
- For endophotocoagulation or for operating microscope use, a separate discrete eye safety filter assembly must be installed into each viewing path of the operating microscope. All eye safety filters have an optical density (OD) at the laser wavelength sufficient to permit long-term viewing of diffuse laser light.

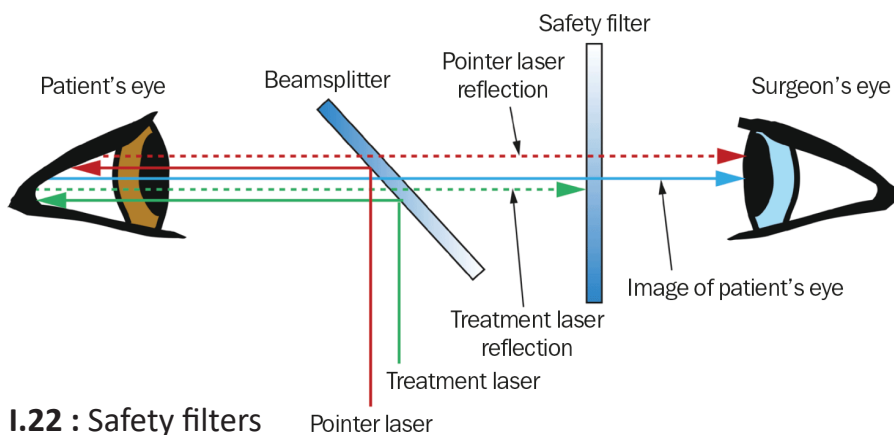


Figure I.22 : Safety filters

Ismael Corderic

I.6. Guidance and Focusing System :

The guidance and focusing system in the PhotoCoagulation system is considered an essential element to ensure the precise directing of the laser beam towards the targeted area inside the eye or the body, while maintaining the appropriate energy concentration for coagulation.

The guidance and focusing system in PhotoCoagulation can be achieved using several methods and techniques, including singleSpot and multiSpot techniques.

the choice depends on the surgical requirements and available technologies to achieve optimal performance.

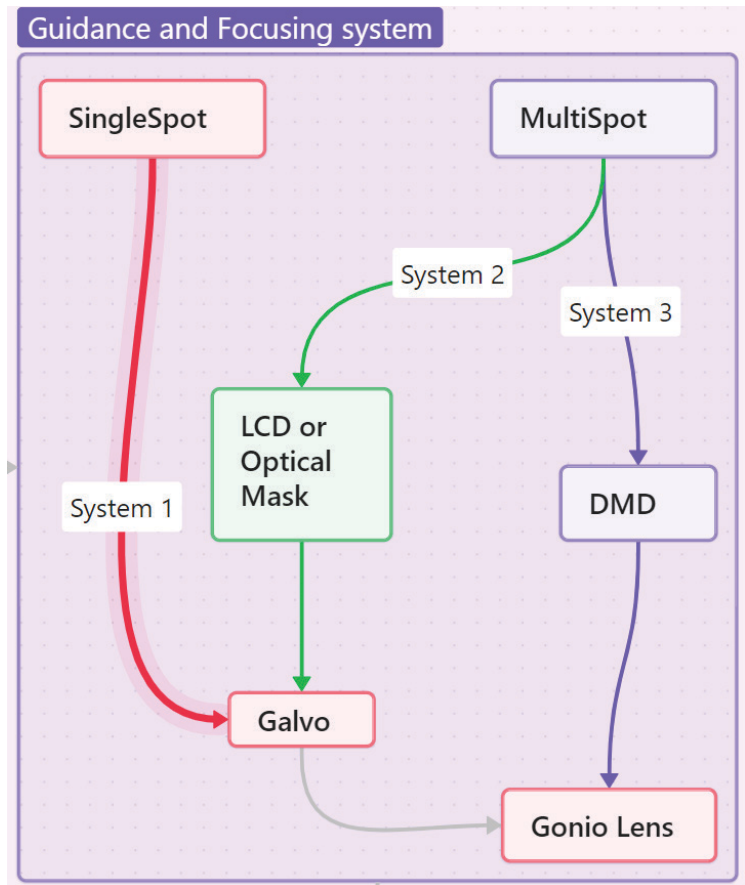


Figure I.23 : Guidance and Focusing System

I.6.1. SingleSpot :

I.6.1.1. System 1 (only Galvo):

The term "Galvo" is derived from "galvanometer," which is an instrument used to measure and detect small electric currents. In the context of laser systems, Galvo scanners are used to reflect and manipulate the laser beam. These scanners consist of two mirrors mounted on galvanometer motors, which can quickly adjust the angle of the mirrors to control the laser beam's position.[23]

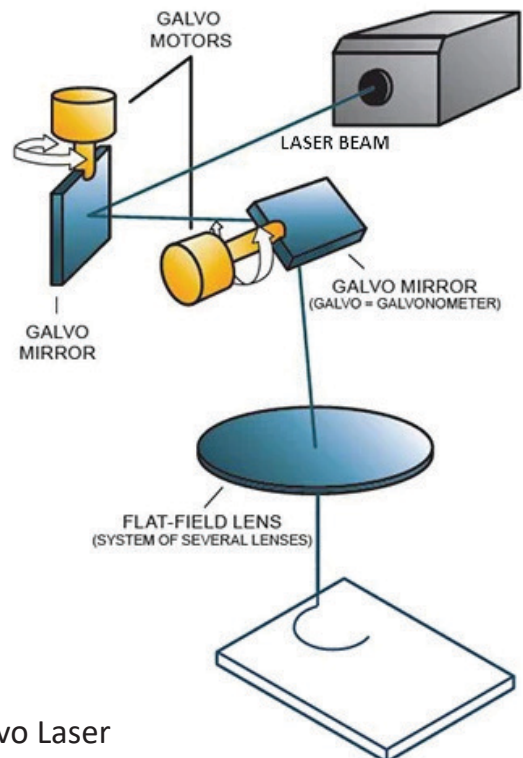


Figure I.24 : Galvo Laser

I.6.2. MultiSpot :

I.6.2.1. System 2 (LCD with Galvo) :

- **Function:** The LCD acts as an optical mask or switch. It selectively allows or blocks parts of the expanded laser beam based on the pattern sent to it.
- **Advantages:** Using an LCD as an optical mask allows for flexible, customizable patterns that can be changed quickly through software,
- LCD allowing for the creation of arbitrary laser spot patterns for retinal photocoagulation.[24]

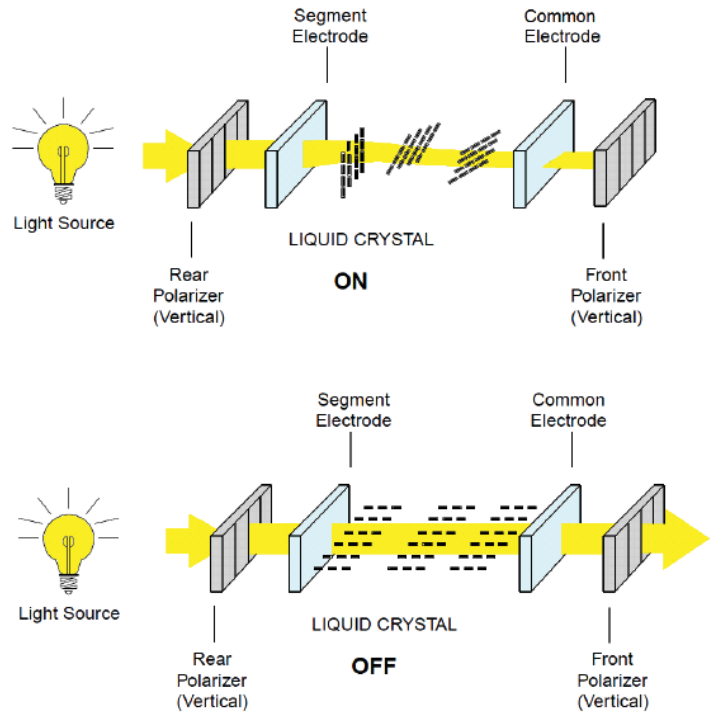


Figure I.25 : Transmissive LCD Display Working

I.6.2.2. System 3 (DMD):

Digital Micromirror Device (DMD) technology uses an array of tiny mirrors that can be individually controlled to reflect or direct light.

The micromirrors are individually controlled by a black and white, or a gray scale level image.

The laser beam reflected by the micromirrors takes the shape of the image displayed on the mirrors.

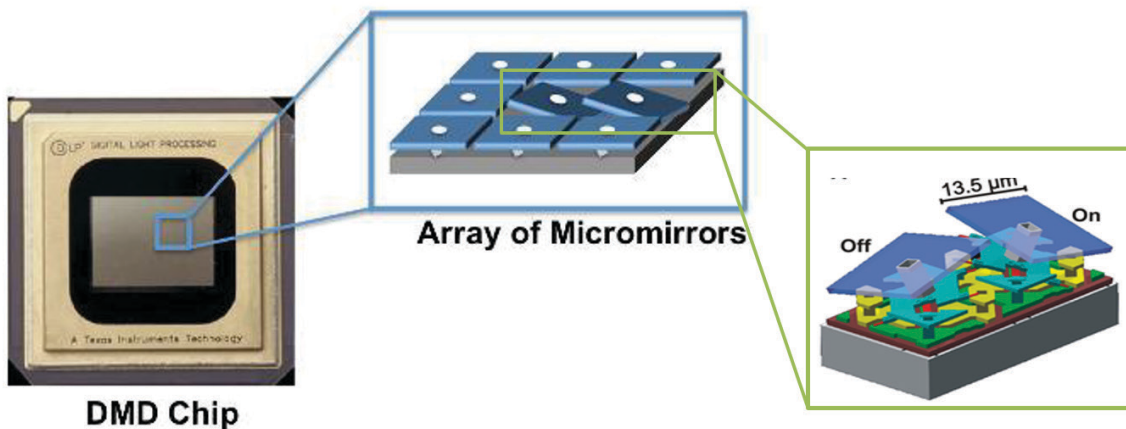


Figure I.26 : DMD chip and micromirrors

- In PhotoCoagulation systems, DMDs are used to precisely guide and focus the laser beam onto the targeted tissue or area within the eye or body.

The ability to control each mirror independently allows for dynamic adjustments in the direction and intensity of the laser beam, enhancing the accuracy and effectiveness of the treatment.

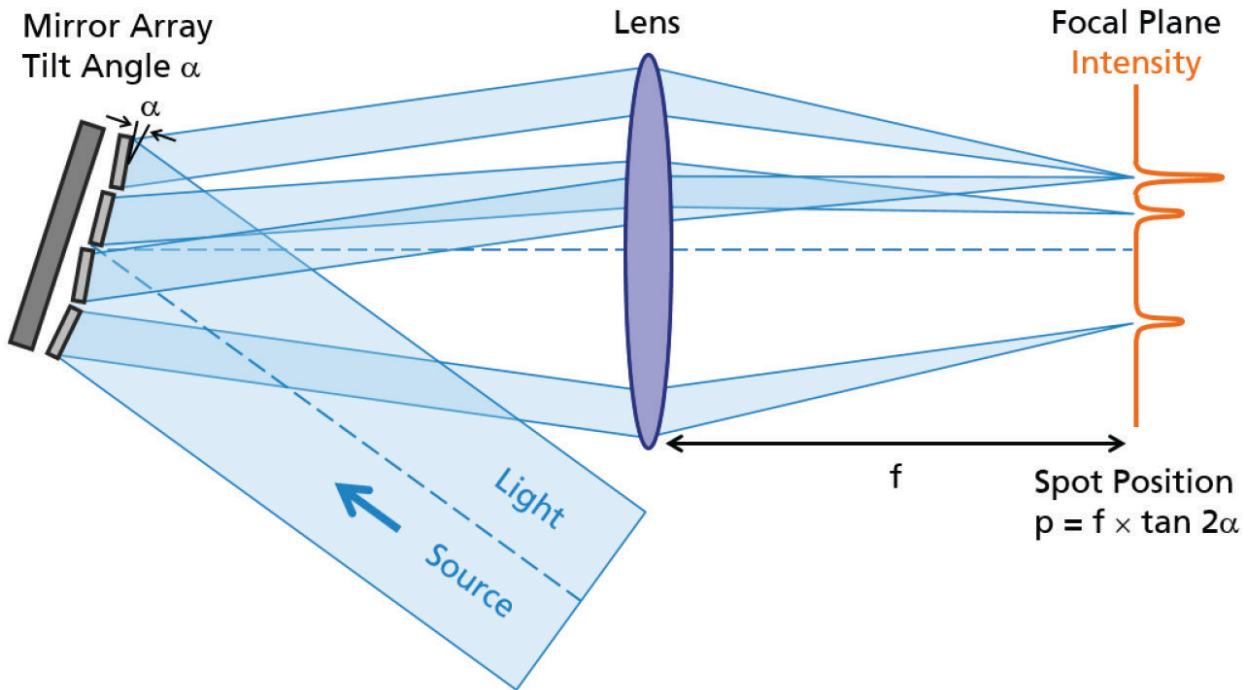


Figure I.27 : DMD Control each Mirror independently

I.7. Conclusion :

Designing the guidance and focusing system requires a precise understanding of the targeted surgical procedure and the tissues to be corrected, in addition to using appropriate and advanced technology to ensure the accuracy and effectiveness of the guidance and focusing process.

In this chapter, we discussed eye diagnostic devices and photocoagulation devices, starting from diagnosing the patient and identifying the disease to the settings and characteristics of these devices in order to design a new Fast and Accurate system based on digital micromirrors.

We observed that the photocoagulation process takes a long time and requires multiple sessions, so the ideal solution is to design a new system that directs a laser beam in the form of patterns and multiple spots.

In the next chapter we design the optical system, and the optics geometric model of the eye to set up our experiment.

CHAPTER II

Design of Optical System for Retina Laser PhotoCoagulation

II. Chapter 2 : Design of optical system for Retina PhotoCoagulation

II.1. INTRODUCTION :

Chapter 2 explores an innovative system that combines laser technology with advanced eye tracking capabilities. This intricate setup integrates hardware components like lasers, optical elements, and digital micromirror devices (DMD) with sophisticated software controls and image processing algorithms. The system’s design aims to precisely direct and modulate laser light onto the human eye while simultaneously tracking eye movements.

This chapter will delve into the system’s key components, including the laser-to-eye pathway, the Galilean beam expander configuration, and the digital control mechanisms. We’ll examine how these elements work in concert to achieve high-precision eye tracking and targeted laser application. Additionally, we’ll discuss the integration of this technology with the complex structure of the human eye, considering factors such as corneal refraction, retinal focusing, and potential clinical applications.

As we progress through this chapter, we’ll analyze the technical challenges, safety considerations, and potential benefits of this cutting-edge approach to ocular interventions and diagnostics.

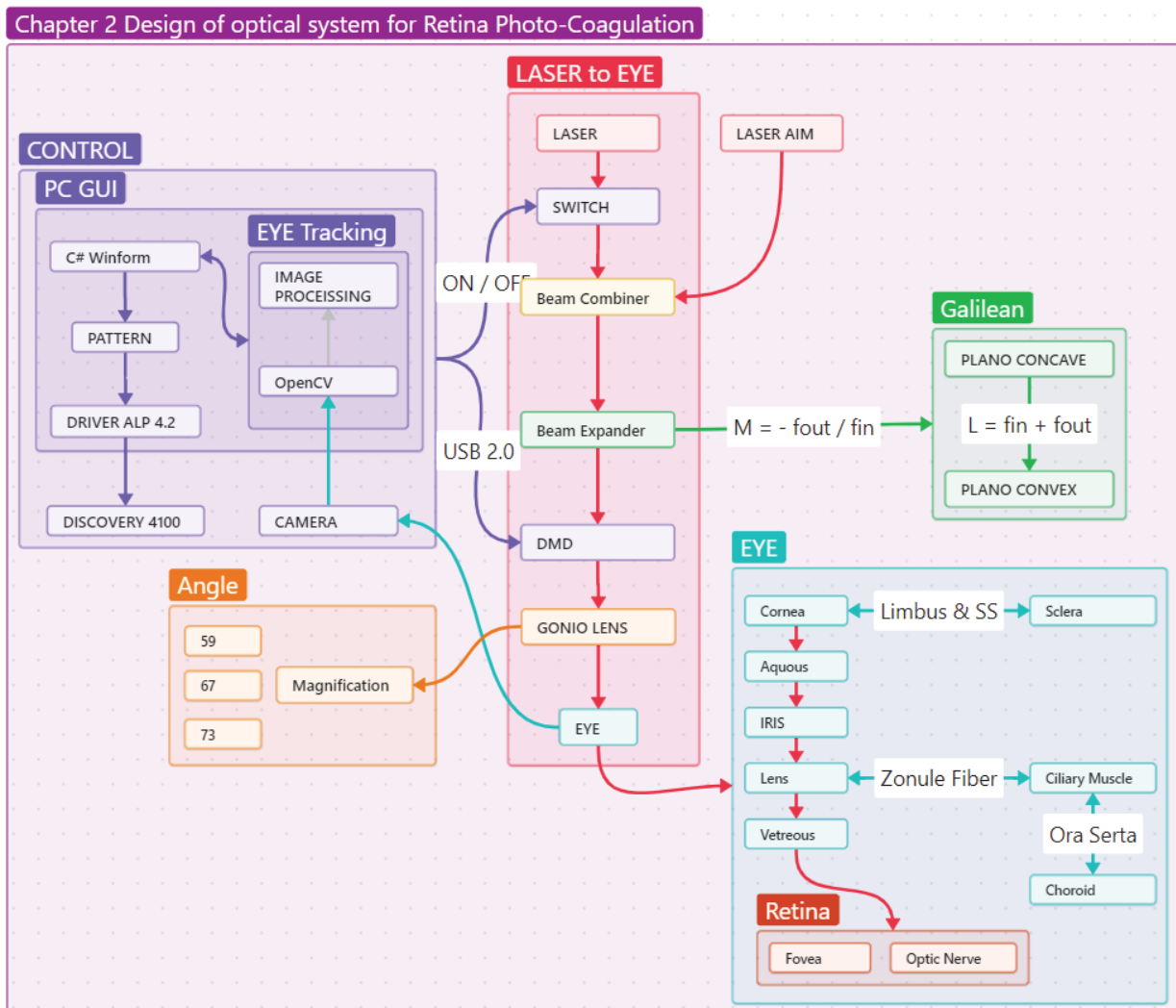


Figure II.1 : Design of Optical System for Retina PhotoCoagulation

II.2. LASER Parameters :

A thorough understanding of the parameters involved in choosing a laser/light treatment as a therapeutic option is essential for safe and effective treatment.

Parameters should be considered each time a laser or light-based device is used: wavelength, power, spot size, pulse width , energy.

If a laser device allowed control of each of these parameters independent of the other, you would be able to adjust the treatment more precisely to match your patient.

Devices that allow the practitioner the freedom to individualize these settings create the ideal environment for maximum efficiency at minimal risk.[25]

II.2.2.1. Power: Number of photons emitted each second and is expressed in watts (W).

II.2.2.2. Exposure time (Pulse width) : The duration in second (sec.) the photons are emitted in each burn from the laser.

II.2.2.3. Wavelength : Wavelength is the distance between two points in a periodic wave which have the same phase.

II.2.2.4. Spot size : The diameter of the focused laser beam and is expressed in micron (μm). Spot size is usually fixed for treatment of a particular lesion.

- However, the energy (Power \times Exposure time) parameters must be decreased or increased, with the decrease or increase in the spot size parameter.
- The spot size when focused on the retina depends on:
- Laser Spot Magnification Factor (LSMF) of the laser lens
- Spot size selected in the Slit-lamp
- Refraction of the eye under treatment.

II.2.2.5. Energy : Number of "photons" emitted during an exposure of any duration and is expressed in joules (J).

So : Energy (Joules) = Power (Watt) \times Exposure time (Second).

II.2.2.6. Power Density : Power and spot size are individual parameters that, when combined, provide power density.

The combination of these 2 characteristics will tell us how much energy and heat are delivered to the desired target By controlling density, devices are able to increase their power output.

Power & Spot size = "Power Density"

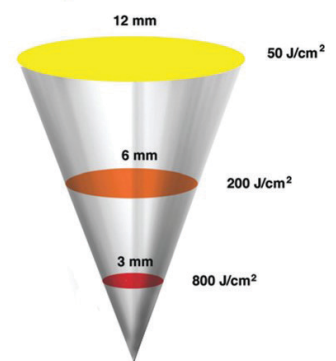


Figure II.2 : Power Density (J/cm²)

II.3. Beam Combiner (Dichroic filter) :

Dichroic filters separate a broad spectrum of light into two components: a reflected component and a transmitted component. They provide the ability to select different bands from a spectrum and direct those bands to where they can either be used or discarded.

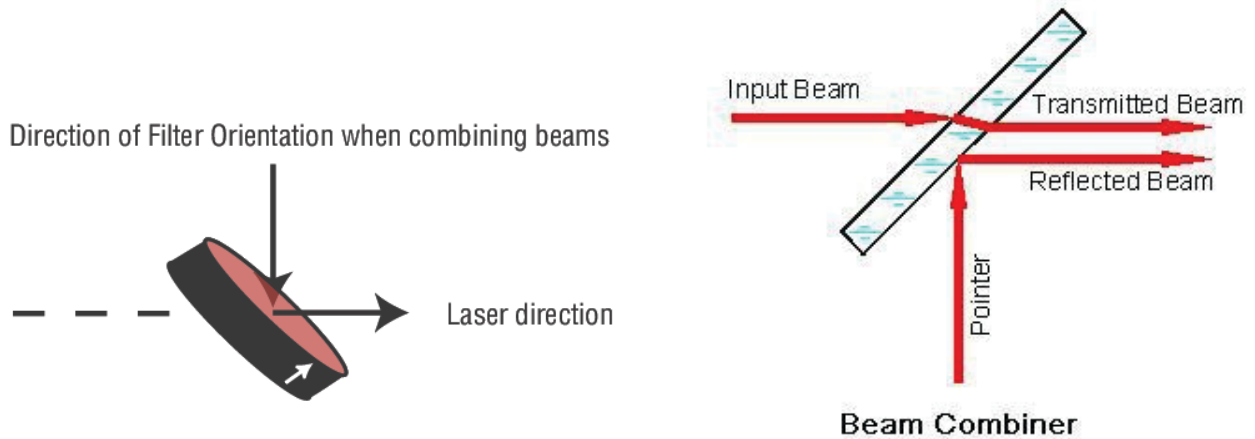


Figure II.3 : Beam Combiner

Beam Combiner is ideal for applications where diode lasers are being used for system alignment. Designed for used at 45 degree, they transmit the long wavelength beam and align it with the 90 degree reflected diode beam.

An ion-beam sputtered coating is applied to laser grade substrates to provide high reflection (>98%) and transmission (>95%) with low scattering. For optimal filter performance, when combining beams, the arrow on the side of the ring should point toward outgoing transmitted & combined laser beam. When separating beams, the arrow on the side of the ring should point toward incoming combined beam and outgoing reflected beam.

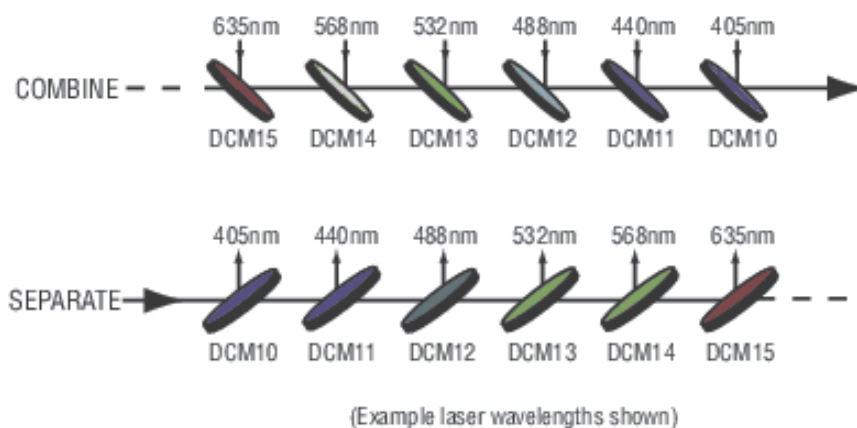


Figure II.4 : Dichroic Combine / Separate

Dichroic laser beam combiners can efficiently combine or separate multiple laser beams at a 45° angle of incidence.

In our case, we use Dichroic to combine two laser beams, one for Aiming and the other for photocoagulation.

II.4. Beam Expander :

Laser beam expanders increase the diameter of a collimated input beam to a larger collimated output beam. Contemporary laser beam expanders are a focal system developed from well-established optical telescope fundamentals. In such systems, the Laser rays enter parallel to the optical axis of the internal optics and exit parallel to them.

The laser beam expanders will increase the diameter of the collimated laser to a larger collimated output laser. Laser beam expanders are similar to telescopes. Both utilising two lenses. The 1st lens has a larger diameter than the laser source. The 2nd lens should also be larger than the desired output size of the laser.[26]

II.4.1. Types of Beam Expanders

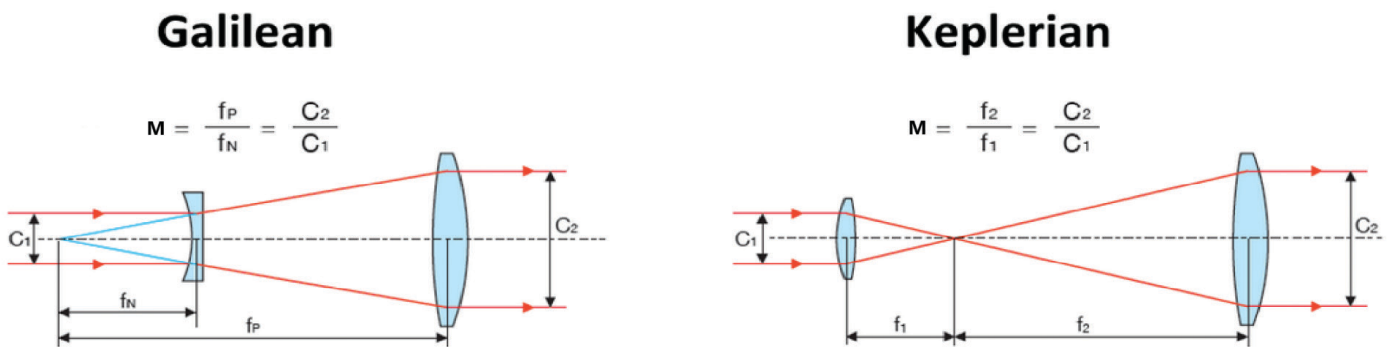


Figure II.5 : Magnification of Galilean & Keplerian Beam Expander

Galilean Type:

- A combination of a convex and concave lens
- Shortens the overall length of the beam expander
- High performance with a small number of lenses
- Usable with high powered lasers

Keplerian Type:

- Utilises two convex lenses.
- Able to insert a pinhole into the expander.
- Able to obtain a clean Gaussian beam emitted by the effect of the pinhole spatial filter.

In our experiment used the Galilean Beam Expander.

II.4.2. Components and Principle of Galilean Beam Expander

- **Negative Lens (Input Lens):** The first lens is a concave lens with a negative focal length. It diverges the incoming collimated beam.
- **Positive Lens (Output Lens):** The second lens is a convex lens with a positive focal length. It converges the diverging beam from the first lens to produce a collimated output beam with a larger diameter.

II.4.3. Magnification of Galilean Beam Expander

The magnification (expansion factor) M of a Galilean beam expander is determined by the focal lengths of the two lenses:

f_{in} is the focal length of the negative lens (input lens).
 f_{out} is the focal length of the positive lens (output lens).

$$M = -\frac{f_{out}}{f_{in}}$$

II.4.4. Beam Diameter Expansion

If the initial beam diameter is D_{in} , the expanded beam diameter D_{out} can be found as:

$$D_{out} = M \cdot D_{in}$$

In our case D_{in} is spot of laser console and D_{out} is active area mirror of DMD.

II.4.5. Lens Separation

The separation between the lenses should be adjusted so that the input beam is correctly diverged and then collimated:

$$L = |f_{out}| - |f_{in}|$$

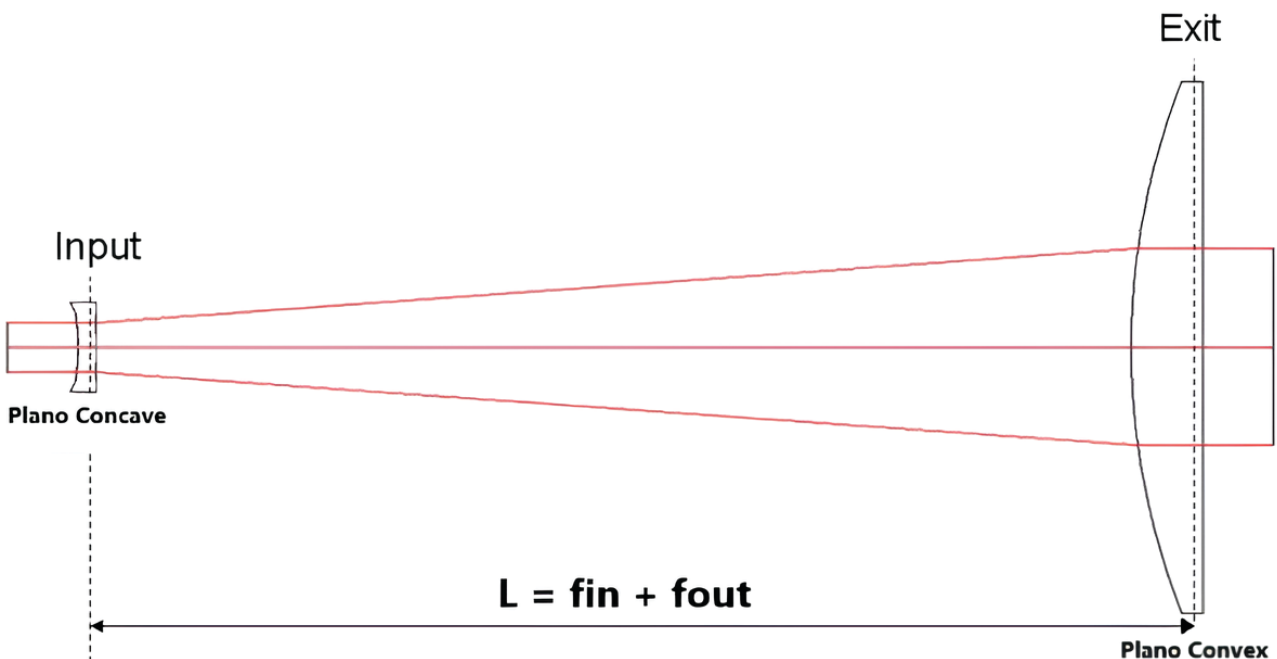


Figure II.6 : Galilean Beam Expander

II.5. Lenses

A lens is a transparent device having at least one curved surface. It bends the ray of light passing through it. The nature of the lens determines how it bends the light rays.

Light travels along a straight line. When it moves from one transparent medium to another in oblique manner, its path will change. This phenomenon is known as the refraction of light. A lens works on this principle. When light rays pass through the transparent material of the lens, they bend, and their path changes. Thus, it appears that the light rays are originating from a source that is closer or farther away than it really is. Therefore, an object appears bigger or smaller than its actual size, when seen through a lens. [27]

II.5.1. Type Of Lenses

There are various types of lenses depending on the curve on each side of the lens.

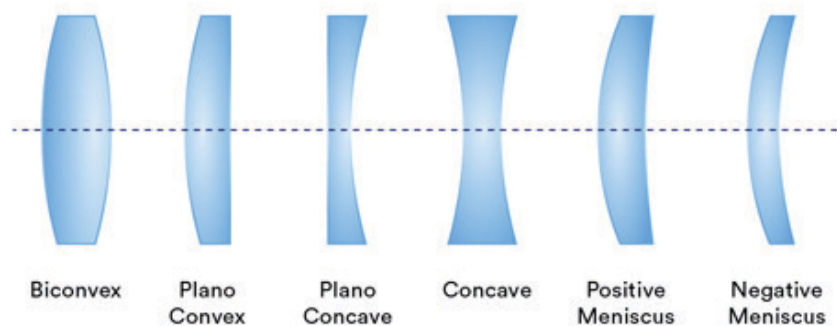


Figure II.7 : Type of Lenses

- **Biconvex Lens** : The bounding surfaces of the lens are spherical and curve inwards.
- **Biconcave Lens** : The bounding surfaces of the lens are spherical and curve outwards.
- **Plano Convex lens** : One of the bounding surfaces is curved inwards and the other is flat.
- **Plano Concave Lens** : One of the bounding surfaces curves outward and the other is flat.
- **Positive Meniscus** : It is a convex-concave lens, thicker at the centre than edges.
- **Negative Meniscus** : It is also a convex-concave lens, thinner at the centre than edges.

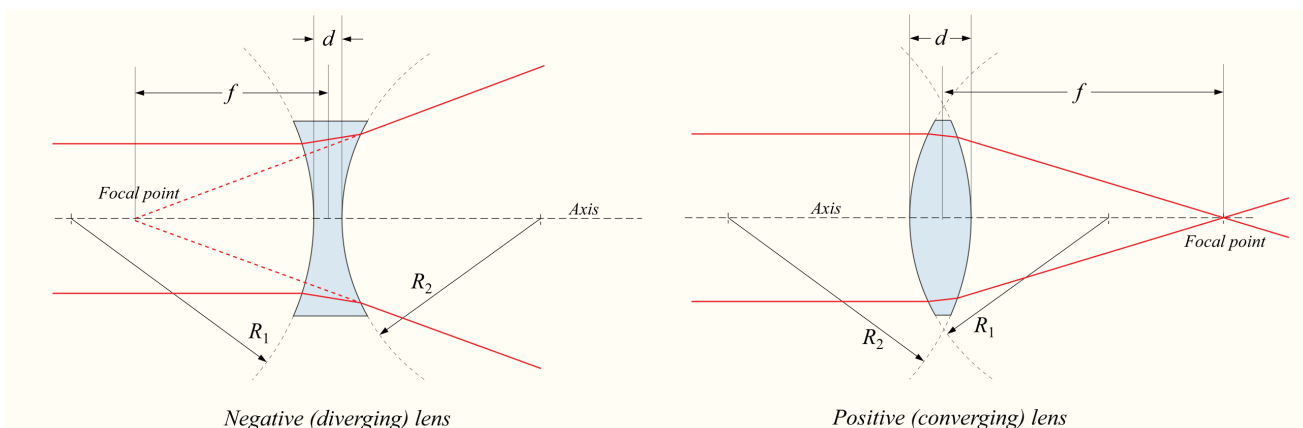


Figure II.8 : Negative and Positive Lens

II.5.2. Lensmaker's Equation

Focal length is a property of the lens and the media around the lens, being positive for convex lens and negative for concave lens.

It is possible to find an expression for the focal length in terms of the radius of curvature R_1 and R_2 of the two refracting surfaces of the lens, the refractive index n_0 of the medium in which lens will be placed, and the refractive index n_l of the material of the lens (Figure). If we ignore the thickness d of the lens, the formula for the inverse of the focal length is :[28]

$$\frac{1}{f} = \left(\frac{n_l - n_0}{n_0} \right) \left(\frac{1}{R_1} - \frac{1}{R_2} \right)$$

This equation is called the lensmaker's equation. By sign convention of refraction from a curved surface, the radius is positive if the center falls on the right of the vertex and negative when it falls on the left.

- if center of sphere is on left then $R < 0$.
- if center of sphere is on right then $R > 0$.

in Figure, $R_1 > 0$ and $R_2 < 0$

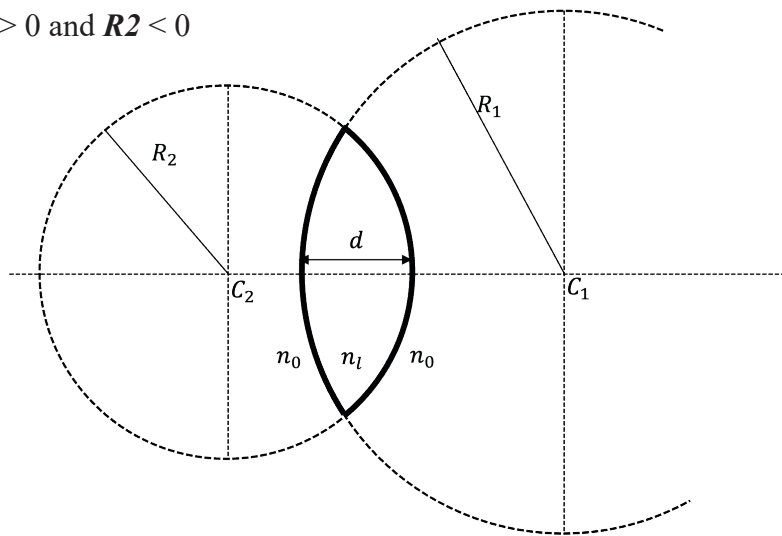


Figure II.9 : The Lens Maker Variables

If the lens is operating in air, then with $n_0 = 1$, this formula will simplify:

$$\frac{1}{f} = (n_l - 1) \left(\frac{1}{R_1} - \frac{1}{R_2} \right)$$

Even the formula with thickness d is not too complicated for lens in air:

$$\frac{1}{f} = (n_l - 1) \left(\frac{1}{R_1} - \frac{1}{R_2} + \frac{(n_l - 1)d}{n_l R_1 R_2} \right)$$

II.5.3. Plano Concave & Plano Convex

- Plano-Concave lenses have negative focal lengths and can be used to diverge collimated beams. In this case, the curved surface of the lens should face the source to minimize spherical aberration.
- Plano-convex lenses have one flat (plano) surface and one outwardly curved (convex) surface. They are used to focus light and are often employed in applications where light needs to be collimated or converged to a point.

The focal length of each lens can be calculated using a simplified thick lens equation:

$$\frac{1}{f} = (n_1 - 1) \left(\frac{1}{R_1} - \frac{1}{R_2} \right)$$

When using the thick lens equation to

calculate the focal length of a Plano-Concave and Plano-Convex lens :

Plano Concave

$$R_1 = -R \quad \text{and} \quad R_2 = \infty$$

$$f = -\frac{R}{n-1}$$

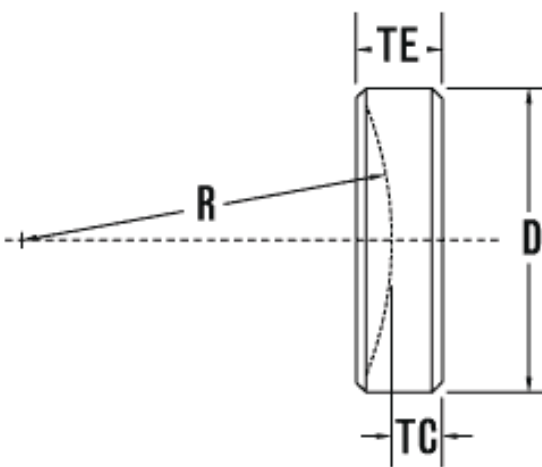


Figure II.10 : Plano-Concave Lens

Plano Convex

$$R_1 = \infty \quad \text{and} \quad R_2 = -R$$

$$f = \frac{R}{n-1}$$

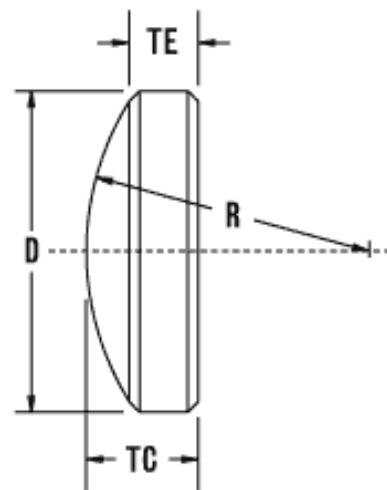


Figure II.11 : Plano-Convex Lens

II.6. Gonio Lens

Gonio lenses are usually indirect lenses such as the three mirrored or four mirrored lenses, although other lenses may be used. These lenses provide visualization of the structures by neutralizing the refractive element of the cornea and giving an oblique view of the structures.

The angles of mirrors in the Goldmann lens are set at 59, 67 and 73 degrees. The smallest mirror is set at 59° and is used to view the angle of the eye. The next larger mirror is set at 67°, and is used to document the iris and angle in an undilated eye, or the iris and lens in a dilated eye. The largest mirror is set at 73° and is used to document the peripheral retina and ciliary body in a dilated eye.[29]



Figure II.12 : Volk Gonio Lens

II.6.1. Direct Lenses

such as the Koeppel, Swan-Jacob, Barkan, Wurst, or Richardson type.

The lens is placed on the eye and saline solution, methylcellulose, or an ophthalmic viscosurgical device is used to fill the space between the cornea and the lens, acting as an optical coupler between the two surfaces.

The goniolens provides direct visualization of the anterior chamber angle (ie, light reflected directly from the angle is visualized).[30]

With a direct lens, the light ray reflected from the anterior chamber angle is observed directly.

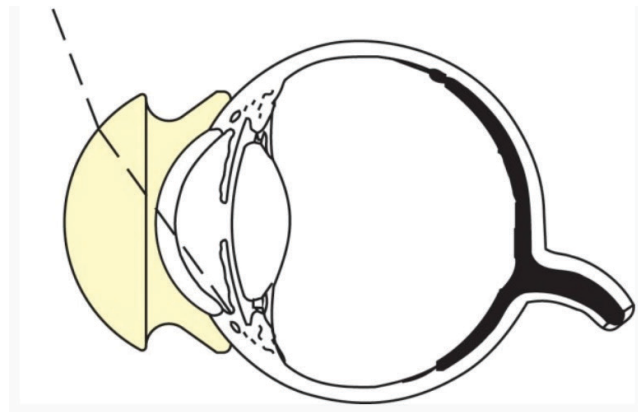


Figure II.13 : Koeppel lens

II.6.2. Indirect Lenses

These are more commonly used in the clinic setting. The viewer will have an inverted and slightly foreshortened image of the opposite angle because the light from the angle is reflected off a mirror and directed towards the viewer.[31]

Examples of indirect gonio lenses include the Posner, Sussman, Zeiss Goldmann.

With an indirect lens, the light ray is reflected by a mirror within the lens.

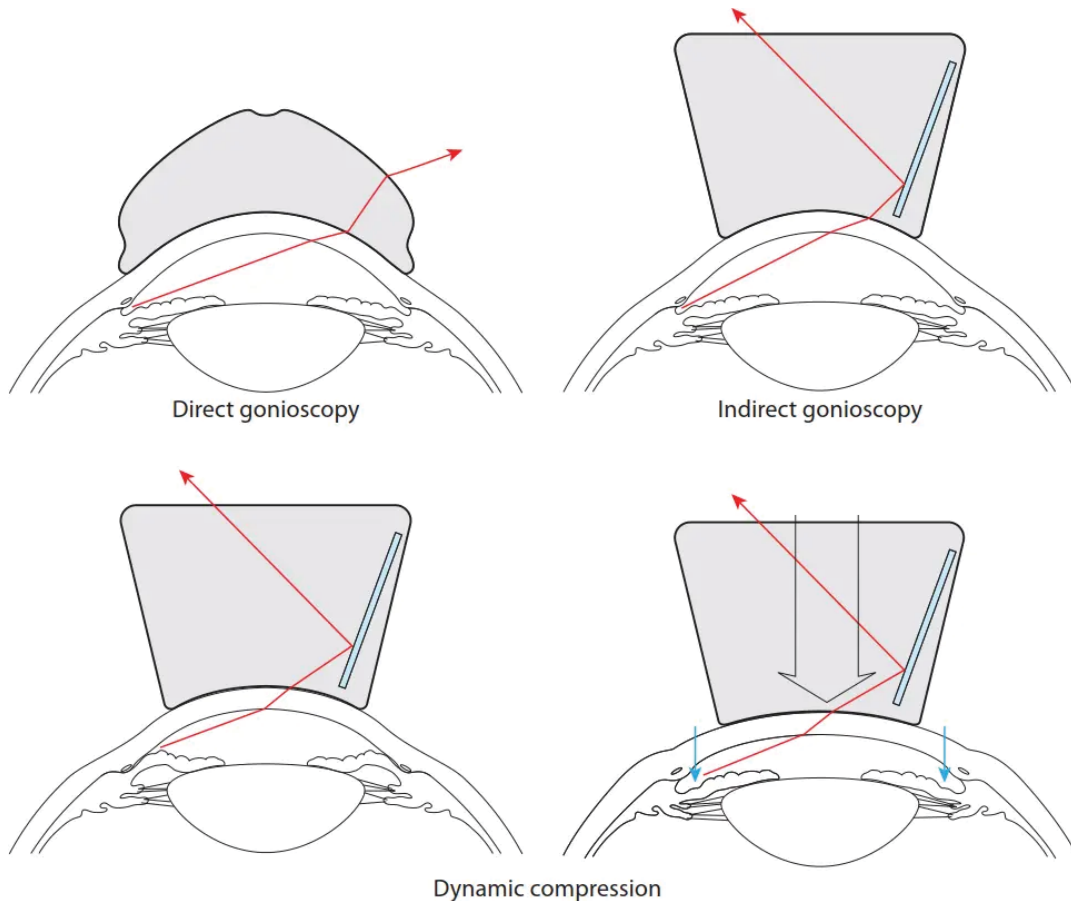


Figure II.14 : Direct vs Indirect gonio lens

For the photocoagulation in our case, one of the most suitable and used lens according to many leading manufacturers in the field such as ocular instruments, Volk et al., is the 3 Mirror Universal Goldmann.



Figure II.15 : Goldmann Three Mirror

II.6.3. Ocular 3 Mirror Universal Goldmann

This classic "Goldmann" type lens has three mirrors angled at 59°, 67° and 73° to permit viewing of the fundus and anterior chamber. Black lens with image magnification of 0.93x, contact diameter of 20mm, laser spot magnification of 1.08x, and a static field of view of 140 degrees. Lens is 33mm high with flange. Manufactured by Ocular.[32]

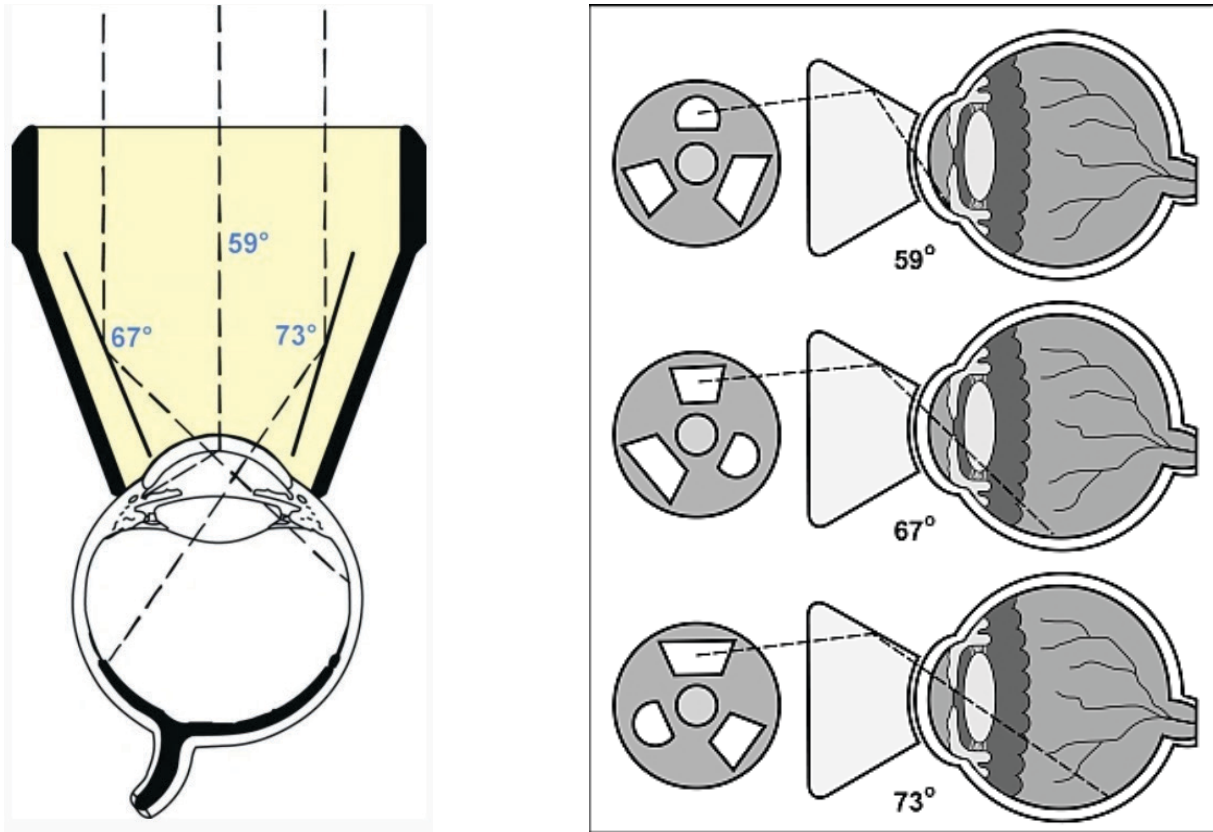


Figure II.16 : Goldmann three mirrors angles


Ocular Three Mirror Universal Lenses								
CE	Product Code	Style	Contact OD (mm)	Lens Height (mm)	Image Mag	Laser Spot Mag	Static Gonio FOV	
	Argon/Diode	OG3MA	Universal	18	32	.93x	1.08x	140°
		OG3MA-2	NMR	16	32	.93x	1.08x	140°
		OG3MFA	with flange	20	33	.93x	1.08x	140°
		OG3MSA	Small	18	24	.93x	1.08x	140°
		OG3MSA-2	NMR Small	16	23	.93x	1.08x	140°
		OG3MPA	17mm	17	26	.93x	1.08x	140°
		OG3MIA	15mm	15	28	.93x	1.08x	140°
		OG3MA-13	NMR Small Fissure	13	28	.93x	1.08x	140°

Figure II.17 : Goldmann Ocular Three Mirror Universal Lenses

II.7. Physics of the EYE :

the eye functions as a sophisticated optical system, with the cornea and lens working together to focus light onto the retina, which is fixed in position. The lens adjusts its power to ensure that objects at varying distances are sharply focused on the retina. The fovea, located at the center of the retina, contains the highest density of light receptors, providing the greatest visual acuity. The pupil's size varies to control light entry, allowing the eye to detect an extensive range of light intensities, up to 10^{10} times greater than the lowest observable level. This adaptability enables the eye to perceive direction, movement, colors, and distance. Visual processing starts with retinal interconnections and continues in the brain, with the optic nerve transmitting visual signals from the eye to the brain.[33]

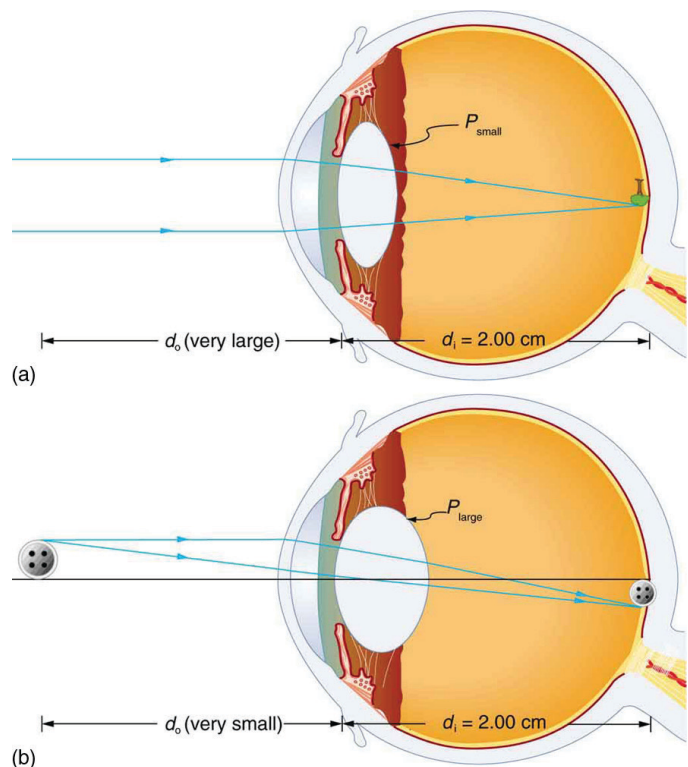
Refractive indices are essential for image formation in the eye, with the most significant change occurring at the cornea, causing substantial bending of light rays. The cornea provides about two-thirds of the eye's optical power due to the dramatic change in light speed from air to cornea. The lens supplies the remaining power needed to focus an image on the retina. Despite light rays passing through multiple layers (cornea, aqueous humor, lens, and vitreous humor), the system can be approximated as a single thin lens. This lens forms an inverted image, which the brain subsequently processes to appear upright.

II.7.1. RELAXED and ACOMODATION :

the image must fall precisely on the retina to produce clear vision—that is, the image distance d_i must equal the lens-to-retina distance. Because the lens-to-retina distance does not change, the image distance d_i must be the same for objects at all distances. The eye manages this by varying the power (and focal length) of the lens to accommodate for objects at various distances. The process of adjusting the eye's focal length is called accommodation. A person with normal (ideal) vision can see objects clearly at distances ranging from 25 cm to essentially infinity. However, although the near point (the shortest distance at which a sharp focus can be obtained) increases with age (becoming meters for some older people).

Figure II.18 : Relaxed and accommodated vision

Relaxed and accommodated vision for distant and close objects. (a) Light rays from the same point on a distant object must be nearly parallel while entering the eye and more easily converge to produce an image on the retina. (b) Light rays from a nearby object can diverge more and still enter the eye. A more powerful lens is needed to converge them on the retina than if they were parallel.



the thin lens equations to examine image formation by the eye quantitatively:

- the power of a lens is given as : $p = \frac{1}{f}$ and $\frac{h_i}{h_o} = -\frac{d_i}{d_o} = m$
- the thin lens equations : $P = \frac{1}{d_o} + \frac{1}{d_i}$
- Power has units of diopters where : $1 \text{ D} = \frac{1}{\text{m}}$

II.8. Index of Refraction (IOR) :

Refractive index, measure of the bending of a ray of light when passing from one medium into another. If i is the angle of incidence of a ray in vacuum (angle between the incoming ray and the perpendicular to the surface of a medium, called the normal) and r is the angle of refraction (angle between the ray in the medium and the normal), the refractive index n is defined as the ratio of the sine of the angle of incidence to the sine of the angle of refraction; i.e., $n = \sin i / \sin r$. Refractive index is also equal to the velocity of light c of a given wavelength in empty space divided by its velocity v in a substance, or $n = c/v$. [34]

$$n = \frac{\text{velocity of light in vacuum } c}{\text{velocity of light in the medium } v}$$

II.8.1. Snell's law

Snell's law, in optics, a relationship between the path taken by a ray of light in crossing the boundary or surface of separation between two contacting substances and the refractive index of each.

Because the ratio n_1/n_2 is a constant for any given wavelength of light, the ratio of the two sines is also a constant for any angle. Thus, the path of a light ray is bent toward the normal when the ray enters a substance with an index of refraction higher than the one from which it emerges; and because the path of a ray of light is reversible, the ray is bent away from the normal when entering a substance of lower refractive index. [35]

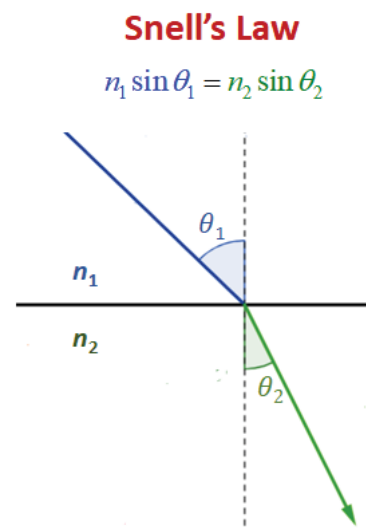
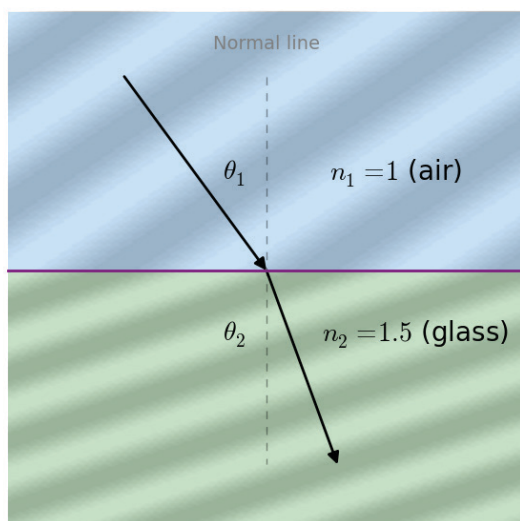
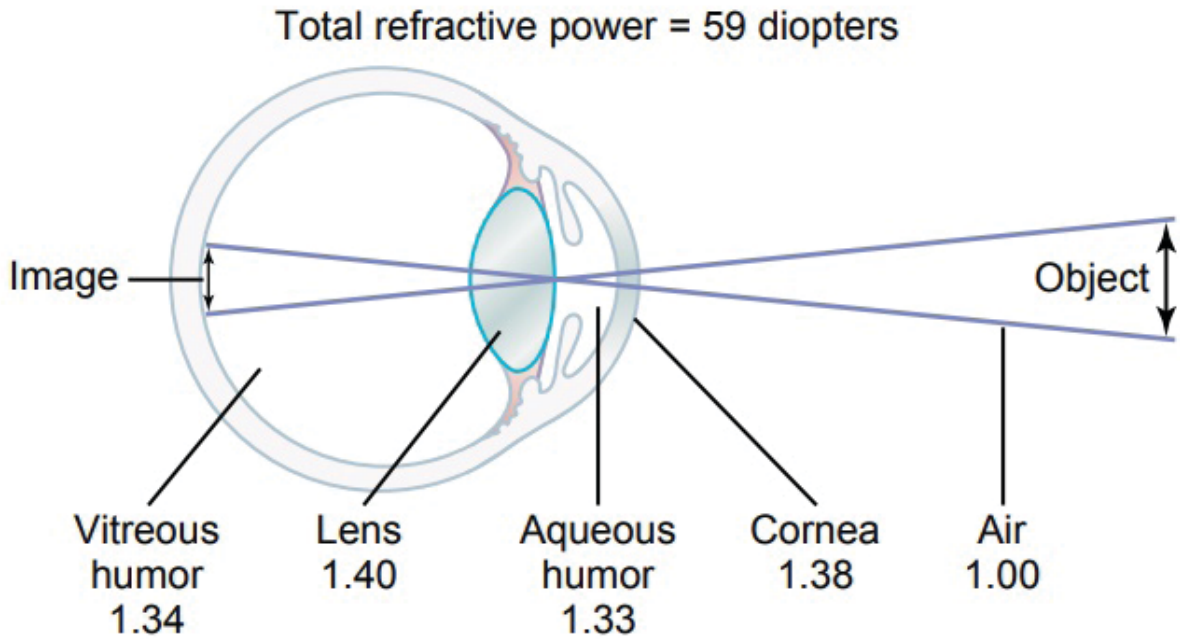


Figure II.19 : IOR & Snell's Law

II.8.2. IOR of the Eye



The eye as a camera. The numbers are the refractive indices.

Figure II.20 : Refractive indices of the Eye

Refractive index in the normal eye: up to 1.4 in the center of the nucleus and a linear variation in the outer region of the nucleus from 1.37 at the cortex. 5 The origin of frame references coincides with the anterior of the area with a higher refractive index. Axis 0, z coincides with the visual axis of the lens.[47]

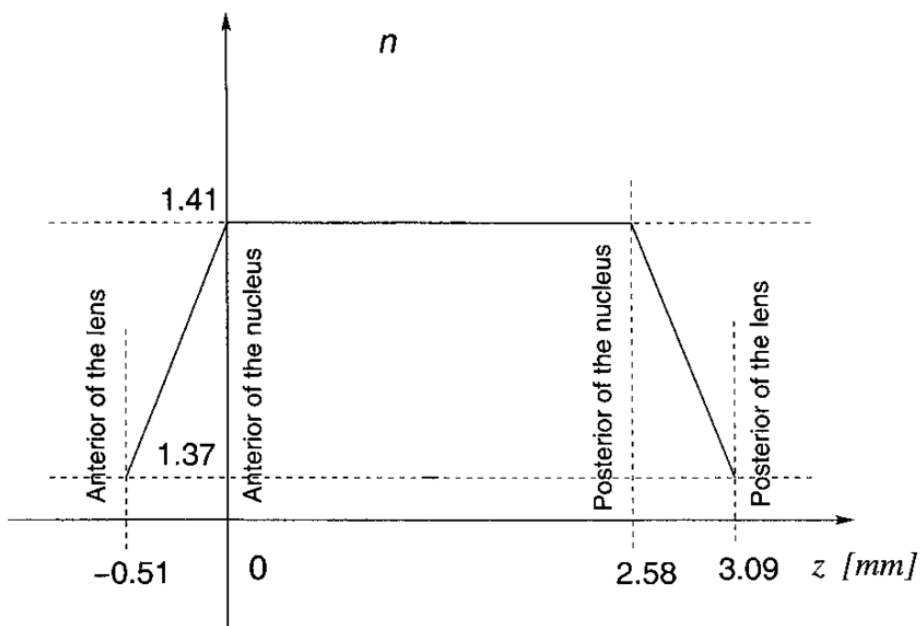


Figure II.21 : Refractive index in Crystalline Lens

II.9. DMD VIALUX V-7000 Module

In our experiment used the DMD V-7000 Module

All V-Modules are based on the DLP Discovery™ 4100 platform and represent the highest performance class of the DLP product family available from catalog.

The ViALUX V-Modules offer unique flexibility in mirror control enabling a wide variety of new emerging applications. Outstanding pattern frequencies of 22 727 global array updates per second are achieved taking advantage of the 50 Gbit/s bandwidth of the DLP Discovery chipset. The usable spectral range covers all wavelengths from 363 nm UV to 2500 nm NIR (All models can be used up to 2500 nm with reduced efficacy).[36]

II.9.1. Overview

- The Type A DMD package has efficient cooling options enabling up to 60 W sustained optical power transfer per DMD
- The V-7000 Hi-Speed V-Module is a compact, cost-effective package for using high-performance DLP technology and to shorten time to market for new emerging products.
- Hi-Speed V-Modules are well suited for education, academic research, proof of concept, and also as OEM components for series production.
- The Hi-Speed V-Module comes with completely configured high-speed FPGA logic and USB controller firmware so that customers save time and costs required for a dedicated hardware and firmware development.

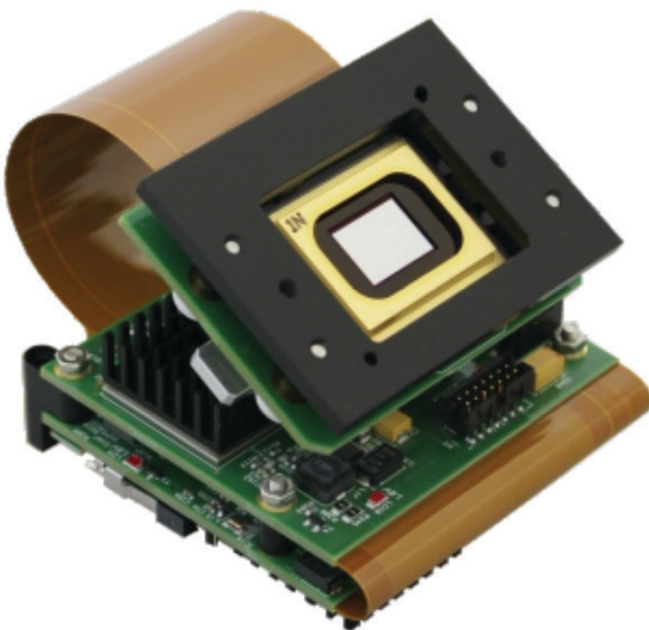


Figure II.22 : VIALUX V-7000 Module

II.9.2. Technical Data

Here is an overview of its specifications :[37]

- **DLP chip** : Discovery™ 4100
- **DMD Type** : 0.7" XGA 2xLVDS (DLP7000)
- **Window Options** : VIS, UV
- **Micromirror Array** : 1024 x 768
- **PC Interface** : USB 2.0
- **Micromirror Pitch** : 13,7 μm
- **Active Mirror Array Area** : 14.0 x 10.5 mm^2
- **Controller Board Type** : V4100
- **Control Board Dimensions** : 71 x 68 mm^2
- **DMD Board Dimensions** : 67 x 50 mm^2
- **PC Transfer Rate** : 800 fps
- **Flexible Cable Length** : 90 mm
- **RAM Capacity on Board** : 16 Gbit
- **Binary Patterns on Board** : 21 845
- **Hardware Trigger** : master / slave
- **Controller Suite** : ALP - 4.2
- **Array Switching Rate** :
 - 1 bit B/W : 22727 Hz
 - 6 bit Gray : 1091 Hz
 - 8 bit Gray : 290 Hz

II.9.3. ALP 4.2 Controller Suite

The ALP-4 Controller Suite is an universal platform enabling advanced control of DLP micromirror systems. Application development is facilitated by an extensive set of library functions designed for use in industry, medicine, research and development.[38]

ALP-4.2 is the according software for ViALUX V-7000 Modules

Customers using ALP-4 can rapidly launch productdesign without the need of time consuming developments for software, firmware and high-frequency FPGA logic code.

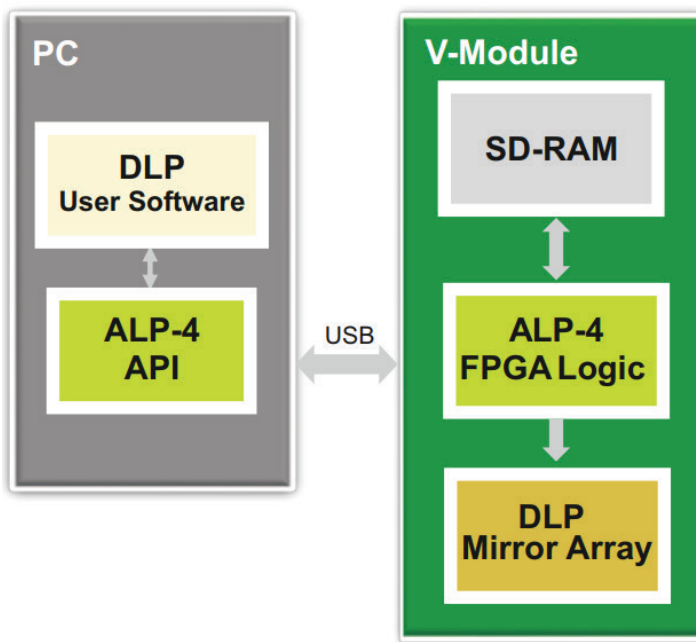


Figure II.23 : Control and Data Flow

The scheme of control and data flow is shown in the block diagram.

The principle of operation is completely different from standard multimedia projection.

Sequences of patterns are generated in the PC and uploaded to on-board memory via compressed USB transfer. Highly sophisticated FPGA logic is applied for processing and streaming the data to the micromirror array.

The ALP-4 Controller Suite is included in all V-Modules and is also available as an accessory for the DLP Discovery 4100 evaluation modules (EVM) of Texas Instruments.

The ViALUX Controller Suite ALP-4.2 drives the high-performance Discovery 4100 chipset of the Hi-Speed V-Modules. The ViALUX proprietary FPGA design is the core of the well proven ALP-4 firmware and software.

The industrial grade USB 2.0 device driver for all current Microsoft® Windows® operating systems guarantees smooth integration with any type of PC. Multiple Hi-Speed V-Modules can be controlled from one computer simultaneously.

The USB 2.0 transfer is speeded up by lossless compression achieving effective PC transfer rates of up to 1.2 Gbit/s. The Hi-Speed V-Module software API, a DLL library, fits seamlessly into standard programming platforms like C++, C#, Visual Basic (.NET), Python, MATLAB, LabVIEW.

II.10. Conclusion

In conclusion, this chapter has explored an innovative laser-based system designed for precise ocular applications. We've examined the intricate interplay of optical components, from the initial laser source through the beam manipulation stages, culminating in highly controlled delivery to the eye.

The integration of advanced technologies such as the digital micromirror device (DMD) and the Galilean beam expander demonstrates the system's capacity for unprecedented precision in laser delivery.

We've also considered the critical interface between this technology and the complex structure of the human eye. Understanding how laser light interacts with various ocular tissues is paramount for both the efficacy and safety of potential applications.

While this system represents a significant advancement in ocular laser technology, it's important to acknowledge that ongoing research and clinical trials will be crucial. Future developments may further refine the system's capabilities, potentially expanding its applications in ophthalmology and vision science.

This chapter underscores the transformative potential of interdisciplinary approaches in medical technology. By combining principles from optics, engineering, and medicine, we're pushing the boundaries of what's possible in ocular care.

CHAPTER III

Modeling & Simulation Eye and Optical System

III. Chapter 3 : Modeling & Simulation Eye and Optical System

III.1. INTRODUCTION :

In this chapter we will design, model and simulate an optical system using 3D software (blender) .

Based on modeling the human eye, its layers and standards according to very precise standards that are very close to reality.

Then design the laser beam and its characteristics, and also designed the beam extender and its lenses to multiply the beam point by 10 using Matlab.

Then model the digital micro-mirrors and simulate how they work.

But designing this system requires a lot of knowledge about the anatomy of the eye, its layers, how it works, and how it deals with light.

The optical system for retinal photocoagulation is difficult to manufacture due to the danger of the laser, the lack of lens standards, and the expensive equipment., So we modeled it.

III.2. Dimensions and Measurements of the Eye :

The significance of numbers in routine clinical practice has grown exponentially. They guide disease diagnoses, treatment choices (in terms of kind, dosage, and duration), aid in surgical precision, determine implant specifications, and even influence follow-up schedules. Daily clinic procedures involve various biometric assessments, generating essential numerical data. In the realm of ophthalmology, sometimes, the sole focus for specialists is a single numeric value, such as normal corneal power, acceptable residual stromal bed levels, or specific anatomical reference values. Despite the advancement of search engines, procuring normal value ranges and their clinical implications remains a cumbersome task. Therefore, there's a strong appreciation among clinicians for a centralized repository of reference values in ophthalmology. This initiative aims to collect and present the latest reference values and their clinical relevance across various ophthalmic conditions. The primary source for these numbers is The American Academy of Ophthalmology's Basic and Clinical Science Course™ book series. Continuous contributions from all members are vital to maintain the page's accuracy and relevance.[39]

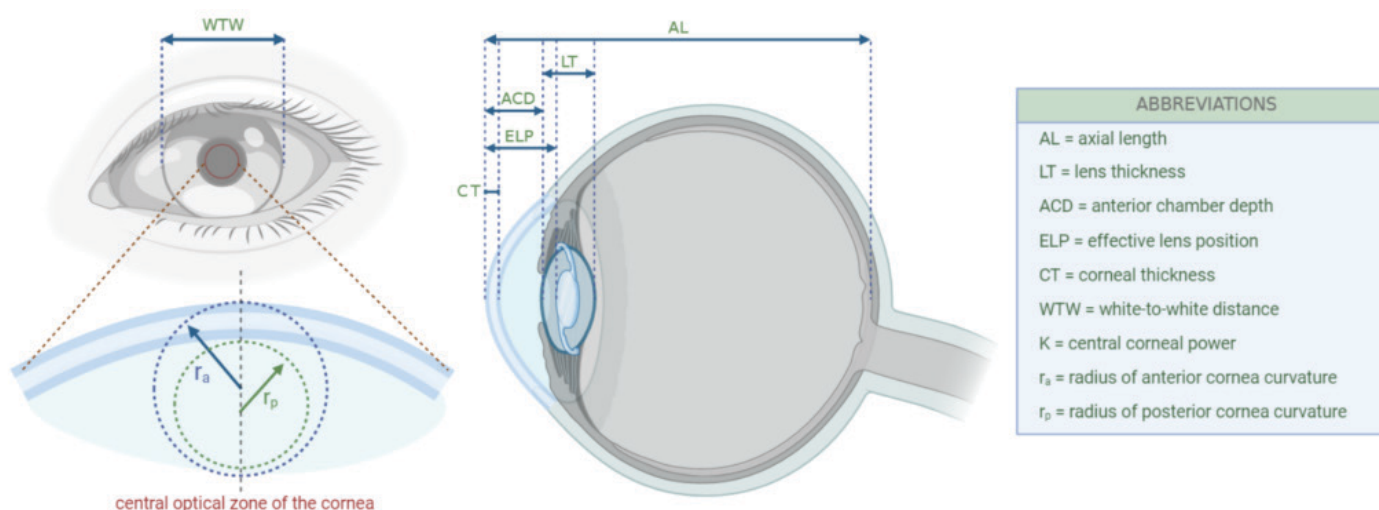


Figure III.1 : Ocular biometric measurements

III.2.1. Axial length (AL):

- Normal length in adults: 23-25 mm
- High myopia (> -6 D): > 26 mm
- Pathologic myopia (> -8 D): 32.5 mm
- Nanophthalmos: < 18 mm in a highly hyperopic eye

III.2.2. Transverse diameter :

- approximately 24 mm (i.e. at its widest point) of the globe.

III.2.3. Cornea:

III.2.3.1. Corneal diameter:

- In adults (reaches adult size by age 2 years):
- **Horizontal:** 12-12.5 mm
- **Vertical:** 11 mm
- **At birth:** 9.5-10.5 mm

Consistency: 70% of its dry weight: type I collagen

III.2.3.2. Power:

- **Average** 43 diopter (D) (air-tear interface)
- **Anterior:** 48 -49 (D)
- **Post:** 5.8-6 (D)

III.2.3.3. Asphericity: A normal cornea is prolate, with an asphericity Q value of -0.26.

III.2.3.4. Corneal thickness:

- **Normal central corneal thickness (CCT):** 540 micron
- **Thickness near limbus:** 700 μ m - 1.0 mm
- **Limbal relaxing incision (LRI depth):** 500-550 μ m
- **Epithelium thickness** 10% of corneal thickness: 50 μ m
- **Bowman layer thickness:** 10 (8-14) μ m
- **Descemet thickness:** At birth: 3 μ m , In adults: 10 - 12 μ m

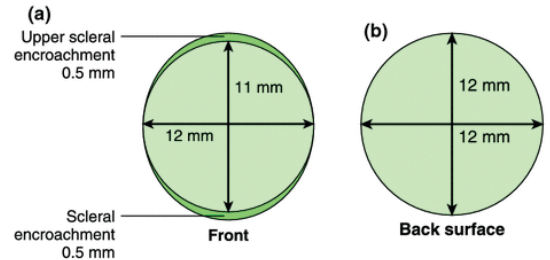
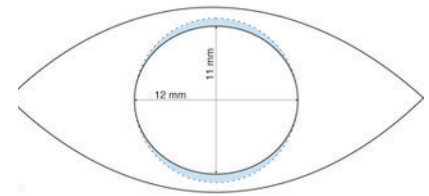


Figure III.2 : Cornea Horizontal Vertical Diameter

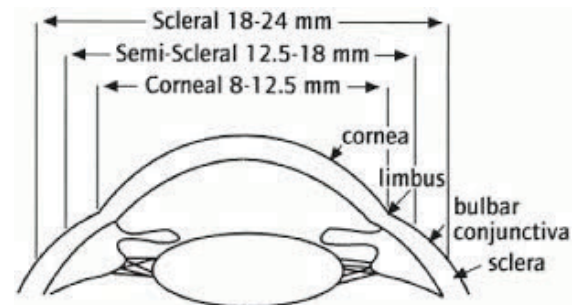


Figure III.3 : Cornea semi-Sclera Sclera Diameter

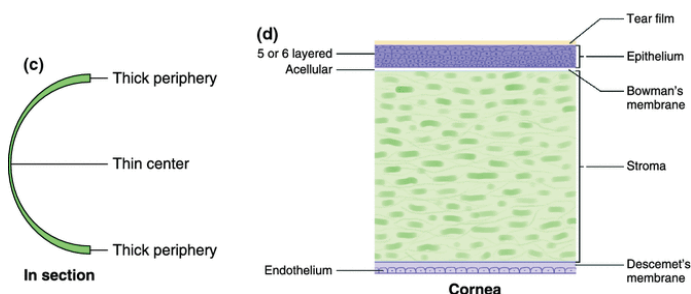


Figure III.5 : Cornea Layers

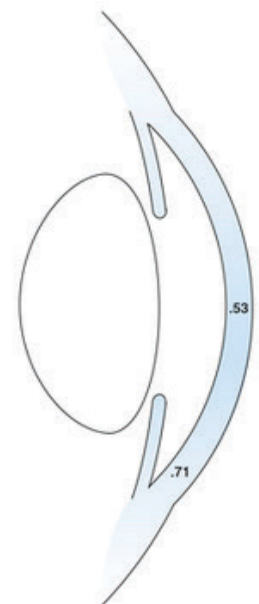


Figure III.4 : Cornea Thickness

III.2.4. Sclera :

Thickness:

- **Thinnest location:** immediately posterior to the insertion of the recti muscles 0.3 mm
- **At the equator:** 0.4-0.5 mm
- **Anterior to muscle insertions:** 0.6 mm
- **Thickest (around the optic nerve head):** 1.0 mm
- **posterior to the limbus :** 5-6 mm (primarily at the inferotemporal quadrant)

This Study on measuring scleral thickness in humans using optical coherence tomography.

Measurements were taken at 8 different meridians around the eye, at 1mm intervals from the scleral spur out to 6mm.

This study provides new data on how scleral thickness varies around the anterior eye in healthy adults, which may have implications for ocular procedures and understanding eye structure.[40]

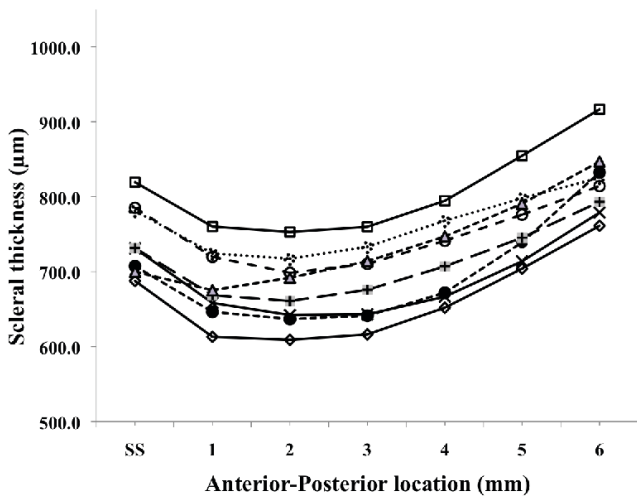


Figure III.6 : AST for all 8 meridians

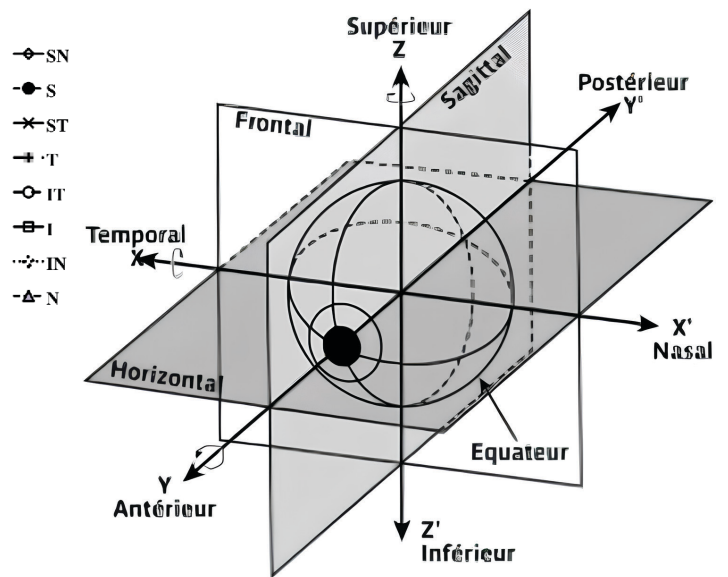


Figure III.7 : Eye Axes

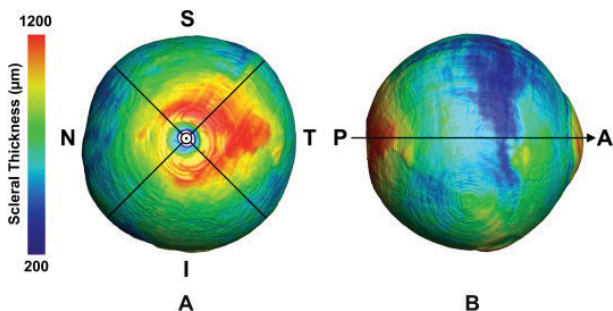


Figure III.8 : Sclera Thickness

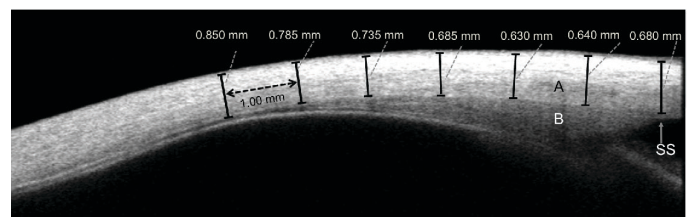


Figure III.9 : OCT image of the temporal sclera (A). Ciliary muscle (B); Scleral spur (SS) Calipers (in black) shown for scleral thickness measurements for 6 mm from the SS at 1 mm intervals (in dotted black)

III.2.5. Anterior chamber:

- **Anterior chamber depth (ACD):** 3 mm
- **Angle:** The critical angle at which total internal reflection occurs at the air-tear interface is approximately 46 degrees.

scleral spur; IA, iris area; IC, iris curvature; LV, lens vault; PD, pupil diameter.

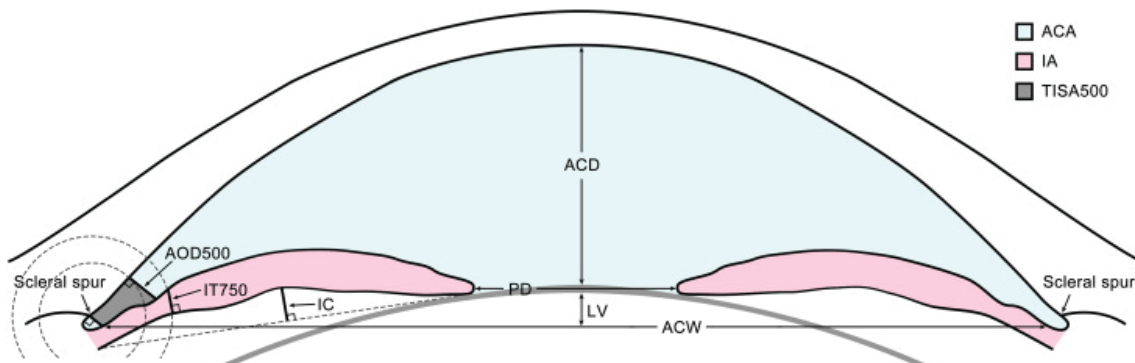


Figure III.10 : Anterior segment parameters

III.2.6. Aqueous humor:

- Volume: 260 microliter
- Anterior chamber (AC): Volume: 200 microliter
- Posterior chamber (PC): Volume: 60 microliter.

III.2.7. Pupil:

- The pupillary light reflex:
- **UNDILATED** : 2 to 4 mm in diameter in bright light
- **DILATED** : 4 to 8 mm in the dark

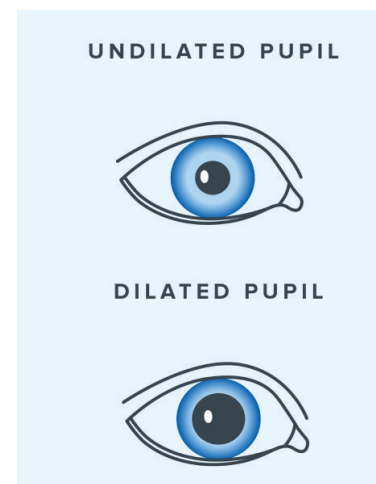


Figure III.11 : Pupil Light Reflex

III.2.8. Iris:

- **Thickness:** 0.35-0.45 mm[1]
- Clinical pearl: iris thickness exceeding 0.7 mm considered increased based on normative values.
- Clinical pearl: Proper iridotomy size: at least 150-200 microns
- ideally 500 micron [2]

III.2.9. Lens:

III.2.9.1. Refractive index: 1.4

III.2.9.2. Refractive power: 20 diopters

III.2.9.3. Equatorial diameter:

- At birth: 6.5 mm
- Adults: 8.54 – 9.70 mm

III.2.9.4. Lens Thickness :

- At birth: 3.5 mm
- Adults: 4.75 – 5 mm

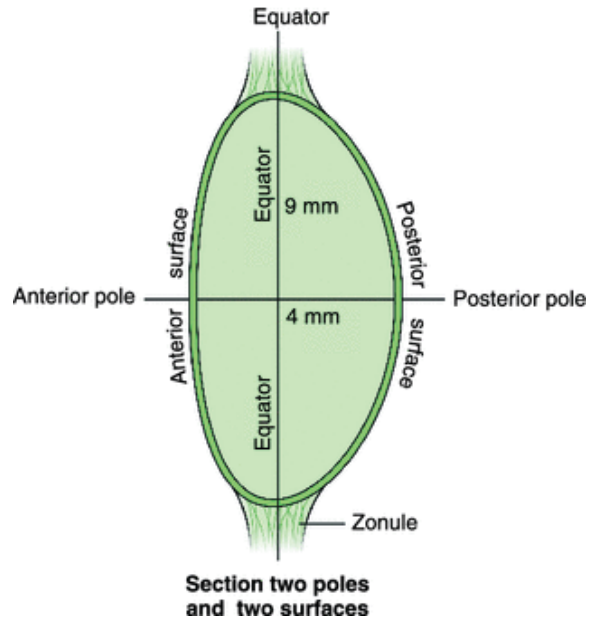


Figure III.12 : Crystalline Lens Dimension

III.2.9.5. Capsule thickness:

- Anterior capsule: 14.0-15.5 microns
- Thinnest point: Posterior capsule: 2.8-4.0 microns
- Thickest point: Posterior pre-equatorial area: 23 microns

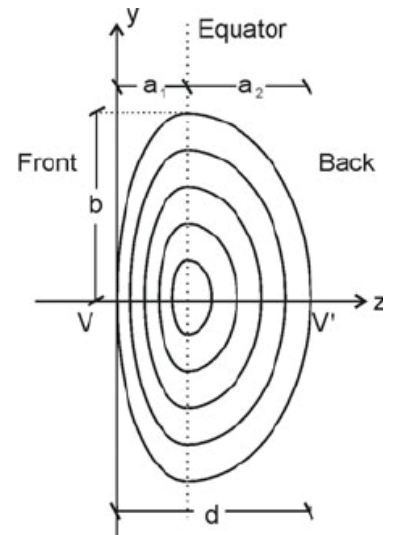


Figure III.13 : Crystalline Lens Parameters

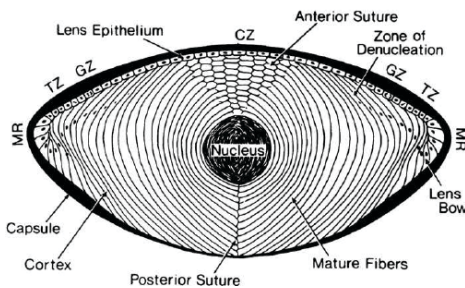


Figure III.14 : Crystalline Lens Diagram

The central lens thickness increases with age, and the slope of age dependence of the lens thickness was estimated to be 0.023 mm/year.[41]

The distance from anterior to posterior pole (i.e. thickness) and radial diameter of human lenses as a function of age :[42]

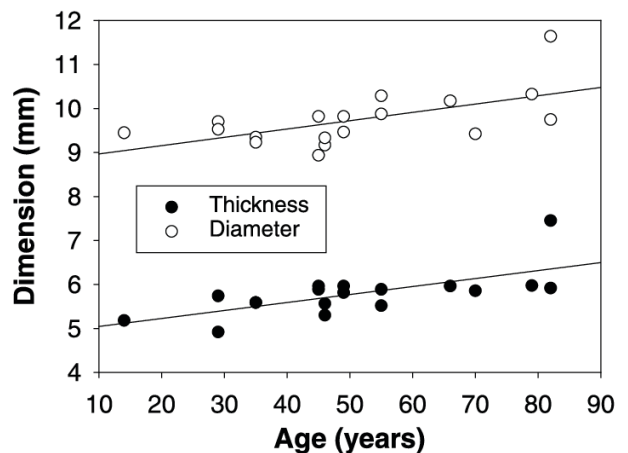


Figure III.15 : Crystalline Lens Dimension/age

III.2.10. Ciliary Body :

The mean and median thickness of the CB were 0.72, 0.71 ± 0.1 mm (range: 0.43 to 1.14 mm)[43]

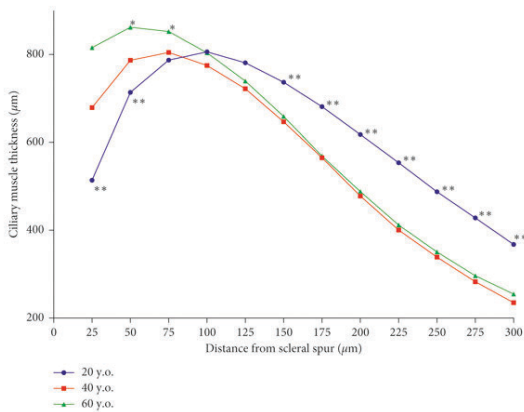


Figure III.16 : Ciliary Body Thickness/SS/Age

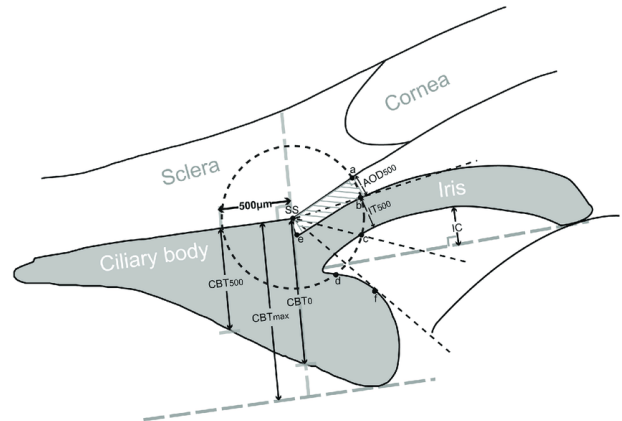


Figure III.17 : Ciliary Body Parameters

III.2.10.1. Pars plana:

- site of intravitreal injections between the horizontal and vertical rectus muscles.

III.2.10.2. Ora serrata (the boundary between the pars plana and the retina):

Distance from limbus/Schwalbe’s line:

- Nasally: 5.75 mm
- Temporally: 6.50 mm

Figure III.18 : Ciliary Body thickness during Accommodation/pars

	Accommodated (Non-cycloplegic)	Unaccommodated (Cycloplegic)	P-value*	Change in Thickness
CBT1	818 ± 40 µm	751 ± 42 µm	< 0.001	+ 66 ± 39 µm
CBT2	445 ± 59 µm	506 ± 66 µm	< 0.001	- 61 ± 43 µm
CBT3	242 ± 50 µm	295 ± 54 µm	< 0.001	- 59 ± 31 µm

CBT1, CBT2 and CBT3 : Measurements of the ciliary body thickness at 1 mm (CBT1), 2 mm (CBT2) and 3 mm (CBT3) distance from the scleral spur.

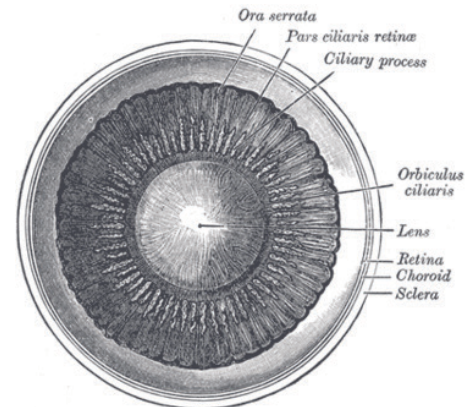
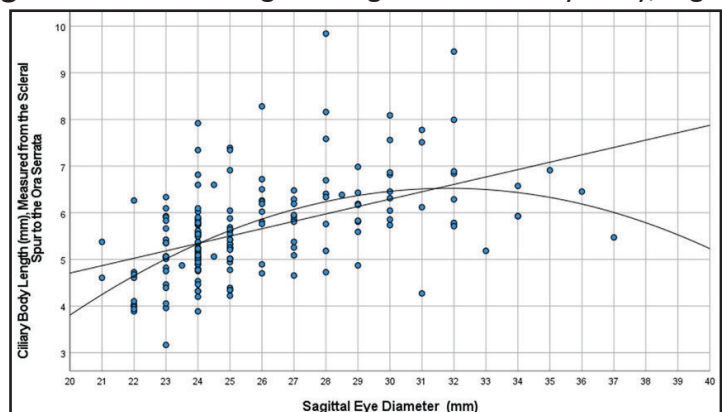


Figure III.19 : plana/Ora serrata

Figure III.20 : Scattergram engh of the ciliary body/sagittal

Scattergram showing the distribution of the length of the ciliary body, measured from the scleral spur to the ora serrata, in dependence of sagittal eye diameter.[44]



III.2.11. Vitreous:

III.2.11.1. Volume :

- Vitreous cavity: 5-6 mL
- Vitreous body: 4 mL

III.2.11.2. Consistence: >99% water

III.2.12. Retina :

The retinal thickness shows greatest variations in the center. The retina is thinnest at the foveal floor (0.10, 0.150-0.200 mm) and thickest (0.23, 0.320 mm) at the foveal rim. Beyond the fovea the retina rapidly thins until the equator. At the ora serrata the retina is thinnest of all (0.080 mm).

this Figure shown The vertical extent of the retina across the horizontal meridian at different eccentricities.[45]

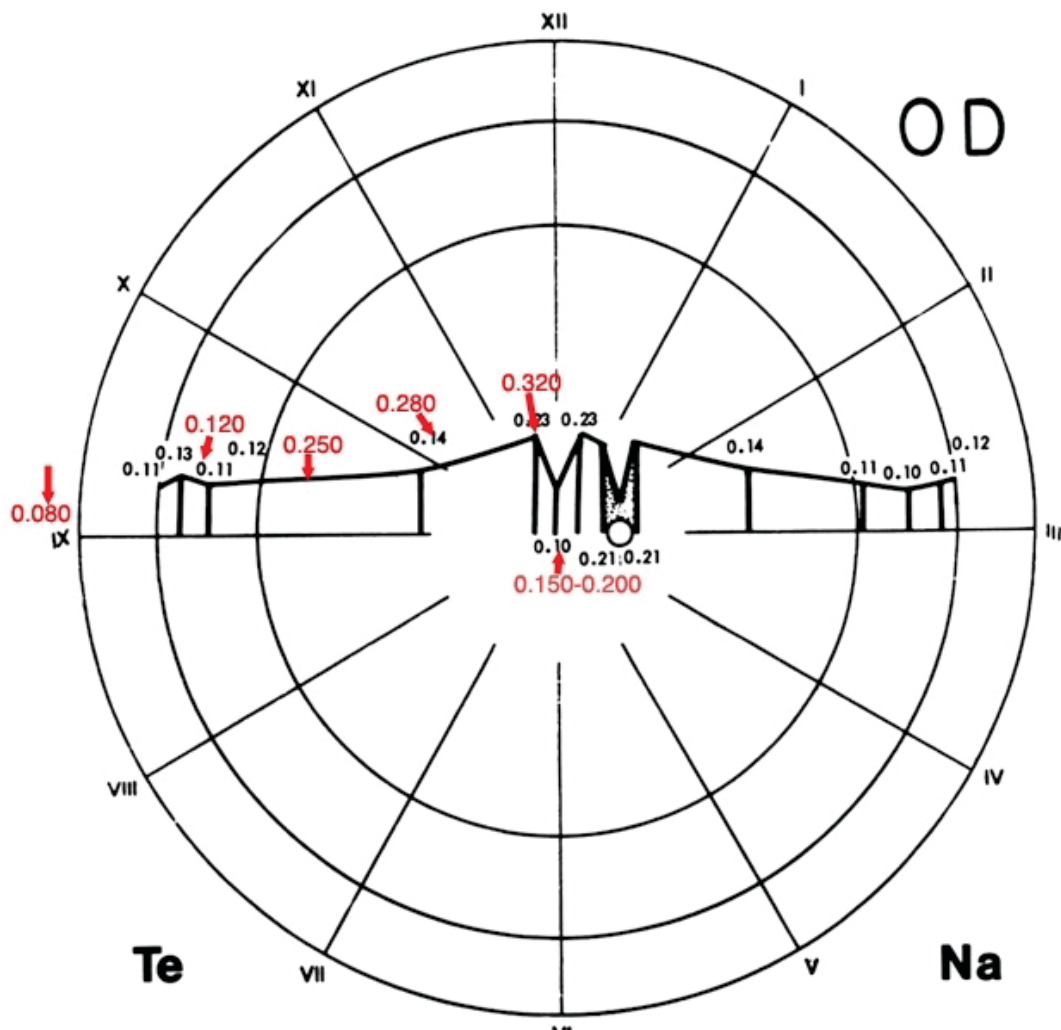


Figure III.21 : The vertical extent of the retina across the horizontal meridian

III.2.13. Macula:

- **Diameter:** 5.5 mm

III.2.14. Fovea :

- These are important to localize visual field defects and find a corresponding pathology.
- **Diameter:** 1.5 mm (5 degrees) in (i.e. the diameter of an average-sized optic disc).

III.2.14.1. Foveal avascular zone (FAZ):

- **Diameter:** 500 microns (1:40 degrees)
- **Clinical pearls:** Should be avoided with laser therapies.

III.2.14.2. Foveola:

- **Location:**
- 4.0-4.5 mm (15 degrees) temporal to the optic disc
- 0.8 mm (2:10 degrees) inferior to the optic disc
- **Diameter:** 350 microns
- **Cells:** all cones
- **Umbo:** **Diameter:** 150 microns

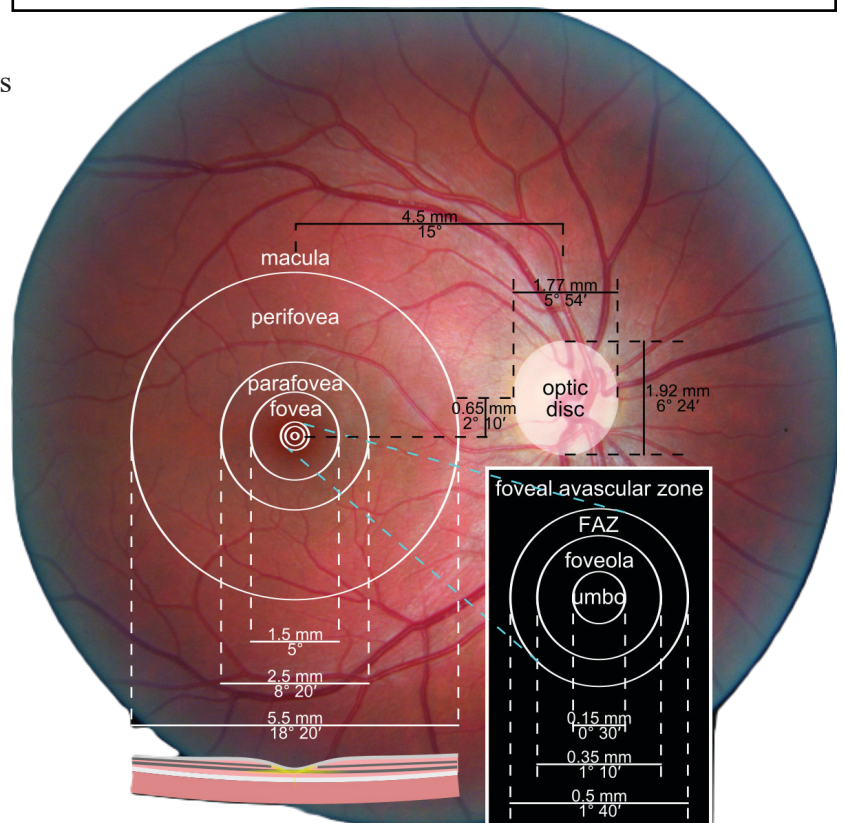
III.2.14.3. ParaFovea:

- Ring width: 0.5 mm
- Outer radius: 2.5 mm
- Inner radius: 1.5 mm

III.2.14.4. PeriFovea:

- Ring width: 1.5 mm wide
- Outer radius: 5.5 mm
- Inner radius: 2.5 mm

Figure III.22 : Foveola-Fovea-centralis-Parafovea-Perifovea



III.2.15. Optic nerve :**III.2.15.1. Optic nerve's (ON) diameter:**

- **Optic nerve's head diameter :** 1.5-2.2 mm
- **Anterior to the lamina cribrosa:**
 - Horizontally: 1.5 mm
 - Vertical: 1.75 mm
- **Behind the lamina cribrosa:** 3 mm
- **Cup-to-disc ratio: Normal:** < 0.5

III.2.15.2. Optic nerve's length:

- Total: Approximately 50 mm
- Intrascleral: 1 mm
- Intraorbital: 25-30 mm (apex to sclera 18 mm)
- Intracanalicular: 10 mm
- Intracranial: 10 mm

III.3. Modeling :

After discussing the dimensions and measurements of the eye, we can model and simulate a 3D eye using the Blender program

III.3.1. Blender :

Blender is the free and open source 3D creation suite. It supports the entirety of the 3D pipeline—modeling, rigging, animation, simulation, rendering, compositing and motion tracking, even video editing and game creation. Advanced users employ Blender’s API for Python scripting to customize the application and write specialized tools; often these are included in Blender’s future releases. Blender is well suited to individuals and small studios who benefit from its unified pipeline and responsive development process .

Blender is cross-platform and runs equally well on Linux, Windows, and Macintosh computers. Its interface uses OpenGL to provide a consistent experience.



blender

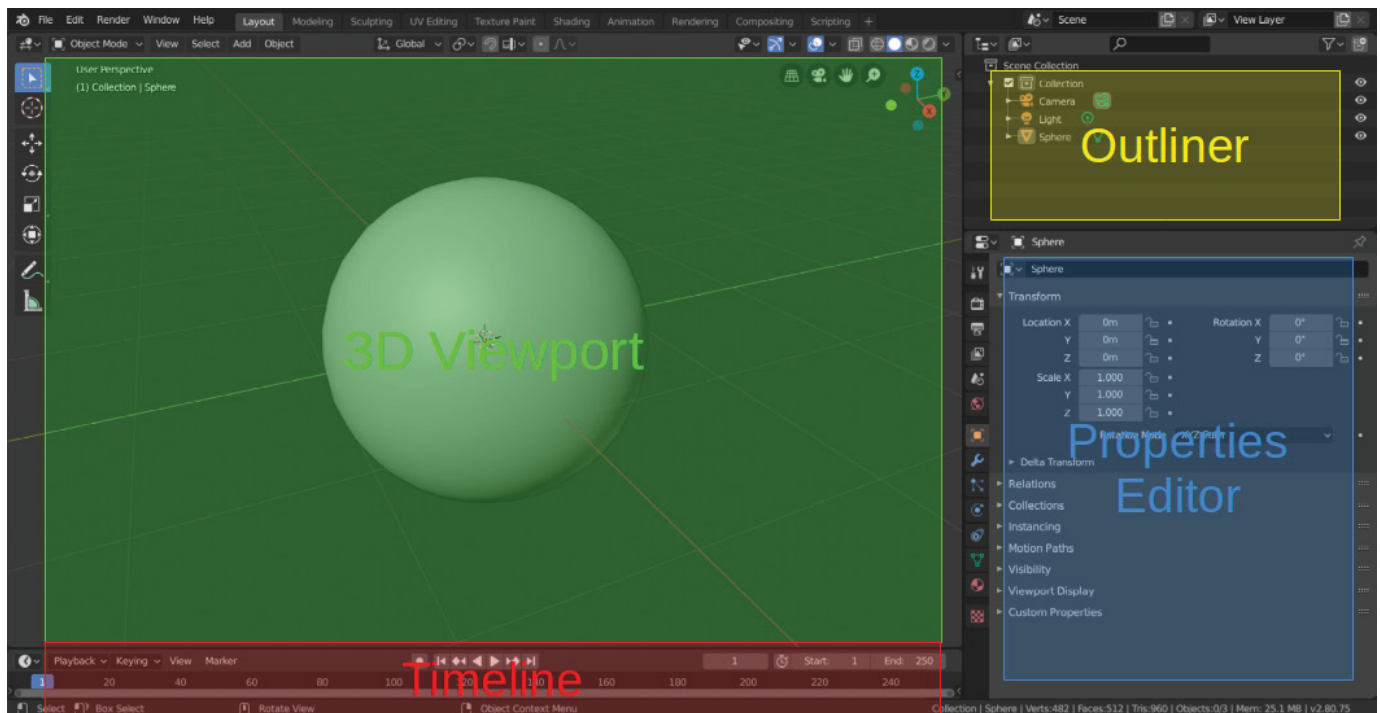


Figure III.23 : Blender Workspace Environment

- **The 3D Viewport** is a sort of visual workshop, where you can add and remove things from your scene.
- **The Outliner** is a hierarchical diagram of your project that shows the relationship between elements of a scene.
- **The Properties Editor** gives you access to many kinds of controls, for display, animation, appearance of objects, and much more.
- **The Timeline** can be expanded and shows video sequencing and animation controls. It allows you to configure motions and property changes over time.

III.3.2. Modeling EYE :

- We designed an accurate and realistic three-dimensional eye model using the most accurate data and measurements available about the structure and layers of the eye.
- We used average eye measurements to ensure the simulation worked well.

III.3.2.1. Modeling Sclera :

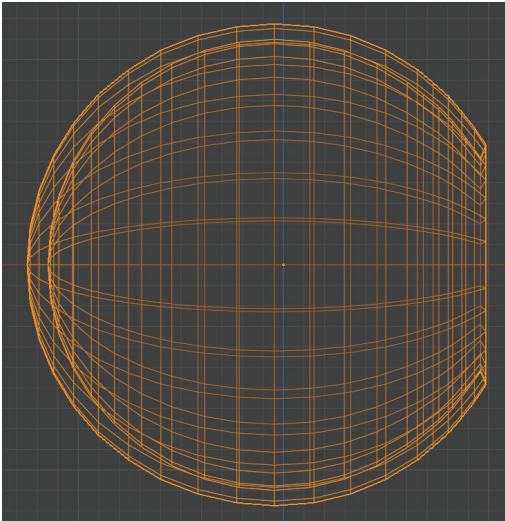


Figure III.24 : 3D Sclera Topology

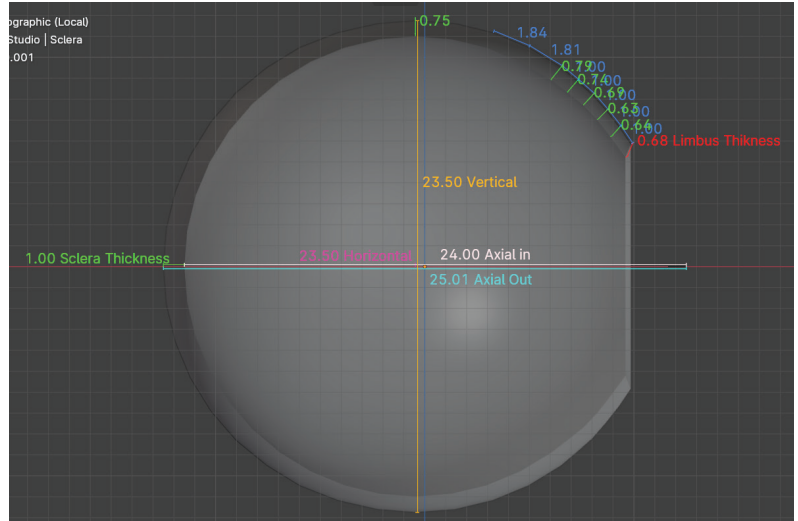


Figure III.25 : 3D Sclera side view

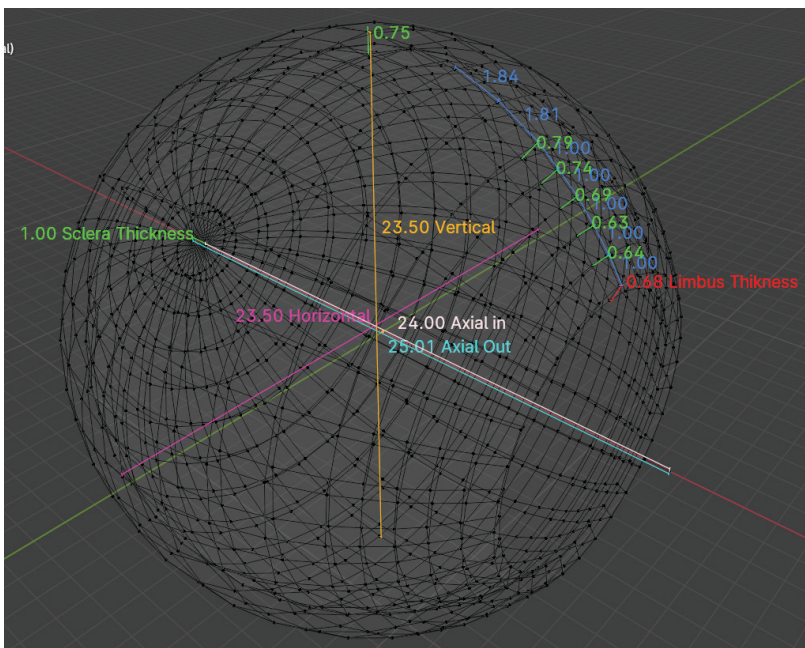


Figure III.26 : 3D Sclera Wireframe

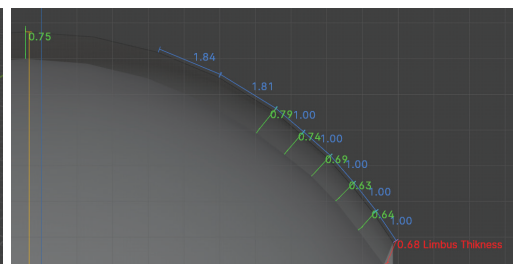


Figure III.27 : 3D Sclera Thickness

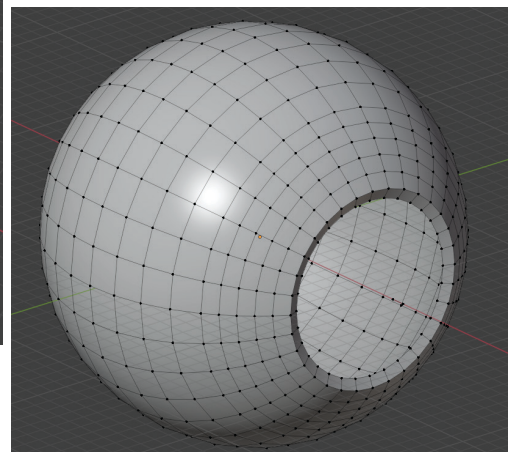


Figure III.28 : 3D Sclera Solid View

III.3.2.2. Modeling Cornea :

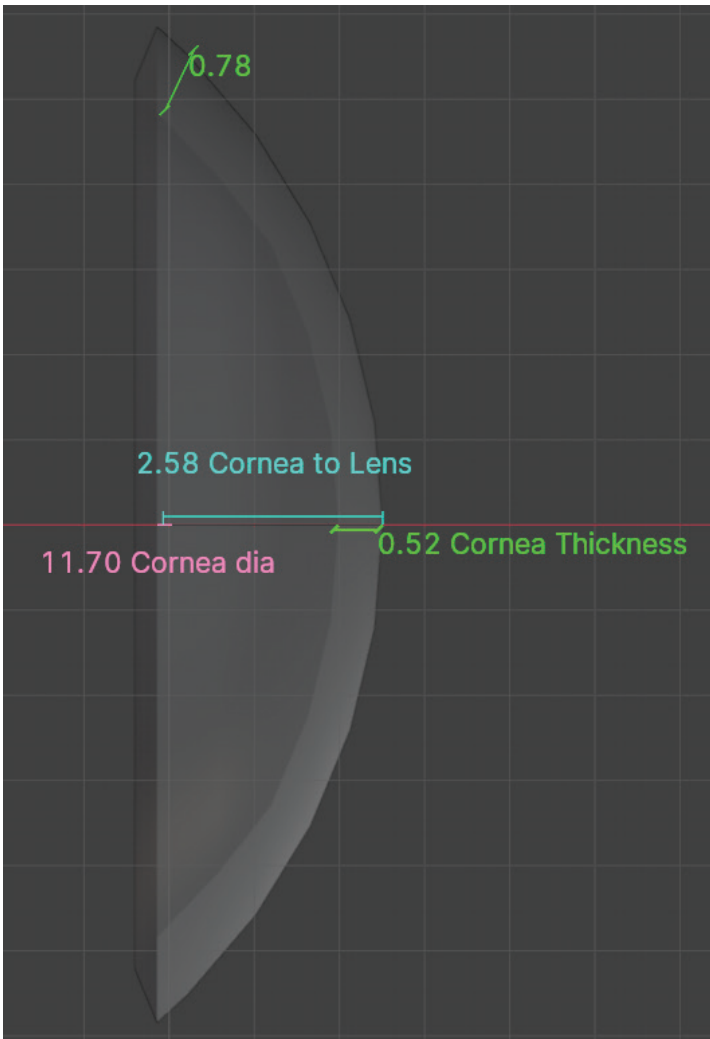


Figure III.29 : 3D Cornea side view

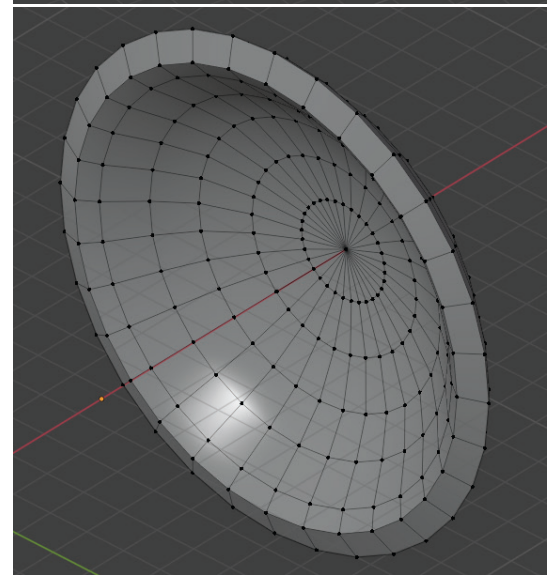
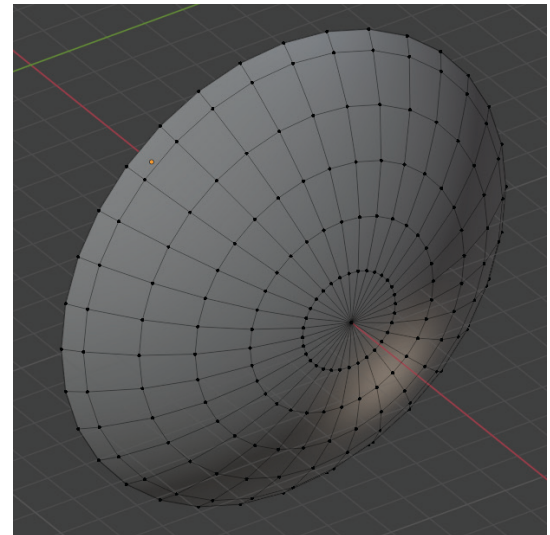


Figure III.30 : 3D Cornea Solid view

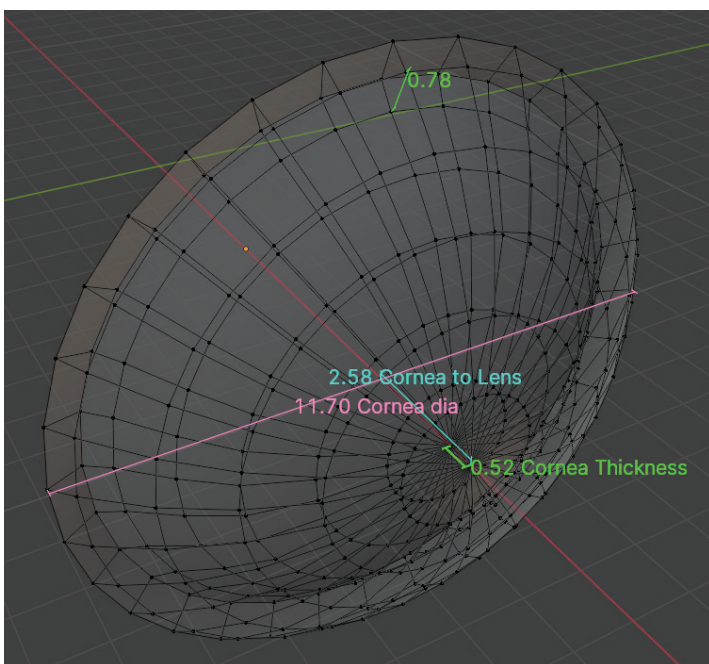


Figure III.31 : 3D Cornea Wireframe Front view

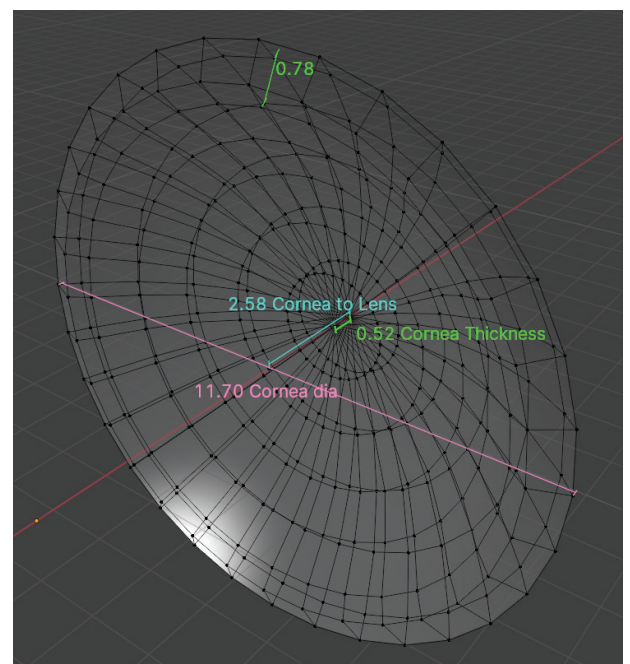


Figure III.32 : 3D Cornea Wireframe Back view

III.3.2.3. Modeling Ciliary Muscle :

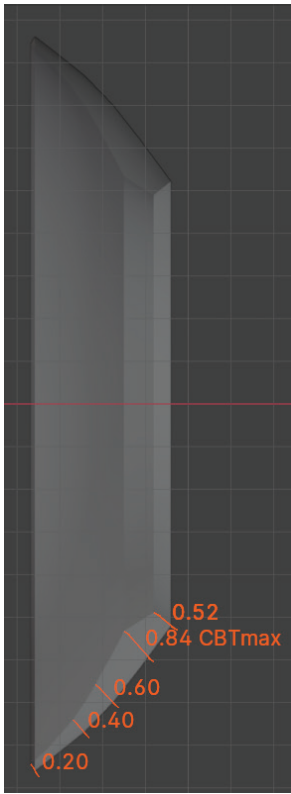


Figure III.33 : 3D Ciliary Muscle side view

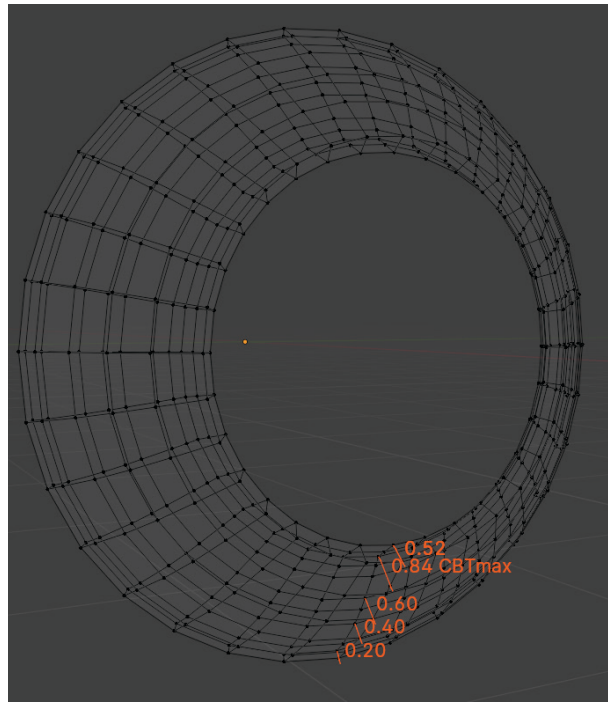


Figure III.34 : 3D Ciliary Muscle Wireframe

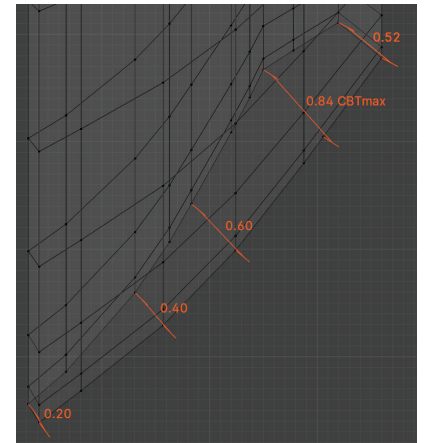


Figure III.35 : 3D Ciliary Muscle Measurement

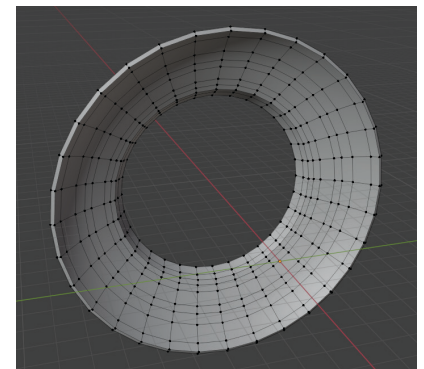


Figure III.36 : 3D Ciliary Muscle Solid view

III.3.2.4. Modeling Choroid & Retina :

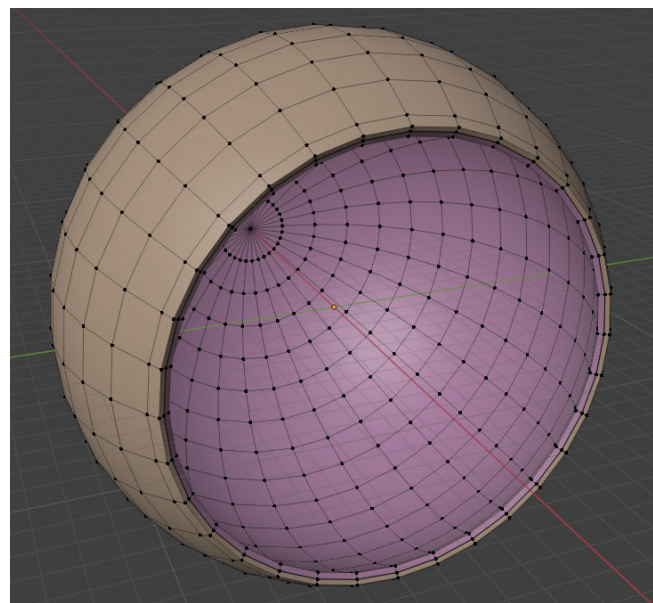
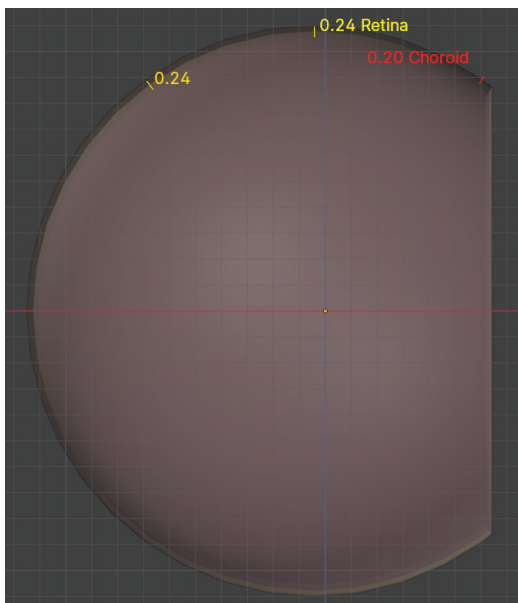


Figure III.37 : 3D Retina and Choroid side & front view

III.3.2.5. Modeling Iris :

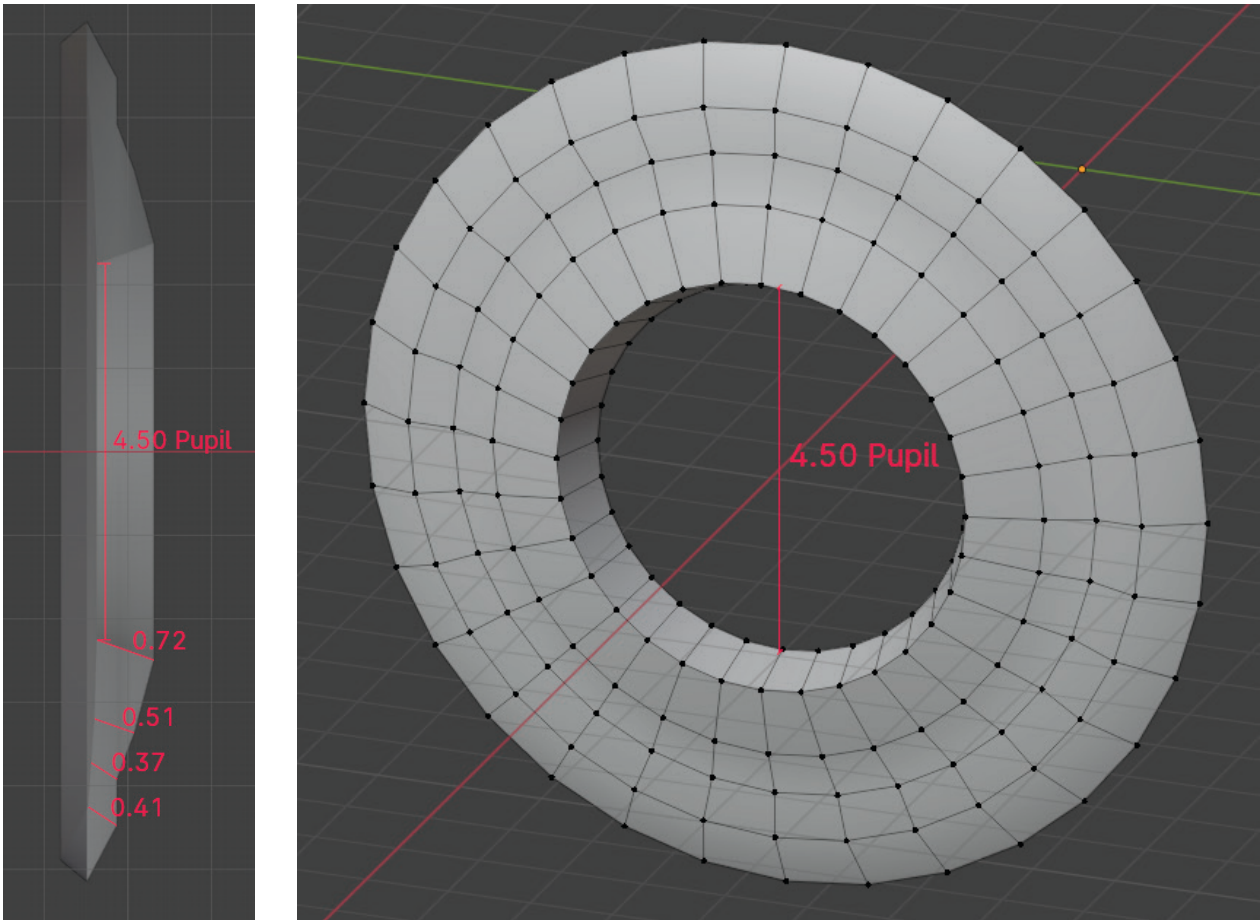


Figure III.38 : 3D Iris side & front view

III.3.2.6. Modeling Vitreous :

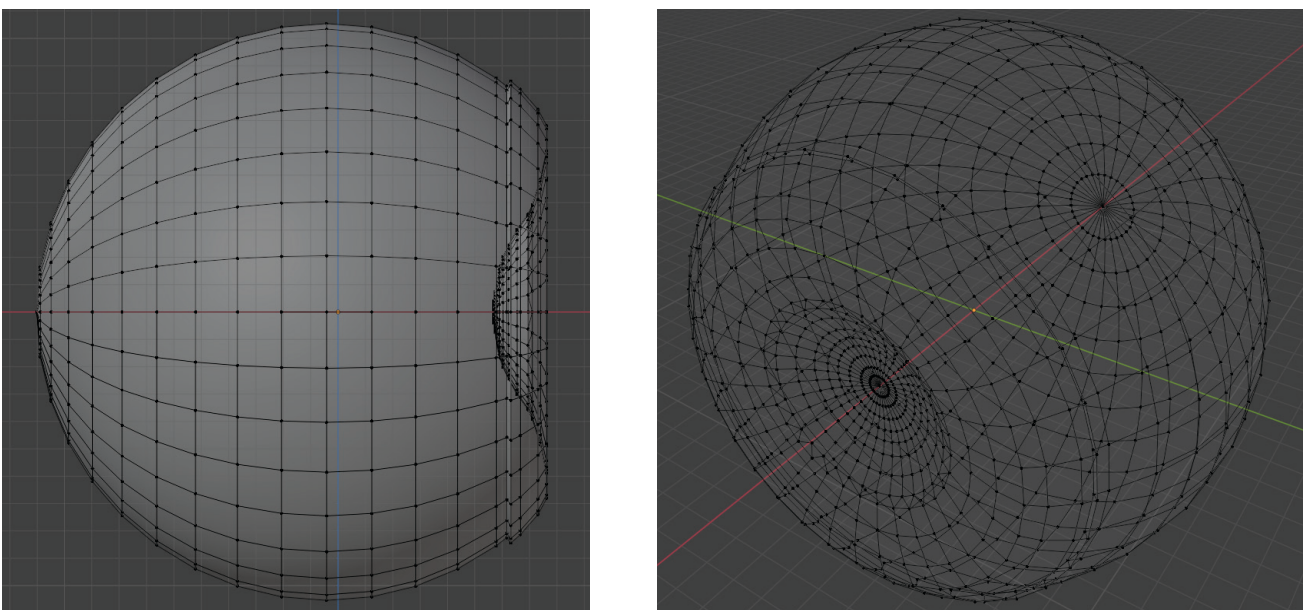


Figure III.39 : 3D Vitreous (side & front view)

III.3.2.7. Modeling Crystalline Lens :

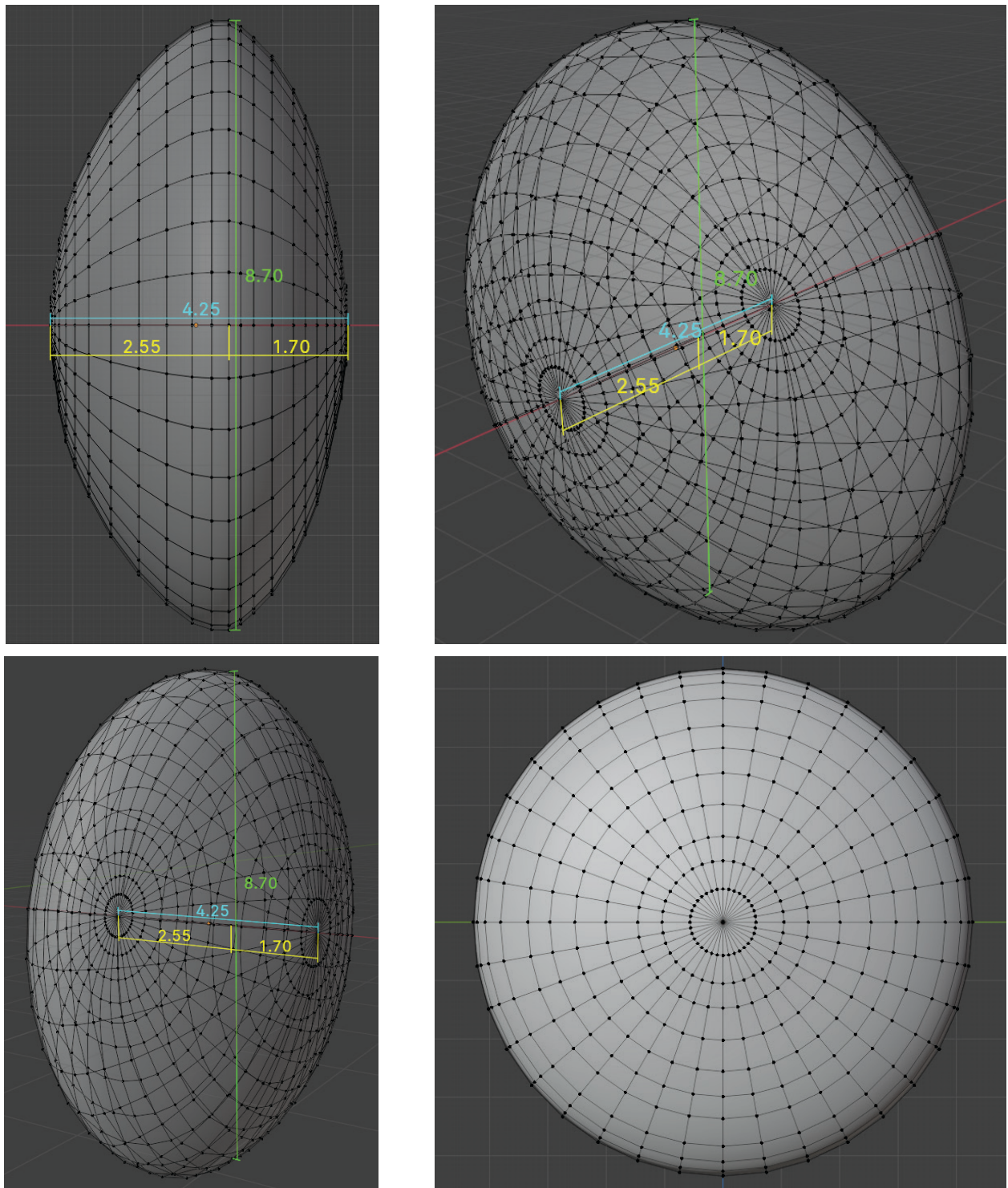


Figure III.40 : 3D Crystalline Lens Measurement (side & front view)

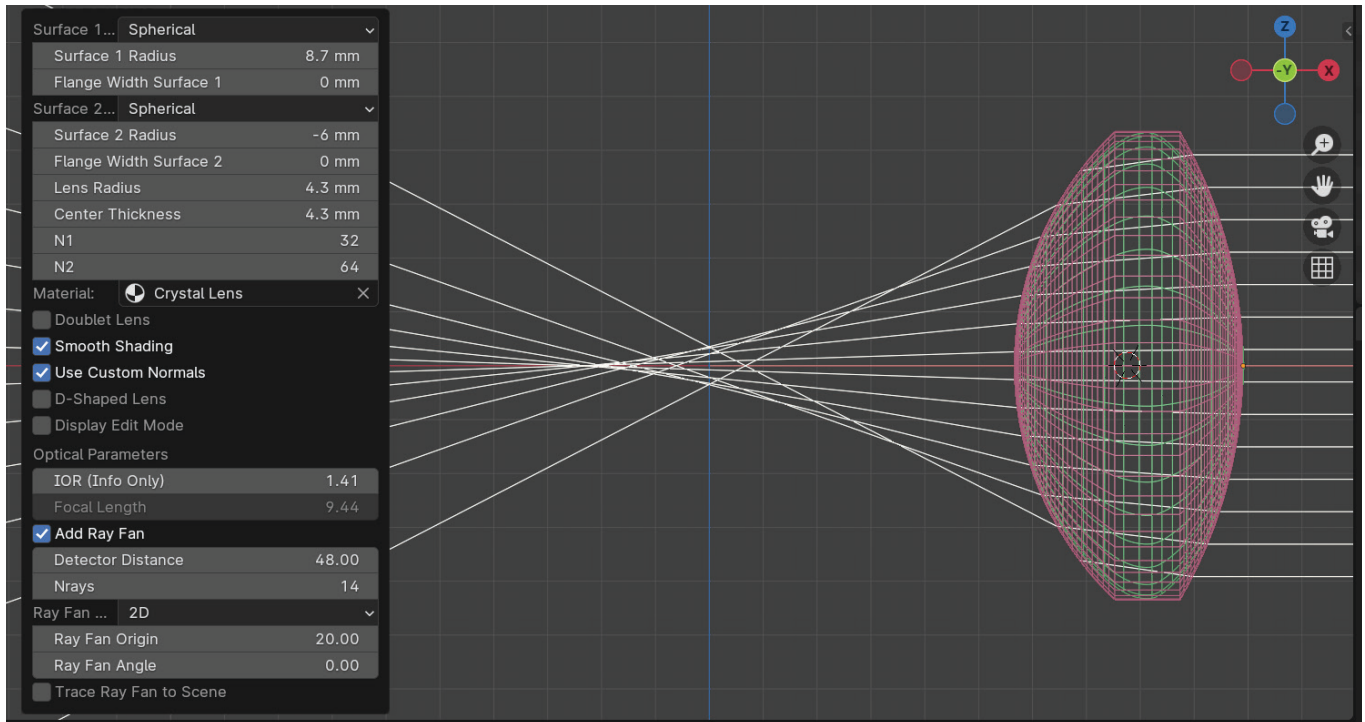


Figure III.41 : 3D Crystalline Lens Parameters (focal Length-R1-R2)

In our experiment : we can Change this parametre

- **R1** : 8.7 mm
- **R2** : -6 mm
- **Lens Radius** : 4.35 mm **==== Lens Diametre** : 8.7 mm
- **Center Thickness** : 4.3 mm
- **Focal Length** : 9.44 mm

While the typical focal length of the crystalline lens in a relaxed state is around 17-20 mm, it can decrease to about 10 mm when fully accommodating for very close objects, especially in younger individuals with flexible lenses. This capacity diminishes with age due to the natural stiffening of the lens.

III.3.2.8. EYE (All in One) :

After assembling all the components of the eye, we get a realistic eye whose optical properties can be simulated.

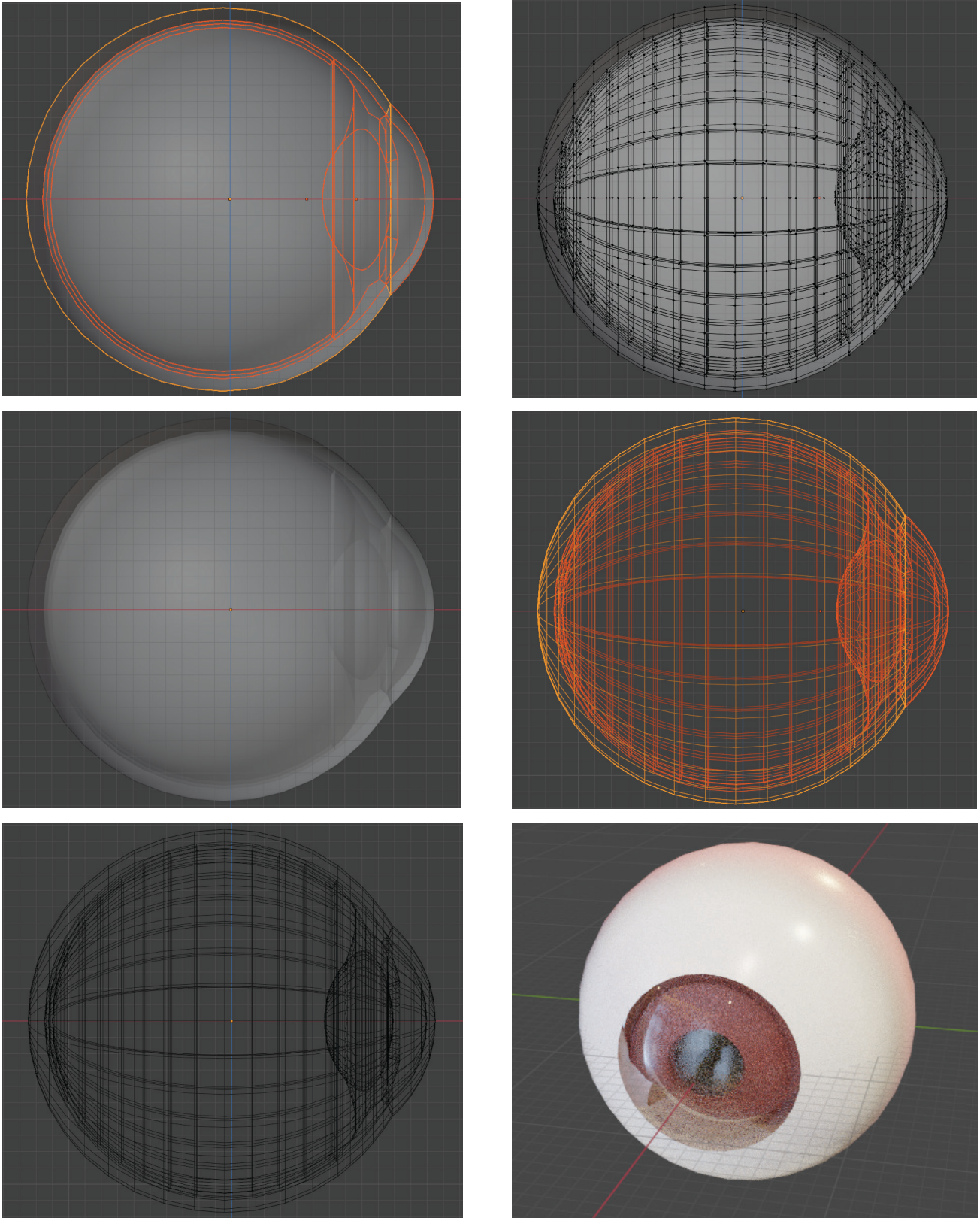


Figure III.42 : EYE (All in One)

III.3.3. Modeling & Calculation of Beam Expander :

We used MATLAB with app designer to create a graphical user interface :

```

1  classdef BeamExpanderCalculator < matlab.apps.AppBase
2
3      % Properties that correspond to app components
4      properties (Access = public) ...
47
48      % Properties that correspond to apps with auto-reflow
49      properties (Access = private)
50          onePanelWidth = 576;
51          twoPanelWidth = 768;
52      end
53
54      % Callbacks that handle component events
55      methods (Access = private)
56
57          % Value changed function: CalculatButtonCocave
58          function CalculatButtonCocaveValueChanged(app, event)
59              R = app.RxEditField.Value;
60              n = app.nxEditField.Value;
61              f = -(R/(n-1))
62              app.fxEditField.Value = f;
63              app.finEditField.Value = app.fxEditField.Value
64          end
65
66          % Value changed function: RxEditField
67          function RxEditFieldValueChanged(app, event)
68              value = app.RxEditField.Value;
69
70          end
71
72          % Value changed function: CalculateButton
73          function CalculateButtonValueChanged(app, event)
74
75              fin = app.finEditField.Value
76              fout = app.foutEditField.Value
77              M = -(fout/fin)
78              app.MEditField.Value = M
79              L = abs(fout)-abs(fin)
80              app.LEditField.Value = L
81          end
82
83          % Value changed function: CalculatButtonConvex
84          function CalculatButtonConvexValueChanged(app, event)
85              R = app.RvEditField.Value;
86              n = app.nvEditField.Value;
87              f = (R/(n-1))
88              app.fvEditField.Value = f;
89              app.foutEditField.Value = app.fvEditField.Value
90          end
91
92          % Changes arrangement of the app based on UIFigure width
93          function updateAppLayout(app, event) ...
127      end

```

Figure III.43 : Matlab Code for GUI

This graphical user interface for Beam Expander calculation:

- Focal Length of PLANO-CONCAVE (**f_{out}**) lens then Raduis of Curvature.
- Focal Length of PLANO-CONVEX (**f_{in}**) lens then Raduis of Curvature.
- **M** the Beam Expander Magnification (LASER Spot Magnification).
- Distance Between two Lenses (**L**)

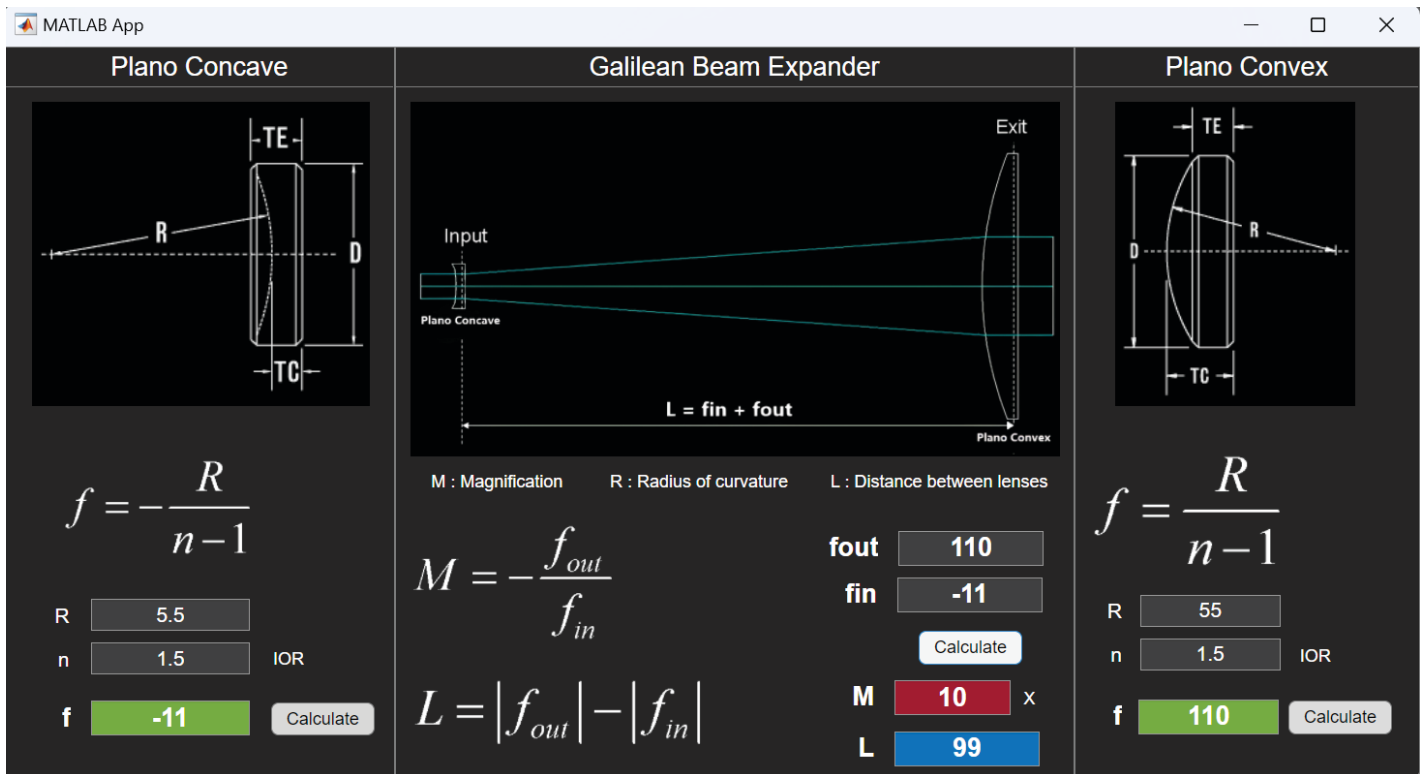


Figure III.44 : Matlab GUI Beam Expander Calculator

After calculating we found:

Plano Concave :

- $R = 5.5$ mm
- Focal Length = -11 mm

Plano Convex :

- $R = 55$ mm
- Focal Length = 110 mm

Beam Expander :

- $M = 10$
- $L = 99$ mm

Then we modeled it in Blender.

- Modeling PLANO-CONCAVE and PLANO-CONVEX lens.

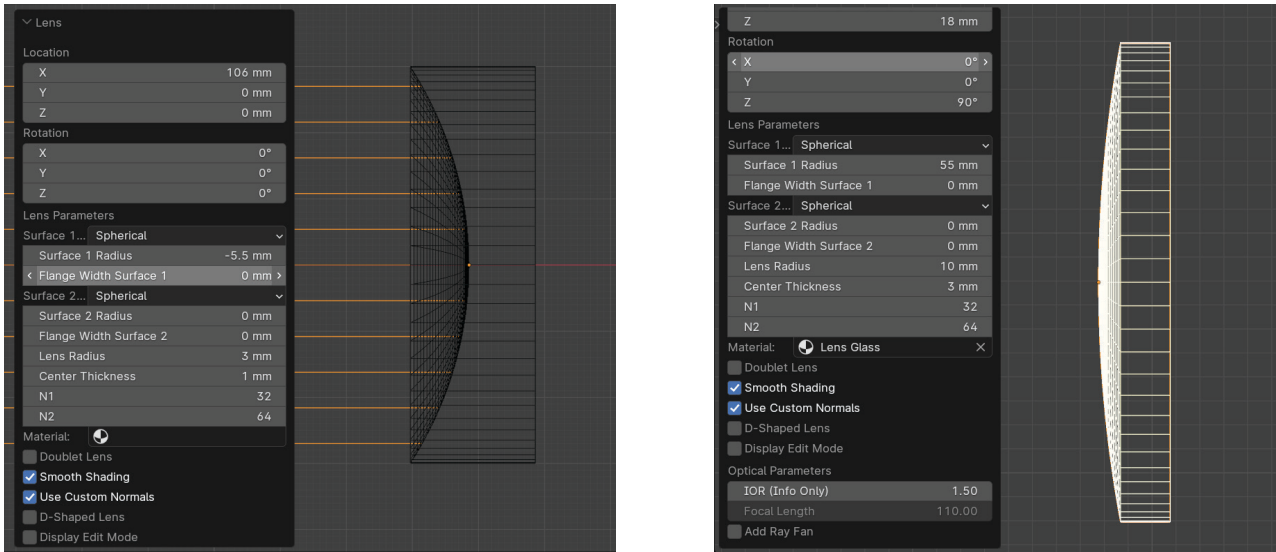


Figure III.45 : Plano Concave and Plano Convex Parameters

- Adjust the distance "L" between two lenses.

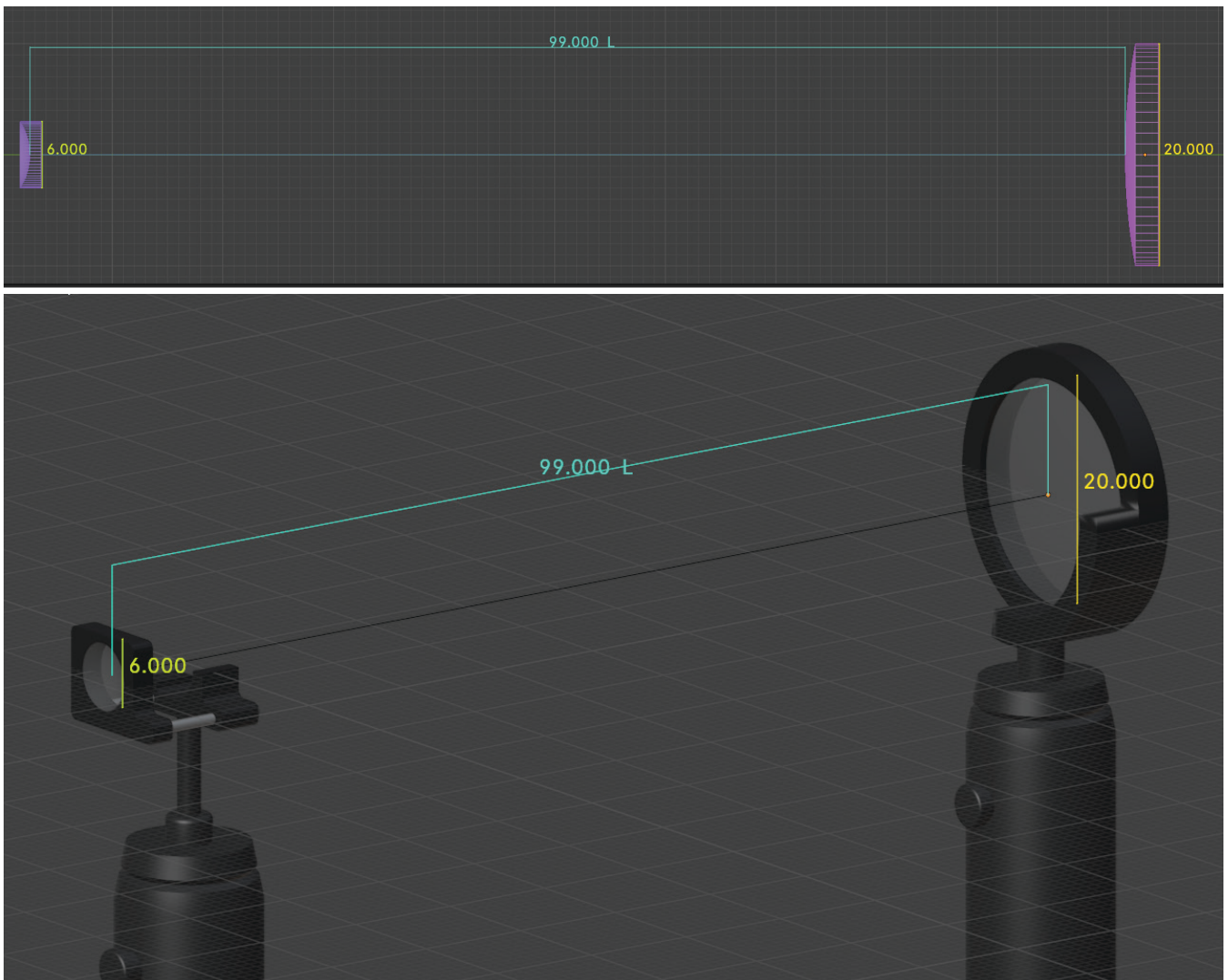


Figure III.46 : Beam Expander Dimension

III.3.4. Modeling DMD :

DMD (DLP7000) Dimension

from Texas Instruments datasheet (DLP7000 DLP® 0.7 XGA 2x LVDS Type A DMD)[46]

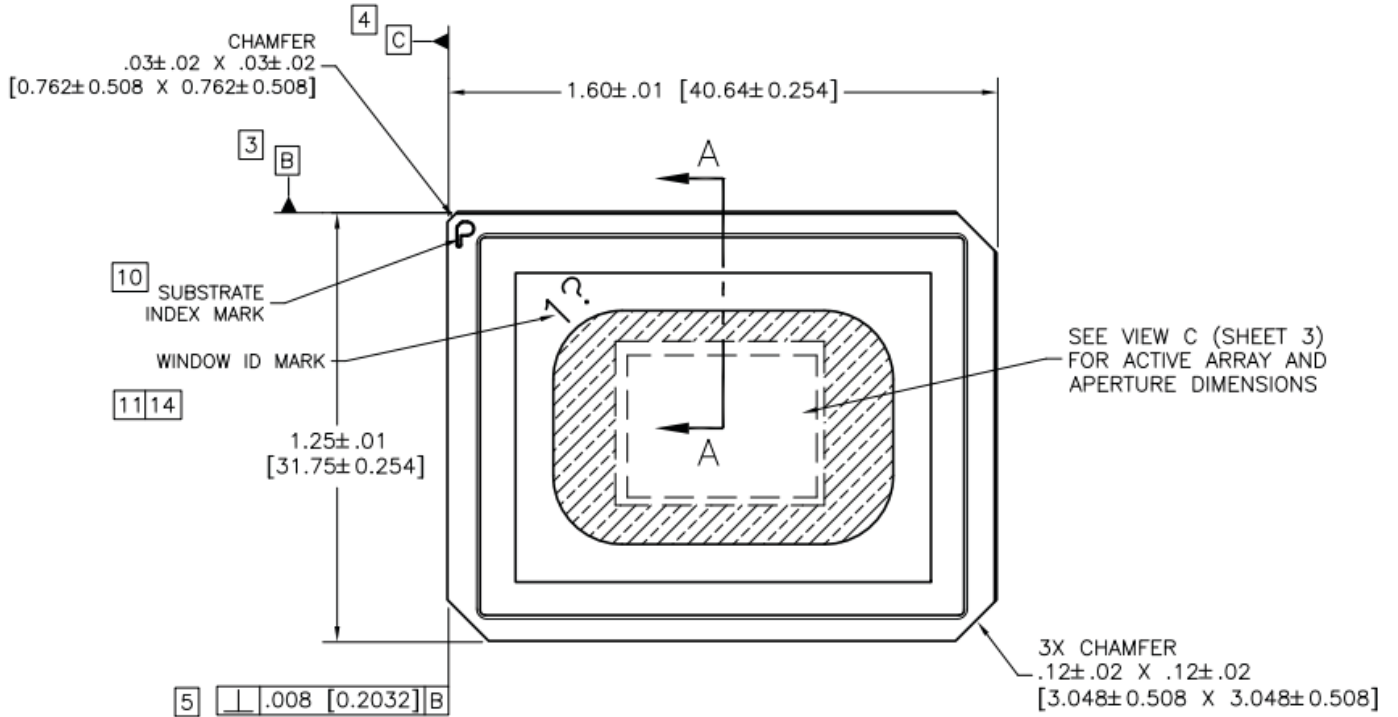


Figure III.47 : DMD Dimensions

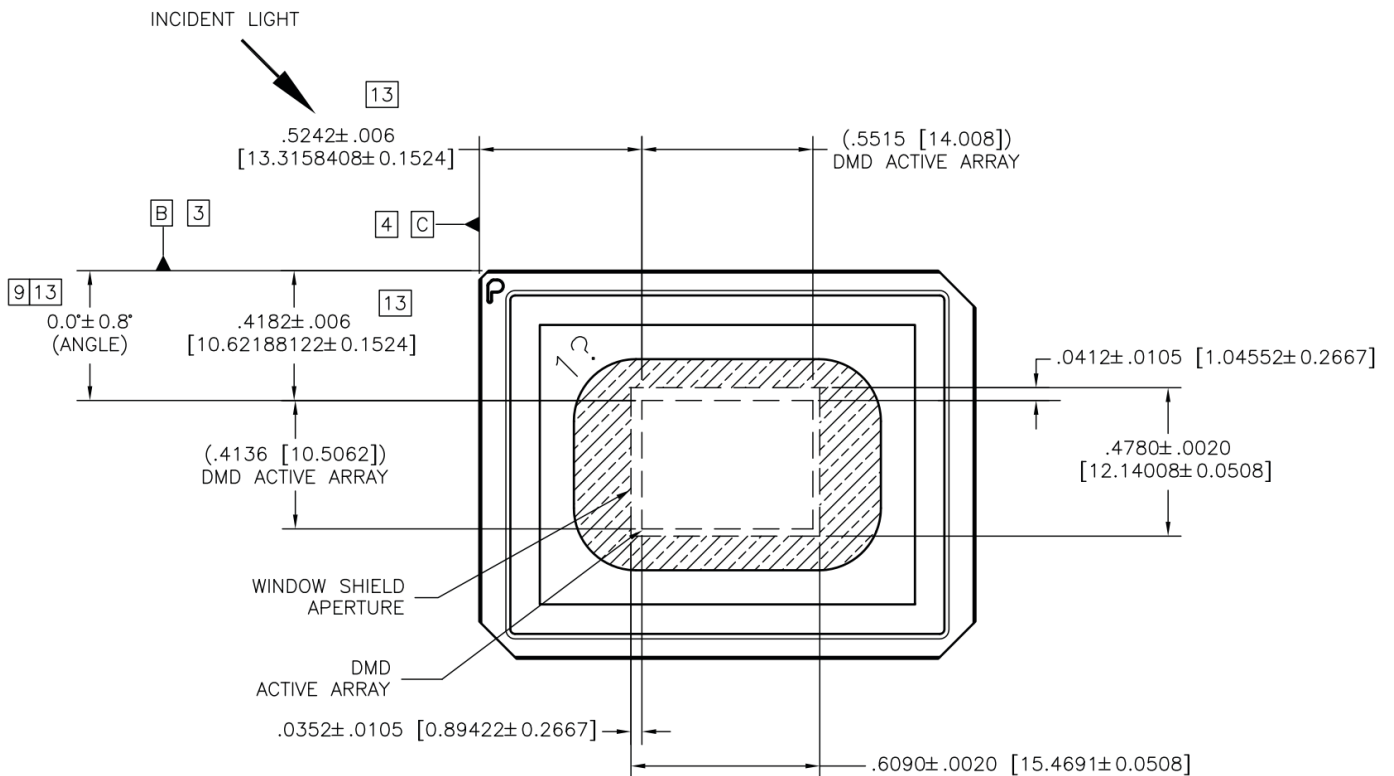


Figure III.48 : DMD ACTIVE ARRAY and WINDOW SHIELD APERTURE

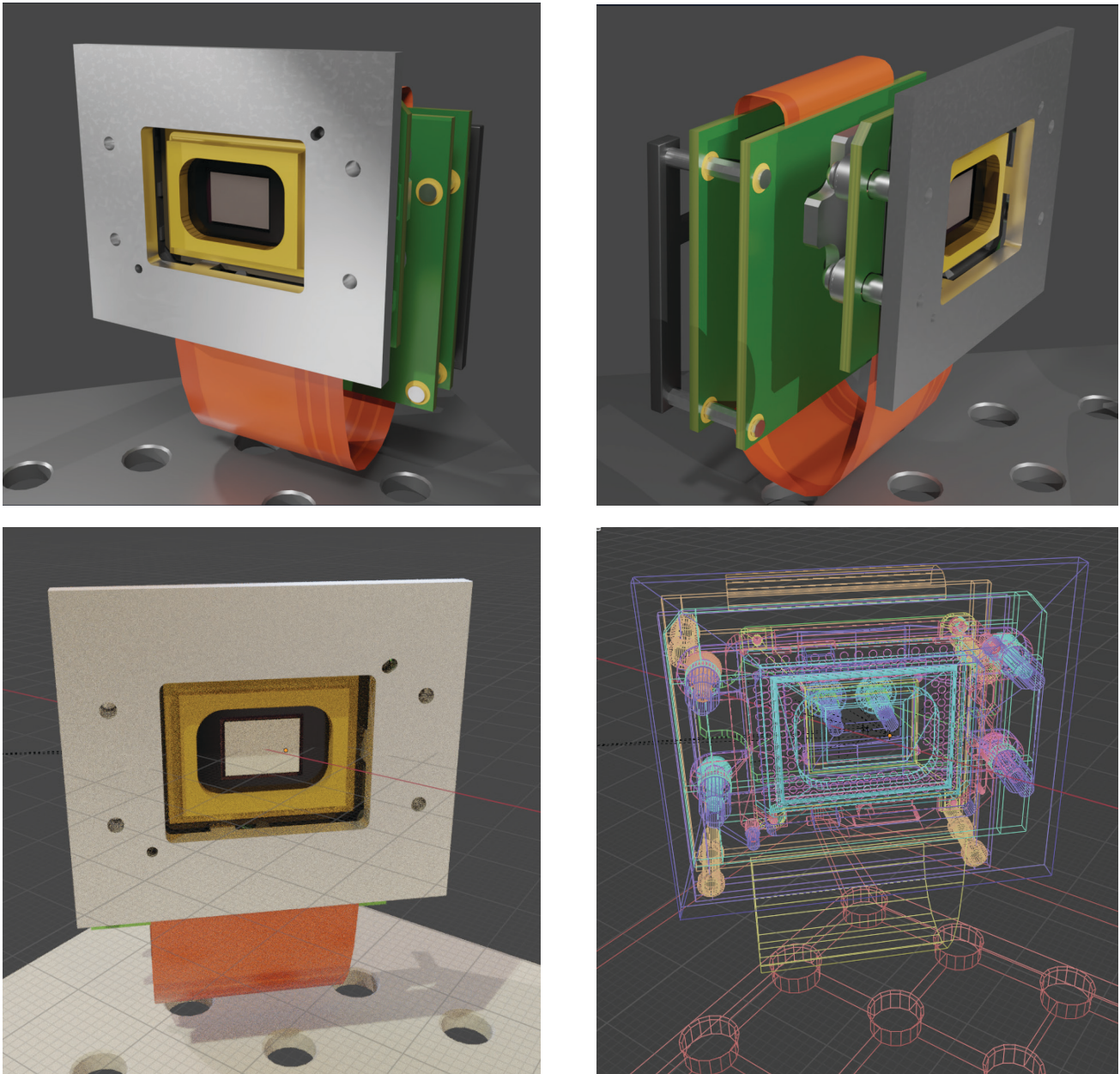


Figure III.49 : 3D Model and Render of DMD

Creating a 3D model of the DLP7000 can be useful for design, simulation, and integration purposes in various optical and electronic systems.

Simulating the DLP7000 DMD in LuxCoreRender involves preparing a detailed 3D model, configuring realistic materials, setting up appropriate lighting, and animating the micromirrors to demonstrate their behavior. LuxCoreRender's physically-based rendering capabilities allow for high-quality visualizations that can be used for design validation, presentations, and educational purposes.

In our experiment used the 3D model of DLP7000 DMD to pattern lasers for eye retina photocoagulation and simulate this process using LuxCoreRender in Blender.

III.3.5. OptoMechanics Component :

Breadboards provide a solid foundation for construction of an optical system.

Postholders and Bases for postholders used with post-mounted holders allow great flexibility of layout and are useful for experimental work.

Direct-mounting screws and bases give a much more stable and compact system, suitable for production as well as prototyping. Component holders are screwed either directly to the breadboard, or to a base on the breadboard. This is feasible because of standardised axis heights.

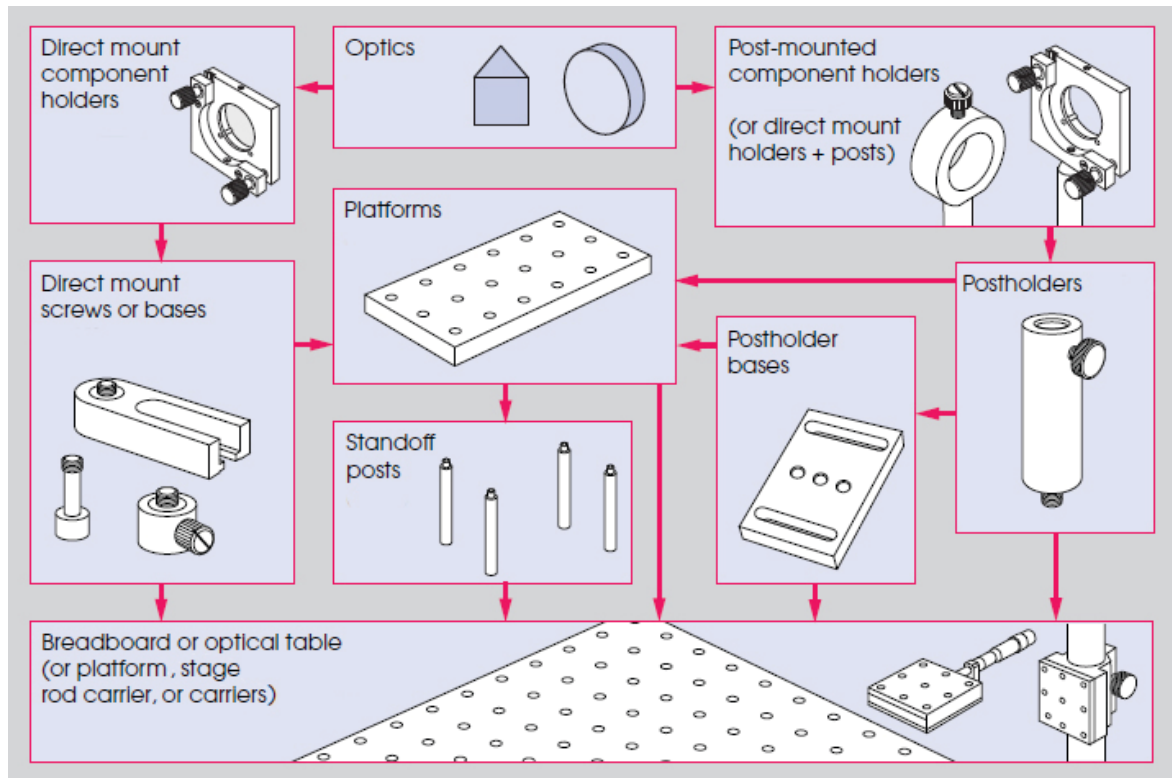


Figure III.50 : BreadBoard & OptoMechanics

III.3.6. Modeling OptoMechanics :

- We do not have this equipment, so we modeled it for use in simulation using Blender.
- The modeling is accurate and realistic.

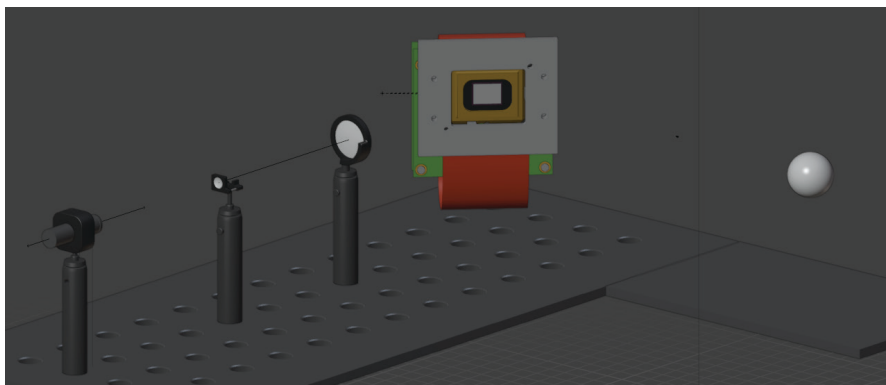


Figure III.51 : Assembly all Components in BreadBoard

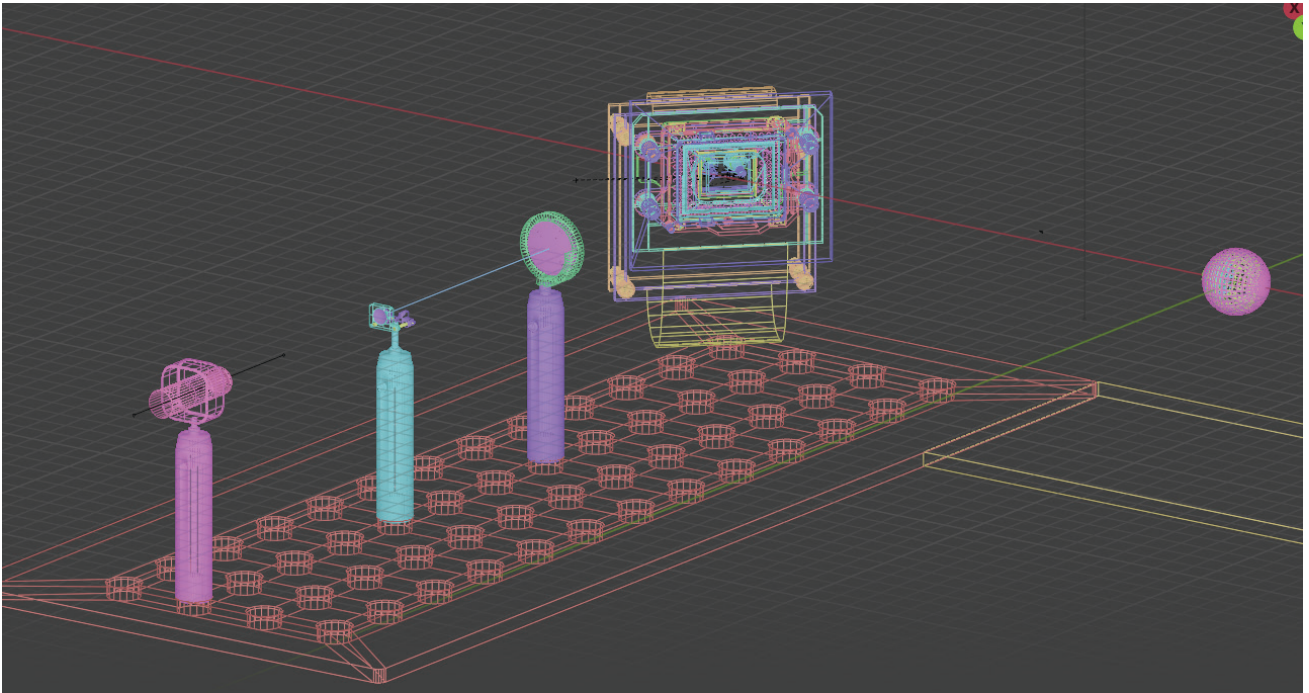


Figure III.52 : Full Optical System (Front view)

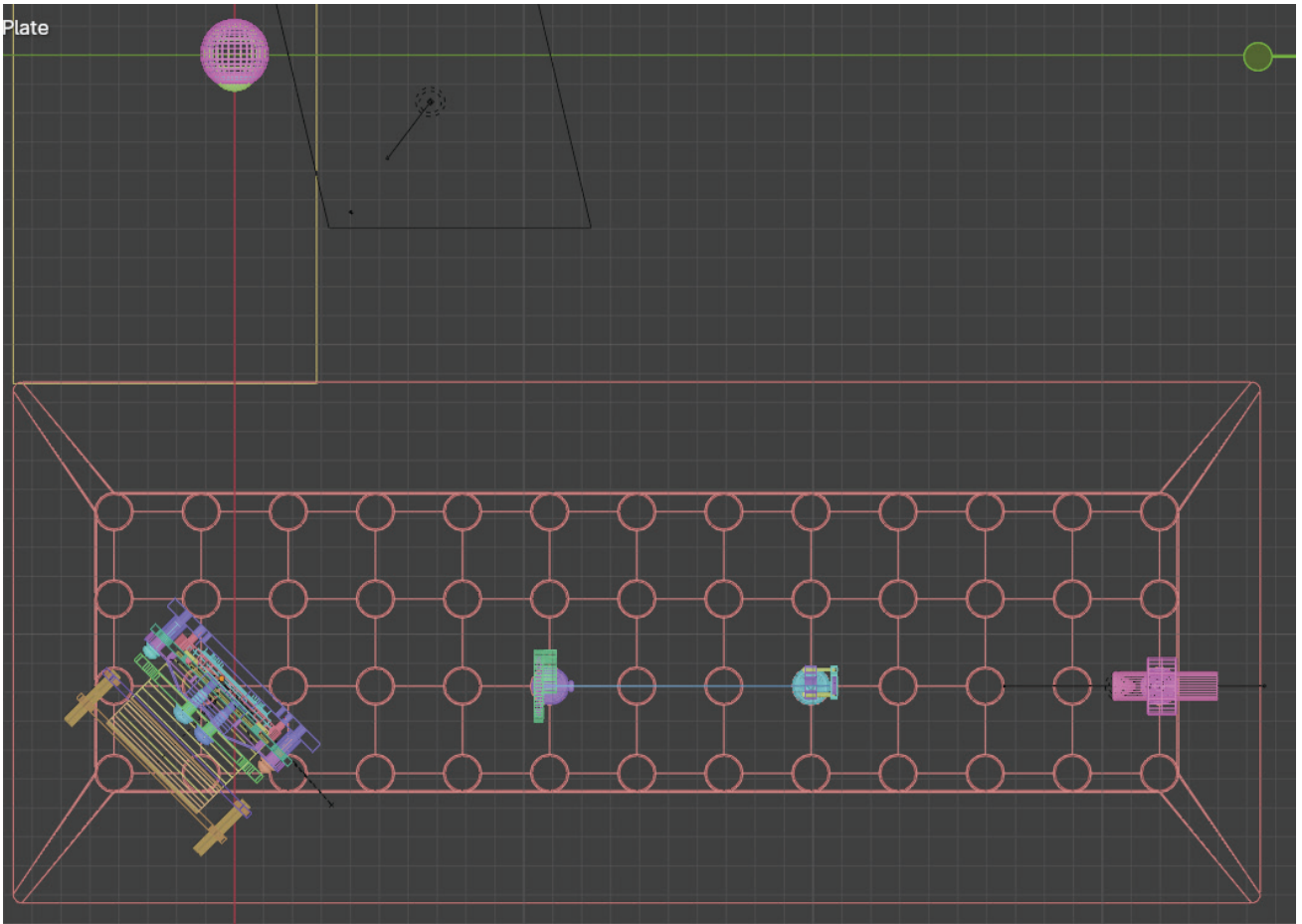


Figure III.53 : Full Optical System (Top view)

III.4. Simulation :

III.4.1. LuxCoreRender :



- **PHYSICALLY BASED RENDERING :**

LuxCoreRender is built on physically based equations that model the transportation of light. This allows it to accurately capture a wide range of phenomena which most other rendering programs are simply unable to reproduce. This also means that it fully supports high-dynamic range (HDR) rendering.

LuxCoreRender features a variety of material types. Apart from generic materials such as matte and glossy, "physically accurate representations of metal, glass," and car paint are present.

LuxCoreRender supports dynamic and interactive scene editing.

LuxCoreRender is a physically based and unbiased rendering engine. Based on state of the art algorithms, LuxCoreRender simulates the flow of light according to physical equations, thus producing realistic images of photographic quality.

- **LuxCoreRender advanced features :**

Materials and Textures :

LuxCoreRender features a variety of material types. Apart from generic materials such as matte, glossy or the Disney principled shader, physically accurate representations of metal, glass, paint are present. All materials can be mixed and modified using textures, most material properties are texturable

Lighting : LuxCoreRender supports emitters and environment light sources.

Volumes : LuxCoreRender includes a powerful volume system capable of physically accurate absorption and scattering. Absorption can be defined by RGB values and scattering supports either single or multiple scattering with user-defined asymmetry. This allows simple setup for internal volumetric effects such as subsurface scattering or volumetric color absorption

Cameras : LuxCoreRender supports orthographic and environment cameras. Using the orthographic camera, one can easily render a front or top view of a model. The environment camera can be used to produce 360° panoramas.

Motion Blur, Depth Of Field and Lens Effects : LuxCoreRender features a tons of extra features such as motion blur depth of field and "lens effects" which gives the user a complete freedom and no limitations.

III.4.2. DMD PATTERN Simulation :

Using the LuxCoreRender Engine, we make the active area of Digital micromirrors work like real by converting between black and white or grayscale.

we Create two Pattern and Test it in simulation and it Work Well.

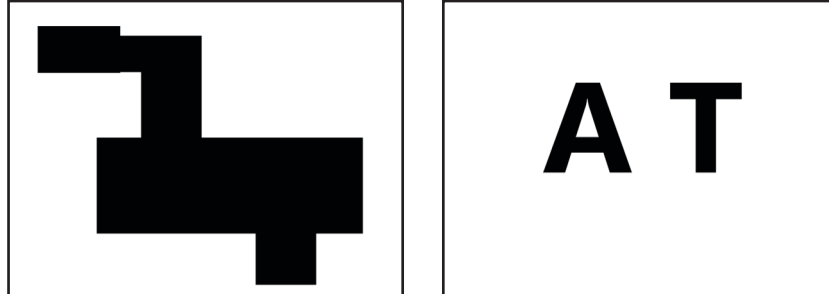


Figure III.54 : DMD Pattern 1024x768 (example)

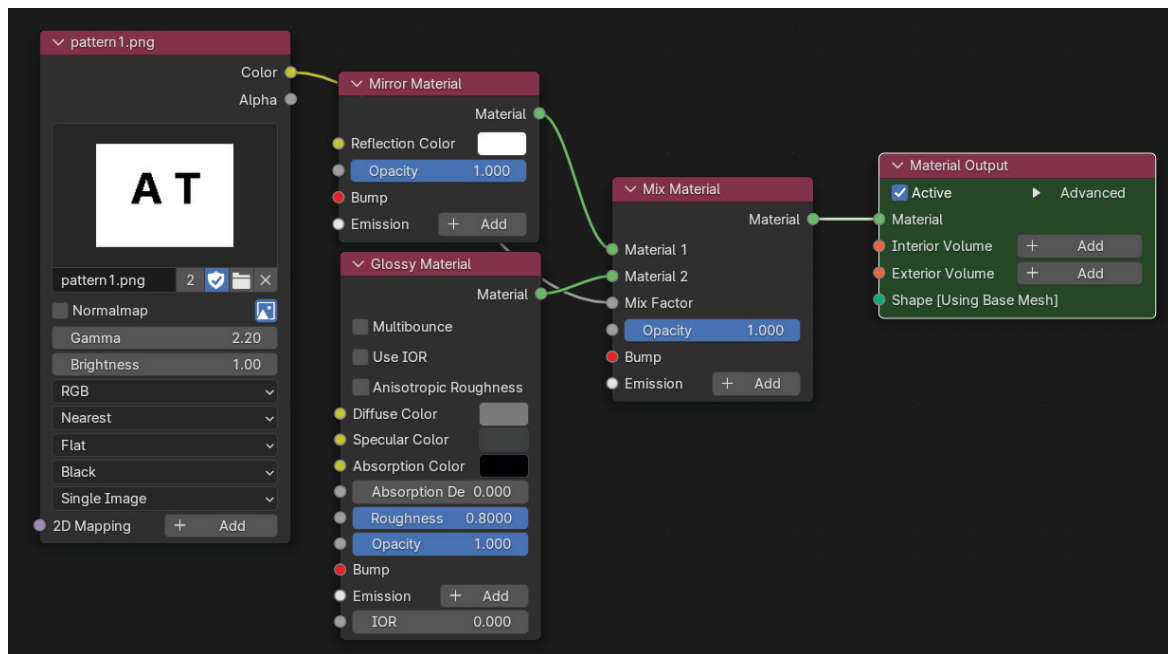


Figure III.55 : DMD Pattern Parameters in Editor

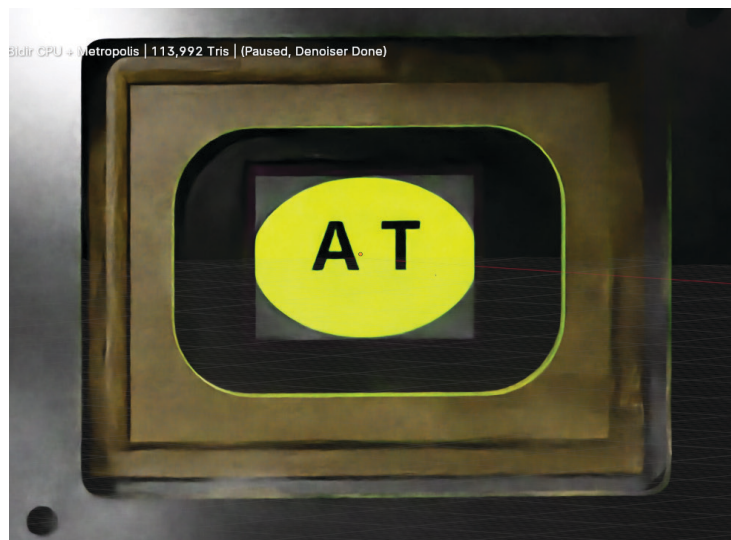


Figure III.56 : Render of DMD Pattern Reflect Laser

III.4.3. Result :

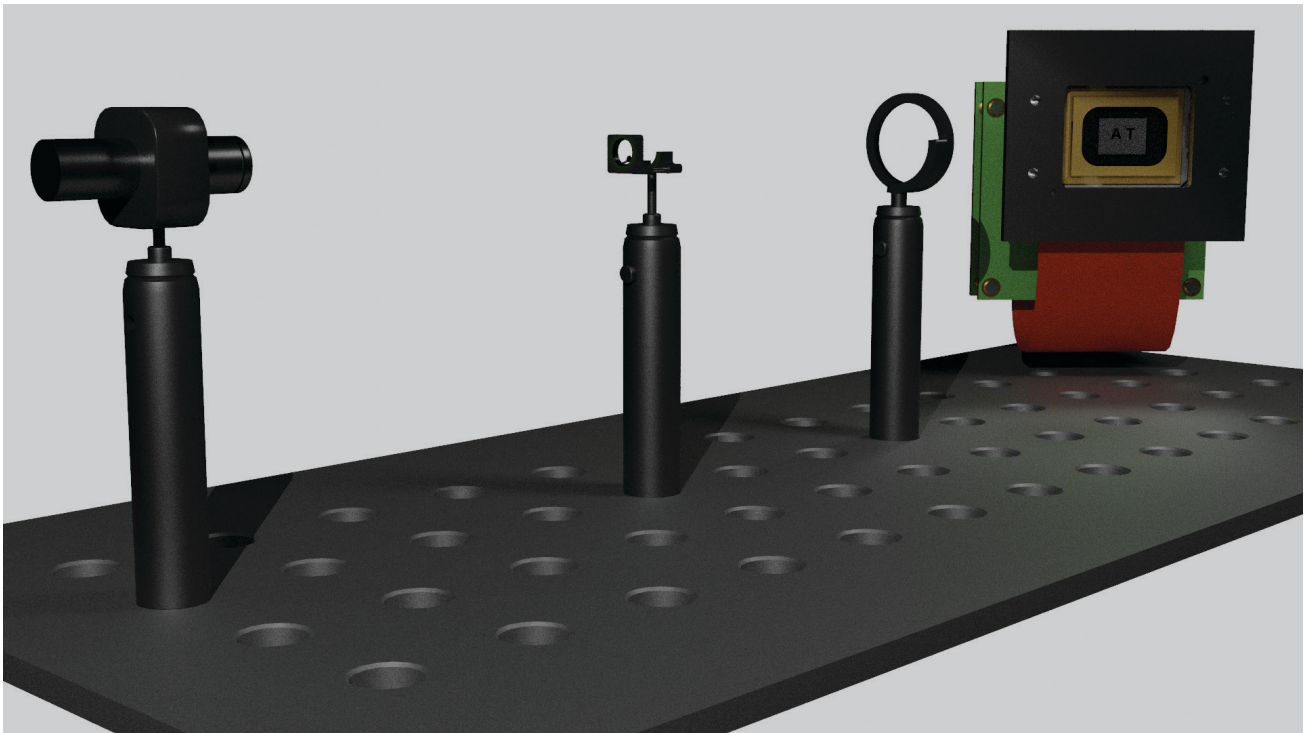


Figure III.57 : Render the Optical System (front view)



Figure III.58 : Render the Optical System (side view)

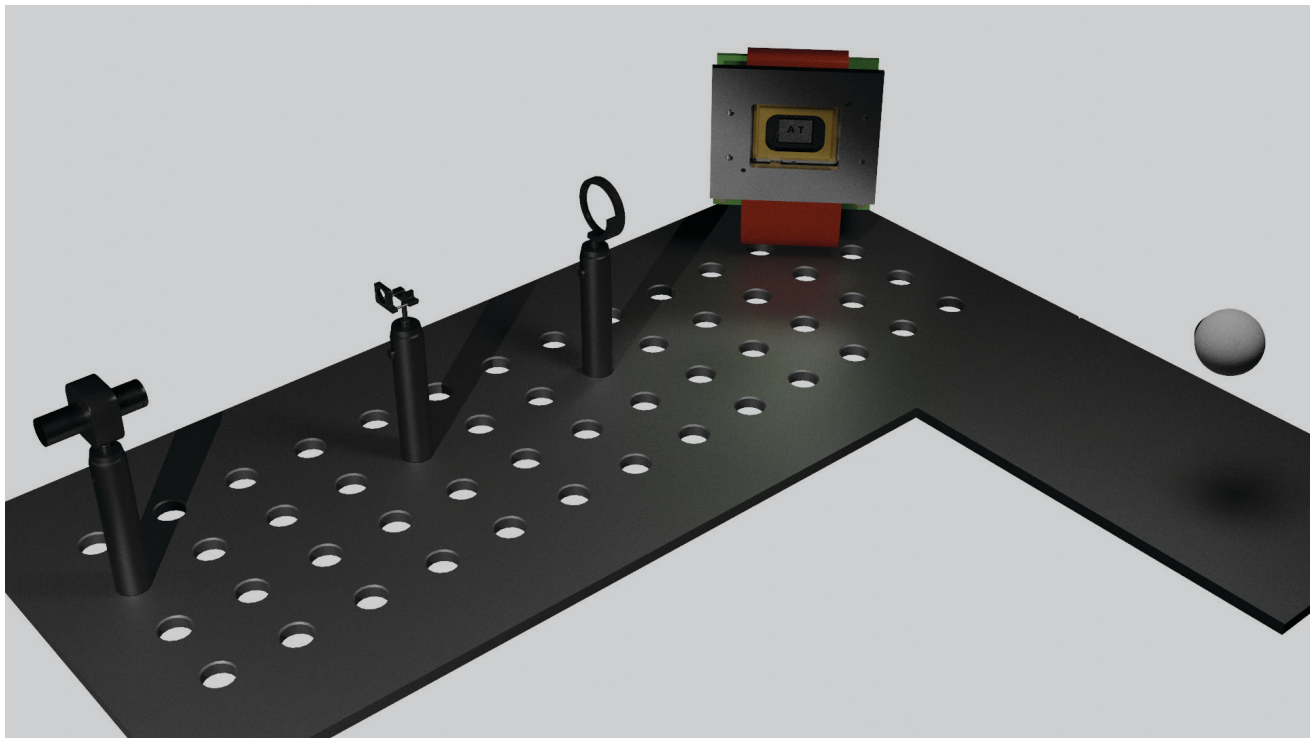


Figure III.59 : Render and Test Full Optical System

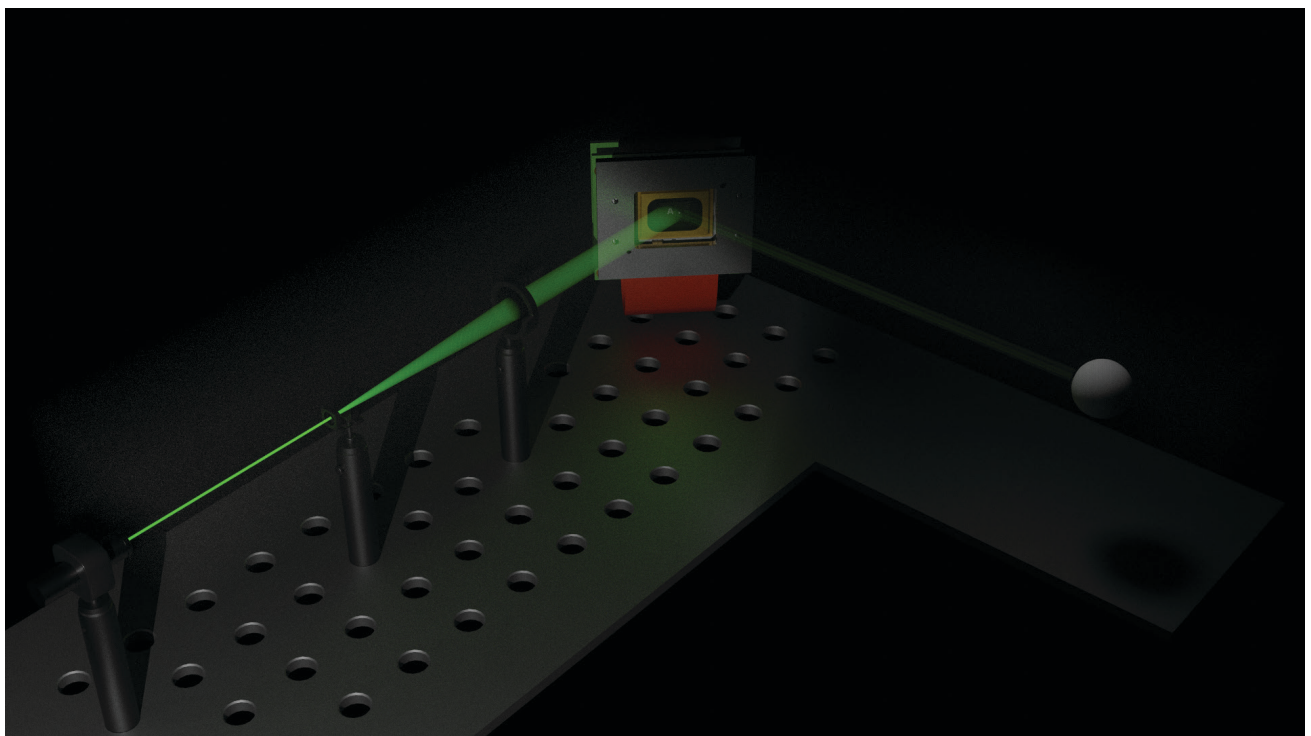


Figure III.60 : Simulate Full Optical System



Figure III.61 : Simulation Laser on Retina (view inside eye)

This image represents the laser applied to the retina in our system.

III.5. Conclusion

In conclusion, in this chapter we successfully demonstrated the feasibility and value of creating a comprehensive virtual model for a retinal photocoagulation optical system. By leveraging the power of 3D modeling in Blender and beam calculations in MATLAB, we have created a highly detailed and anatomically accurate representation of the human eye, integrated with a sophisticated laser delivery system including digital micro-mirror device and its functioning in the system. This approach overcomes the significant challenges associated with physical prototyping of such systems, including safety concerns, high costs, and lack of standardized components. Our model not only provides a platform for visualizing the complex interactions between the laser system and ocular anatomy but also serves as a valuable tool for further research and development in ophthalmic instrumentation. By bridging the gap between theoretical design and practical application, this virtual prototype paves the way for safer, more efficient development of retinal photocoagulation systems, potentially accelerating advancements in the treatment of various retinal disorders.

General Conclusion

This project presents a comprehensive approach to the development and optimization of a retina laser photo-coagulation system, integrating background research, detailed system design, and advanced visualization techniques.

In the first chapter, we provided a thorough background on retinal laser application devices and fundamentals about laser interactions with retina, exploring current technologies, and clinical significance. This foundational knowledge established the context for our project, highlighting the importance of precision and control in retinal laser treatments.

Chapter two focused on the detailed design and implementation of the system, as illustrated in the provided schema. We described the workflow and integration of various components, including the laser source, beam combiner, beam expander, Digital Micromirror Device (DMD), and Gonio lens. The Galilean beam expander's configuration was detailed, emphasizing its role in modifying the laser beam's properties for accurate focus on the retina. The anatomical model of the eye was also discussed, highlighting the importance of understanding eye structures for effective laser delivery.

The final chapter utilized Blender for advanced 3D visualization of the entire system. These visualizations provided a comprehensive and intuitive understanding of the optical setup and its interaction with the eye, enhancing the ability to optimize the design and ensure precise laser targeting. The visual models created in Blender allowed us to better communicate the system's functionality and improve its practical application.

Overall, this project successfully combines theoretical research, detailed system design, and advanced visualization to enhance the precision and efficacy of retina laser photo-coagulation treatments. By integrating multidisciplinary approaches and leveraging state-of-the-art tools, we have developed a robust framework that not only addresses current challenges but also sets the stage for future innovations in ophthalmic laser procedures.

Annex

absorption : change of radiant energy to a modified form of energy by interaction with matter resulting in decrease in power of light passing through a substance.

beam : a group of light rays that can be parallel, or diverge, or converge.

beam diameter (1/e²) : the diameter of that particular irradiance contour in a laser beam of which the irradiance has fallen to 1/e² (13.5%) of the peak or axial irradiance.

beam divergence : the full angle of the beam spread between diametrically opposed (or 1/e²) irradiance points: usually measured in milliradians (1 mrad = 3.4' of arc).

beam splitter : an optical device which uses controlled reflection to produce two beams from a single incident beam.

beam spot size : the diameter of the laser beam between the 1/e² power points; sometimes used loosely to mean the area of the beam cross section between the 1/e² points.

coherent light : radiation in which there is a fixed phase relationship between any two points in the electromagnetic field.

collimated beam : a beam of light where the rays are parallel with very small divergence or convergence.

energy(Q) : the capacity for doing work; energy content is commonly used to characterize the output from pulsed lasers, and is generally measured in joules (J).

continuous wave (cw) : a laser whose output lasts for a comparatively long uninterrupted time, while the laser is actuated (as compared to a pulsed laser); occasionally, a laser emitting continuously for greater than 0.25 sec.

focal length : the length between the secondary nodal point of a lens and the primary focal point. For a thin lens, the focal length is the length between the lens and the focal point.

focal point : the focus point toward which light waves converge or from which they diverge or appear to diverge.

gaussian distribution : a frequency distribution curve for a population or collection of variable data, frequently shown as a bell-shaped curve symmetrical about the mean of the data; frequently called normal distribution. A beam having a gaussian irradiance profile is given by an equation of the form $I = I_0 e^{-2r^2/w^2}$, where I_0 is the beam centerline irradiance, e is the base of the natural system of logarithms, r is the radius of the contour for irradiance I , and w is the radius of the 1/e²

irradiance contour by which beam radius is defined. Both r and w are measured in a plane perpendicular to the beam.

ion laser : a laser for which the active medium is an ionized gas, such as argon or krypton.

atomic laser : a gas laser in which the medium is of atomic form rather than molecular.

chemical laser : a laser that obtains population inversion directly by a basic chemical reaction.

joule (J) : a unit of energy; 1 joule = 1 watt for one second (W .sec) or 107 ergs, or 0.239 calorie.

joule/cm² (J/cm²) : a unit of radiant exposure utilized when measuring the amount of energy per unit area of surface or per unit area of a laser beam.

energy density : the energy per units area expressed in units of joules per square centimeter (J·cm⁻²)

infrared radiation : electromagnetic radiation the wavelengths for which are within the spectrum range of 0.7 μm to 1 mm. This portion of the spectrum is often separated into three bands by wavelength: IR-A (0.7-1.4 μm), or near infrared; IR-B (1.4-3 μm); and IR-C (3 μm -1 mm), or far infrared.

electromagnetic radiation : energy flow formed by vibrating electric and magnetic fields at right angles and lying transverse to the direction of energy. Examples are X rays, ultraviolet light, visible light, infrared radiation, and radio waves, all of which occupy various portions of the electromagnetic spectrum and differ in frequency, wavelength, and energy of a quantum.

emission duration : the temporal duration of a pulse, a series of pulses, or continuous operation, expressed in seconds, during which human access to laser or collateral radiation could be permitted as a result of operation, maintenance, or service of a laser product.

wavelength : the distance between two points in a periodic wave which have the same phase.

laser : acronym for light amplification (by) stimulated emission (of) radiation. Lasers generate or amplify electromagnetic oscillations at wavelengths from the far infrared (submillimeter) to the ultraviolet. The laser oscillator needs two basic elements: an amplifying medium and a regeneration or feedback mechanism (resonant cavity). The amplifying medium can be any of a variety of substances, such as a gas, semiconductor, dye solution, etc. Feedback is generally created by two mirrors.

The distinctive properties of the resulting electromagnetic oscillations include monochromaticity, extremely high intensity, very small bandwidth, very tight beam divergence, and phase coherence.

laser safety officer : one who is knowledgeable in the evaluation and control of laser hazards and has authority for supervision of the control of laser hazards.

maser : acronym for a device for radio microwave amplification (by the) stimulated emission (of) radiation. In contrast to a laser which emits light, a maser emits microwave radiation.

micrometer (μm) : a length equal to 10^{-6} m or 10,000 nm, often termed micron.

microsecond (μsec) : a unit of time equal to 10^{-6} sec.

millisecond (msec) : a unit of time equal to 10^{-3} sec.

monochromaticity : the condition of containing or generating light of only one wavelength from a range of wavelengths present in a beam.

nanometer (nm) : a unit of length equal to 10^{-9} m, 10^{-7} cm, 10^{-3} μm , or 10 Å. The nanometer is beginning to replace the angstrom as the principal unit of electromagnetic wavelength.

nanosecond (nsec) : a unit of time equal to 10^{-9} sec.

optical fiber : a long, thin thread of fused silicon or other transparent substance, used to transmit light.

picosecond (psec) : a unit of time equal to 10^{-12} sec.

photon : the quantum of electromagnetic energy, equal to the product of Planck's constant and the frequency of the radiation.

power (W) : the time rate at which energy is given off, received, or used in some fashion; expressed in watts or in joules per second.

power, average : with a pulsed laser, the pulse energy (joules) times the frequency of the pulse (Hertz), expressed in watts; as compared to the average power of a pulse

power density : denotes the power per unit area (e.g., W cm^{-2}) contained in a laser beam, or falling on a given target area.

reflection : the casting back, turning back, or deviation of radiation following its hitting a surface.

semiconductor laser : a laser formed from an active material that is a semiconductor, which can be a diode or homogeneous. Commercial types are usually diodes in which lasing takes place at the junction of n- and p-type semiconductors, typically gallium aluminum arsenide or gallium arsenide. Homogeneous types are composed of undoped semiconductor material and are energized (pumped) by an electron beam.

stimulated emission : emission (radiation) of electromagnetic energy during a transition from a higher-energy state to a lower-energy state in an activated laser medium. The emission is made possible by the presence of a radiation field (stimulating radiation). The stimulated emission is practically the same in every way (frequency, wavelength, momentum, phase, polarization) to the stimulating radiation.

tunable laser : a laser that allows continuous variation of laser emission across a broad wavelength region. A single laser system can be "tuned" to radiate laser light over a continuous spectrum of wavelengths or frequencies.

ultraviolet radiation : electromagnetic radiation that has wavelength from soft X ray to visible, violet light. The spectral region is frequently categorized into three separate bands by wavelength: UV-A (315-400 nm), UV-B (280-315 nm), and UV-C (200-280 nm). Ultraviolet wavelength is shorter than wavelength for visible radiation.

watt (W) : the unit of power or radiant flux; 1 J/sec.

watt/cm² : a term used as a unit of incident power density or irradiance to express the amount of power per unit area of absorbing surface, or per unit area of a cw laser beam.

Concave lens : it is a lens that produce a negative focal power and add divergence to incident rays of light .

Convex lens : it is a lens that produce a positive focal power and add convergence to incident rays of light.

Plano lens : it is a lens that produce zero focal power and do not change the vergence of incident rays of light.

Radius Of Curvature : radius of curvature R, is the reciprocal of the curvature. For a curve, it equals the radius of the circular arc which best approximates the curve at that point.

Bibliography

- [1] Vanessa Caceres, verywellhealth, 2023, Available: <https://www.verywellhealth.com/laser-photocoagulation-5219365>
- [2] "Kellogg Eye Center", Available: <https://www.umkelloggeye.org/conditions-treatments/anatomy-eye>
- [3] Assil Gaur Eye Institute, 2024. Available: <https://assileye.com/library/retina-diagnostic-tests>.
- [4] Assil Gaur Eye Institute, 2024. Available: <https://assileye.com/library/retina-diagnostic-tests>.
- [5] Assil Gaur Eye Institute, 2024. Available: <https://assileye.com/library/retina-diagnostic-tests>.
- [6] Tower Clock Eye Center, 2024. Available: <https://www.towerclockeyecenter.com/blog-2/oct-exam/>
- [7] B. Bhattacharyya, Step by Step® Laser in Ophthalmology, Jaypee Brothers Medical Publishers, 2009.
- [8] American Academy of Ophthalmology, "EyeWiki," 2024. [Online]. Available: [https://eyewiki.aao.org/Lasers_\(surgery\)](https://eyewiki.aao.org/Lasers_(surgery)).
- [9] B. Bhattacharyya, Step by Step® Laser in Ophthalmology, Jaypee Brothers Medical Publishers, 2009.
- [10] American Academy of Ophthalmology, "EyeWiki," 2024. [Online]. Available: [https://eyewiki.aao.org/Lasers_\(surgery\)](https://eyewiki.aao.org/Lasers_(surgery)).
- [11] American Academy of Ophthalmology, "EyeWiki," 2024. [Online]. Available: https://eyewiki.aao.org/Panretinal_Photoocoagulation.
- [12] I. Cordero, "The Community Eye Health Journal," 2016. [Online]. Available: <https://www.cehjournal.org/article/understanding-and-safely-using-ophthalmic-lasers/>.
- [13] F. A. L'Esperance, Jr., E. F. Labuda, and A. M. Johnson, "Photocoagulation delivery systems for continuous-wave lasers," *Brit. J. Ophthal.*, vol. 53, no. 5, pp. 310-322, 1969.
- [14] Jordan P. Farkas, John E. Hoopman, Jeffrey M. Kenkel, Five Parameters You Must Understand to Master Control of Your Laser/Light-Based Devices, *Aesthetic Surgery Journal*, Volume 33, Issue 7, September 2013, Pages 1059–1064, <https://doi.org/10.1177/1090820X13501174>
- [15] Cleveland Clinic, 2022. [Online]. Available: <https://my.clevelandclinic.org/health/diagnostics/24422-slit-lamp-exam>.
- [16] Cordero, Ismael. (2014). Understanding and caring for an operating microscope. *Community eye health / International Centre for Eye Health*. 27. 17.
- [17] "Wikipedia," 2009. [Online]. Available: https://en.wikipedia.org/wiki/Operating_microscope.
- [18] F. A. L'Esperance, Jr., E. F. Labuda, and A. M. Johnson, "Photocoagulation delivery systems for continuous-wave lasers," *Brit. J. Ophthal.*, vol. 53, no. 5, pp. 310-322, 1969.
- [19] H.-J. Kong, "ResearchGate," 2009. [Online]. Available: https://www.researchgate.net/publication/260385532_Indirect_Ophthalmoscopic_Stereo.
- [20] IRIDEX, "IRIDEX," 2022. [Online]. Available: <https://www.irdex.com/Portals/0/downloads/2022/88287%20Iridex%20Retina%20Portfolio%20>.
- [21] American Academy of Ophthalmology, "EyeWiki," 2024. [Online]. Available: [https://eyewiki.aao.org/Lasers_\(surgery\)](https://eyewiki.aao.org/Lasers_(surgery)).
- [22] I. Cordero, "The Community Eye Health Journal," 2016. [Online]. Available: <https://www.cehjournal.org/article/understanding-and-safely-using-ophthalmic-lasers/>.
- [23] MimoWork Laser, 2023. [Online]. Available: <https://www.mimowork.com/laser/laser-knowledge-what-is-galvo-laser>.
- [24] Omnia Hamdy, Sadeq S. Alsharafi, Mahmoud F. Hassan, Amr Eldib, Nahed H. Solouma, A multi-spot laser system for retinal disorders treatment : Experimental study, *Optik*, Volume 185, 2019, Pages 609-613, ISSN 0030-4026, <https://doi.org/10.1016/j.ijleo.2019.03.158>.
- [25] Jordan P. Farkas, John E. Hoopman, Jeffrey M. Kenkel, Five Parameters You Must Understand to Master Control of Your Laser/Light-Based Devices, *Aesthetic Surgery Journal*, Volume 33, Issue 7, September 2013, Pages 1059–1064, <https://doi.org/10.1177/1090820X13501174>

- [26] iLASER, <https://www.ilasersg.com/knowledge/components/beam-expander/>
- [27] companions, <https://assetlibrary.kompanions.com/learn/physics/lens/>
- [28] Physics Bootcamp, Samuel J. Ling, <https://www.physicsbootcamp.org/lens-maker-equation.html>
- [29] Ophthalmic Photographers' Society, <https://www.opsweb.org/page/gonio>
- [30] <https://www.aaopt.org/education/bcscsnippetdetail.aspx?id=4229c5b0-f873-48d4-9262-9d38fd8405a3>
- [31] EyeWiki, <https://eyewiki.aaopt.org/Gonioscopy>
- [32] Keeler, <https://www.accutome.com/three-mirror-universal-with-flange-laser-20mm>
- [33] lumenlearning, <https://courses.lumenlearning.com/suny-physics/chapter/26-1-physics-of-the-eye/>
- [34] Britannica, The Editors of Encyclopaedia. "refractive index". Encyclopedia Britannica, 19 May. 2024, <https://www.britannica.com/science/refractive-index>. Accessed 27 June 2024.
- [35] Britannica, The Editors of Encyclopaedia. "Snell's law". Encyclopedia Britannica, 7 Jun. 2024, <https://www.britannica.com/science/Snells-law>. Accessed 27 June 2024.
- [36] Vialux Gmbh, https://www.vialux.de/Website/PDF/ALP/E_Hi-Speed-V-Module-Overview.pdf
- [37] Vialux Gmbh, <https://www.vialux.de/en/hi-speed-specification.html>
- [38] Vialux Gmbh, https://www.vialux.de/Website/PDF/ALP/E_ALP-4%20Controller-Suite.pdf.
- [39] American Academy of Ophthalmology, "EyeWiki," 2024. [Online]. Available: https://eyewiki.org/Eye_in_Numbers
- [40] Buckhurst, Hetal & Gilmartin, Bernard & Cubbidge, Robert & Logan, Nicola. (2015). Measurement of Scleral Thickness in Humans Using Anterior Segment OCT. *PloS one*. 10. e0132902. 10.1371/journal.pone.0132902.
- [41] Gupta, A., Ruminski, D., Villar, A.J. et al. Age-related changes in geometry and transparency of human crystalline lens revealed by optical signal discontinuity zones in swept-source OCT images. *Eye and Vis* 10, 46 (2023). <https://doi.org/10.1186/s40662-023-00365-y>
- [42] Moffat, B.A & Atchison, David & Pope, James. (2002). Age-related changes in refractive index distribution and power of the human lens as measured by magnetic resonance micro-imaging in vitro. *Vision research*. 42. 1683-93. 10.1016/S0042-6989(02)00078-0.
- [43] Yousef, Y. A., Mohammad, M., AlNawaiseh, I., Aljabari, R., Toro, M. D., Gharaibeh, A., Rejdak, R., Nowomiejska, K., Zweifel, S., Avitabile, T., Rejdak, M., & Nazzal, R. (2022). Ultrasound Biomicroscopy Measurements of the Normal Thickness for the Ciliary Body and the Iris in a Middle East Population. *Clinical ophthalmology (Auckland, N.Z.)*, 16, 101–109. <https://doi.org/10.2147/OPTH.S297977>
- [44] Panda-Jonas, Songhomitra & Auffarth, Gerd & Jonas, Jost & Jonas, Rahul. (2022). Elongation of the Retina and Ciliary Body in Dependence of the Sagittal Eye Diameter. *Investigative ophthalmology & visual science*. 63. 18. 10.1167/iovs.63.10.18.
- [45] Kolb H. Facts and Figures Concerning the Human Retina. 2005 May 1 [Updated 2007 Jul 5]. In: Kolb H, Fernandez E, Nelson R, editors. *Webvision: The Organization of the Retina and Visual System* [Internet]. Salt Lake City (UT): University of Utah Health Sciences Center; 1995-. Fi, [The retinal thickness shows greatest...]. Available from: <https://www.ncbi.nlm.nih.gov/books/NBK11556/figure/ch38facts.F3/>
- [46] Texas Instruments, <https://www.ti.com/lit/ds/symlink/dlp7000.pdf?ts=1721076551258>
- [47] Barbara Pierscionek, R.J. Green, Sergey Dolgobrodov, 2001, <http://dx.doi.org/10.1364/AO.40.006340>